APPLICATION OF THE LINE-SPRING MODEL TO CRACKS WITH PARTIAL CLOSURE

by

JAMES JOHN LUZ

B.S.M.E. UNIVERSITY OF RHODE ISLAND
(1980)

SUBMITTED TO THE DEPARTMENT OF
MECHANICAL ENGINEERING IN
PARTIAL FULFILLMENT OF THE
REQUIREMENTS FOR THE
DEGREE OF

MASTER OF SCIENCE
IN MECHANICAL ENGINEERING

at the

MASSACHUSETTS INSTITUTE OF TECHNOLOGY

September, 1985

Signature of Author Signature redacted
Department of Mechanical Engineering
September 6, 1985

Certified by Signature redacted
David M. Parks
Thesis Supervisor

Accepted by Signature redacted
Departmental Graduate Committee

APPLICATION OF THE LINE-SPRING MODEL TO CRACKS WITH PARTIAL CLOSURE

by

JAMES JOHN LUZ

Submitted to the Department of Mechanical Engineering on September 6, 1985 in partial fulfillment of the requirements for the Degree of Master of Science in Mechanical Engineering

ABSTRACT

The linear-elastic and elastic-plastic line-spring models are valuable tools in the analysis of surface-cracked plates and shells in which crack surface contact is not of concern. The linear-elastic line-spring model has been extended to include nonlinear-elastic response resulting from partial external closure of surface cracks. Closure lengths and crack tip stress intensities can now be obtained for the partially-closed surface crack. This capability has been incorporated into the ABAQUS © finite element program.

Characteristics of the partially-closed crack are evaluated using a double iterative solution scheme which utilizes multiple interpolation of discrete parametric finite element data.

The case of an axially-cracked, pressurized cylinder has been examined in two ways due to the absence of numerically accepted solutions. The results of a complex plane strain finite element analysis with gap elements defining the crack surface have been compared to those of a simple finite element analysis utilizing shell elements and a single nonlinear-elastic line-spring. Closure lengths and crack tip stress intensities obtained by the two methods compare very favorably. The line-spring model solution was found to be applicable over a limited range of closure due to a lack of parametric data available for interpolation. The lack of data was found to be most severe in the small closure range where the largest displacement variations occur.

In general, the nonlinear-elastic line-spring model is shown to be a viable alternative to complex finite element models in analyzing partial external closure of surface-cracked plates and shells.

Thesis Supervisor: Dr. David M. Parks

Title: Associate Professor of Mechanical Engineering

ACKNOWLEDGEMENTS

I express my appreciation to Professor David M. Parks for his many hours of consultation, and his advice and encouragement.

I am grateful to the General Electric Company, Steam Turbine Generator Division for providing my sponsorship.

Sincere thanks are extended to Samir D. Sayegh, GE Advanced Supervisor for his continual encouragement and assistance through the ABC program.

Special thanks go to Susan MacCormack for her time and effort in typing this document.

And I express my deepest thanks to Steve for his friendship and help throughout the Advanced Course Program. From drop forge to thesis, without him my sanity may not have remained intact.

Most importantly, I thank my wife and my friend, Audree for her unending love, support and patience and I thank my family for their love and support.

TABLE OF CONTENTS

TABLE OF CONTENTS
(continued)

LIST OF FIGURES

LIST OF FIGURES
(continued)

LIST OF TABLES

NOMENCLATURE

a	-	Crack depth of edge-cracked strip
$a(x)$	-	Crack depth profile of surface crack
c	-	Closure length of edge-cracked strip
c'	-	One-half width of semi-elliptical surface crack
$[C]$	-	Cracked contribution to the total tangent compliance matrix of cracked strip
$[C_t]$	-	Total tangent compliance matrix of cracked strip
C_{ij}	-	Tangent compliance matrix coefficients
CMOD	-	Crack mouth opening displacement
COD	-	Crack opening displacement
d	-	CMOD contributions
E'	-	Modulus of elasticity
I	-	Moment of inertia of uncracked strip
J	-	J-integral of cracked strip
k	-	Stress intensity factor contributions of partially-closed crack
k'	-	General stress intensity factor contributions
k^M	-	Total stress intensity factor per unit applied bending moment for partially-closed crack
K_I	-	Total stress intensity factor
l	-	Length from crack plane to the far-field for edge-cracked strip
M	-	Applied bending moment
N	-	Applied membrane force
R	-	Average Radius
R_i, R_o	-	Inner Radius, Outer Radius
$[S_t]$	-	Total tangent stiffness matrix of cracked strip
w	-	Thickness of cracked strip
W_c	-	Strain energy of partially-closed edge-cracked strip
α	-	Slope of closure length ratio versus load ratio curve
δ	-	Far-field displacement contributions
δ^M	-	Total cracked displacement per unit applied bending moment
θ	-	Far-field rotation contributions

Θ^M - Total cracked rotation per unit applied bending moment

$\bar{\lambda}$ - Load ratio (=Nw/M)

ξ_a - Crack depth ratio (=a/w)

ξ_c - Closure length ratio (=c/w)

σ - Stress contributions

Subscripts[1]

app - applied in the far-field (M, N)

c - cracked contributions (δ, Θ)

crit - critical for onset of closure (M, $\bar{\lambda}$)

fc - full closure ($\bar{\lambda}$)

M - due to applied bending moment (d, k, k', K_I, δ, Θ, σ)

mod - modeled (ξ_c)

N - due to applied membrane force (d, k, k', K_I, δ, Θ, σ)

nc - uncracked contributions (δ, Θ)

p - due to resultant crack face pressure distribution (K_I)

symm - symmetrical closure ($\bar{\lambda}$)

[1] The subscripts apply to the variables following the definition.

1. INTRODUCTION

In the design and analysis of typical engineering structures fracture mechanics principles can be applied to a great extent in the evaluation of overall structural component integrity. Among the types of problems which lend themselves to a fracture mechanics approach, perhaps the most common can, in their most basic form, be classified as "part-through surface-cracked plates and shells". In any geometry, beyond the fact that a crack or "defect" is present, it is necessary to characterize the severity of the crack tip singularity. In the case of linear-elastic fracture mechanics the crack tip singularity is characterized by the stress intensity factor. An accurate evaluation of the stress intensity factor is vital in determining the overall structural integrity of the component (i.e., to evaluate the fatigue crack growth characteristics or to determine the potential for catastrophic failure).

A considerable amount of work has been done in two-dimensional SIF calibrations for a number of geometrically linear crack and loading configurations. However, for thick curved shells ($R/w \leq 10$) and fully three-dimensional geometric and kinematic configurations stress intensity factor calibrations are severely lacking; the main stumbling blocks being the complexity of fully 3-D elastic analyses, and the computational and mesh generation costs associated with complete 3-D finite element models with sufficient accuracy and convergence characteristics. These stumbling blocks become even more restrictive when considering the class of problems mentioned above loaded in such a way that partial closure of the

crack occurs. The phenomenon of partial closure introduces highly non-linear aspects into an already complex finite element or analytical model.

The weight function method has been used successfully to characterize crack tip singularities in two and three dimensions. Bueckner's [1] development of weight functions for a notched bar allowed for easy computation of stress intensity factors for a variety of symmetric loading configurations. Similarly, stress intensity factors for semi-elliptical surface cracks in finite thickness plates have been examined by Mattheck et al [2,3] using weight functions and by Isida et al [22].

A related and perhaps more general analytical tool which can be applied to many types of surface cracks (2- or 3-D) is the "line-spring" model of Rice and Levy [4]. Within the past 5-10 years, the "line-spring" model has received renewed interest in its application to 3-D part-through surface-cracked plates and shells. The line-spring considerably simplifies the analysis of this type of problem by reducing the fully three-dimensional problem to effectively one dimension in plate or shell theory. In linear elasticity the line-spring model has been found to estimate stress intensity factor distributions along a crack front to within a few percent of accepted numerical solutions. Through further recent development by Parks et al [5], the line-spring model has been incorporated into the ABAQUS © finite element program. However, to date the applications and development of the line-spring model (Parks, et al [5-8]) have been limited to linear-elastic and

elastic-plastic analyses. Geometrically nonlinear elastic configurations (partial crack closure) have not been addressed.

For a surface-cracked specimen subjected to a linear traction distribution through the thickness there are only two types of closure which can be obtained; "internal" and "external". These can be characterized as follows:

Internal Closure - Crack closure begins at the crack tip. In this type of closure a shallower surface crack results with a stress intensity factor of zero.

External Closure - Closure begins at the mouth of the crack. This type of closure effectively results in a non-surface (central) crack configuration with a non-zero stress intensity factor at the crack tip.

In the present work, the nonlinear characteristics of partial external closure of part-through surface cracks in Mode I are developed and incorporated into the linear-elastic line-spring model formulation and into the ABAQUS © finite element program. Internal crack closure is discussed briefly in Appendix I.

1.1 External Closure of Surface Cracks

With respect to the finite element line-spring model formulation which will be reviewed in Section 2.1, let it suffice to say that a fully 3-D part-through surface-cracked plate or shell can be modeled by a series of single edge-cracked strips. To this end, the phenomenon of partial external closure of

three-dimensional cracks can be characterized by examining an edge-cracked strip.

Consider the edge-cracked strip of Figure 1.1-1 subjected to far-field membrane force, N (per unit width) and bending moment, M (per unit width). The positive sense of each load is as shown; resulting in separation of the crack surfaces. For a constant tensile force, $N = N_{app}$, consider the application of a bending moment, $M = -M_{crit}$ such that the outer edge of the crack (crack mouth) just comes into contact as shown in Figure 1.1-2. If the far-field moment is decreased further, $M = M_{app} < -M_{crit}$ one of the two configurations depicted in Figures 1.1-3 will result. That shown in Figure 1.1-3(a) considers a purely linear superposition of the membrane and bending loading. This superposition neglects the interference which actually develops between the crack surfaces (i.e., it allows for overlap of the crack surfaces). In accounting for the interference, the true equilibrium configuration as depicted in Figure 1.1-3(b) is obtained. Over the area of contact a pressure distribution will be developed between the crack surfaces. This pressure distribution, when superposed on the configuration of Figure 1.1-3(a), results in additional crack surface separation, effectively stiffening the strip. This stiffening results in a contact length (closure length) less than that determined by purely linear superposition and also results in a decrease in the far-field work-conjugate displacements, δ and θ corresponding to N_{app} and M_{app}, respectively.

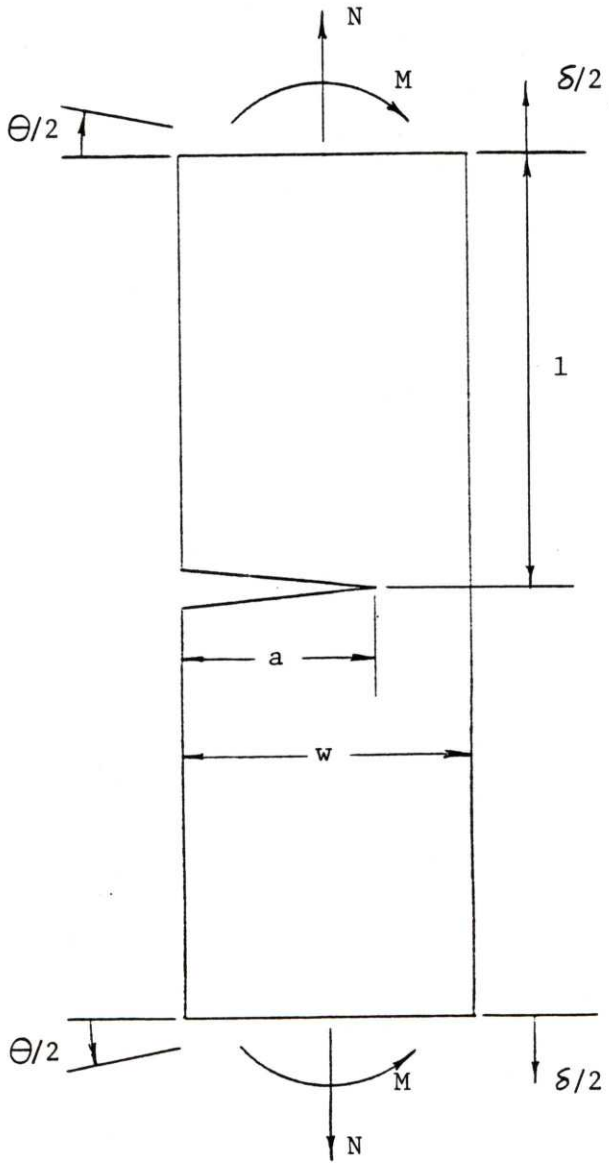

Figure 1.1-1

Single Edge-Cracked Strip Used to Model Partial Crack Closure

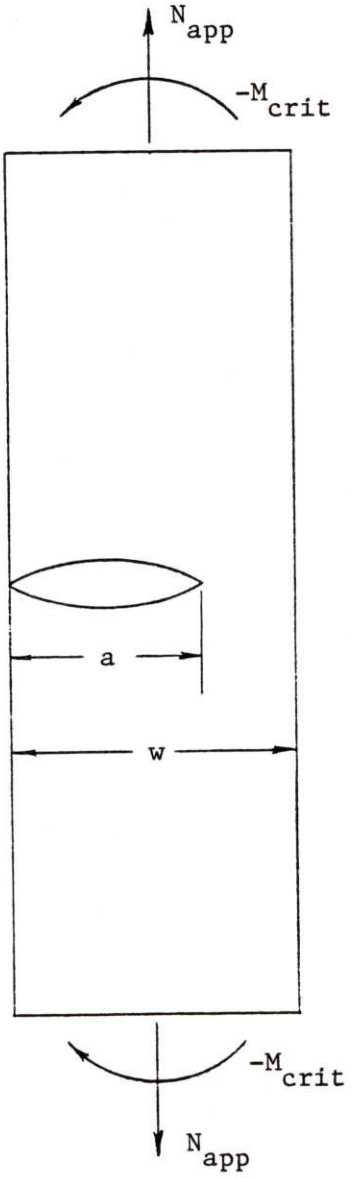

Figure 1.1-2

Onset of Closure for an Edge-Cracked Strip

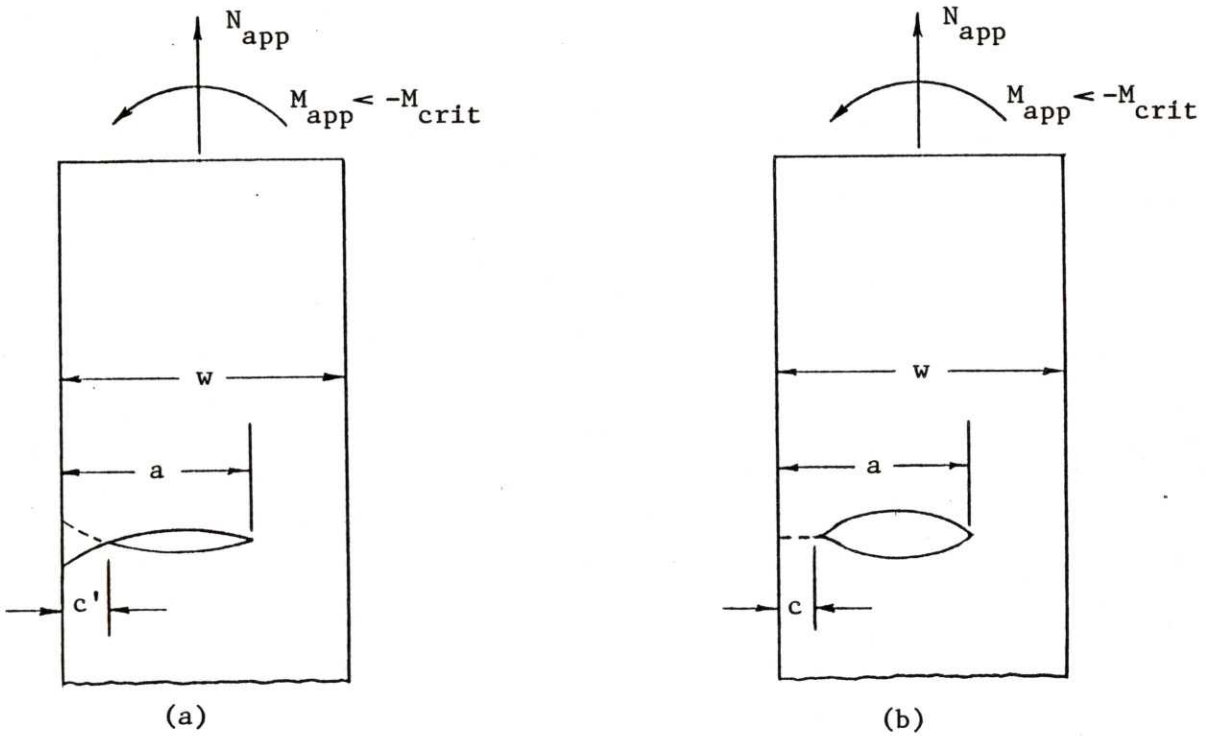

Figure 1.1-3

Partially-Closed Edge-Cracked Strip

(a) by Direct Superposition and (b) by Including Surface Interference

The effect of crack closure interface on the stress intensity factor can be deduced by considering the true configuration to be the superposition of the three loadings of Figure 1.1-4. The applied tensile membrane force, N_{app} causes a positive stress intensity factor, $+K_{IN}$ at the crack tip. The "closing" moment, M_{app} introduces what can effectively be considered a negative SIF contribution, $-K_{IM}$. The third component, the resultant pressure distribution, has associated with it a positive contribution, $+ K_{Ip}$. The ratio of the stress intensity factor allowing overlap (Figure 1.1-3(a)) to that for the true configuration (Figure 1.1-3(b)) is then

$$\frac{K_{I\ overlap}}{K_{I\ closure}} = \frac{K_{IN} - K_{IM}}{K_{IN} - K_{IM} + K_{Ip}}. \qquad (1.1\text{-}1)$$

As the sense of the K_I contributions have already been included, it can be seen that this ratio is always less than one for any non-zero closure length. Therefore, by neglecting the stiffening effects of the crack surface interference an unconservative estimate of the stress intensity factor is obtained. For pure bending the error has been evaluated by Bowie and Freese [12] to be 9% (within 1%) for a wide range of crack depth ratios, $\xi_a = a/w > 0.5$.

The effect of this underestimation on a fatigue life basis can be seen more clearly by considering the limiting case of pure cyclic bending (Figure 1.1-5). For fatigue life estimates it is necessary to know the range of the stress intensity factor and its mean value. As before, the SIF contribution due to

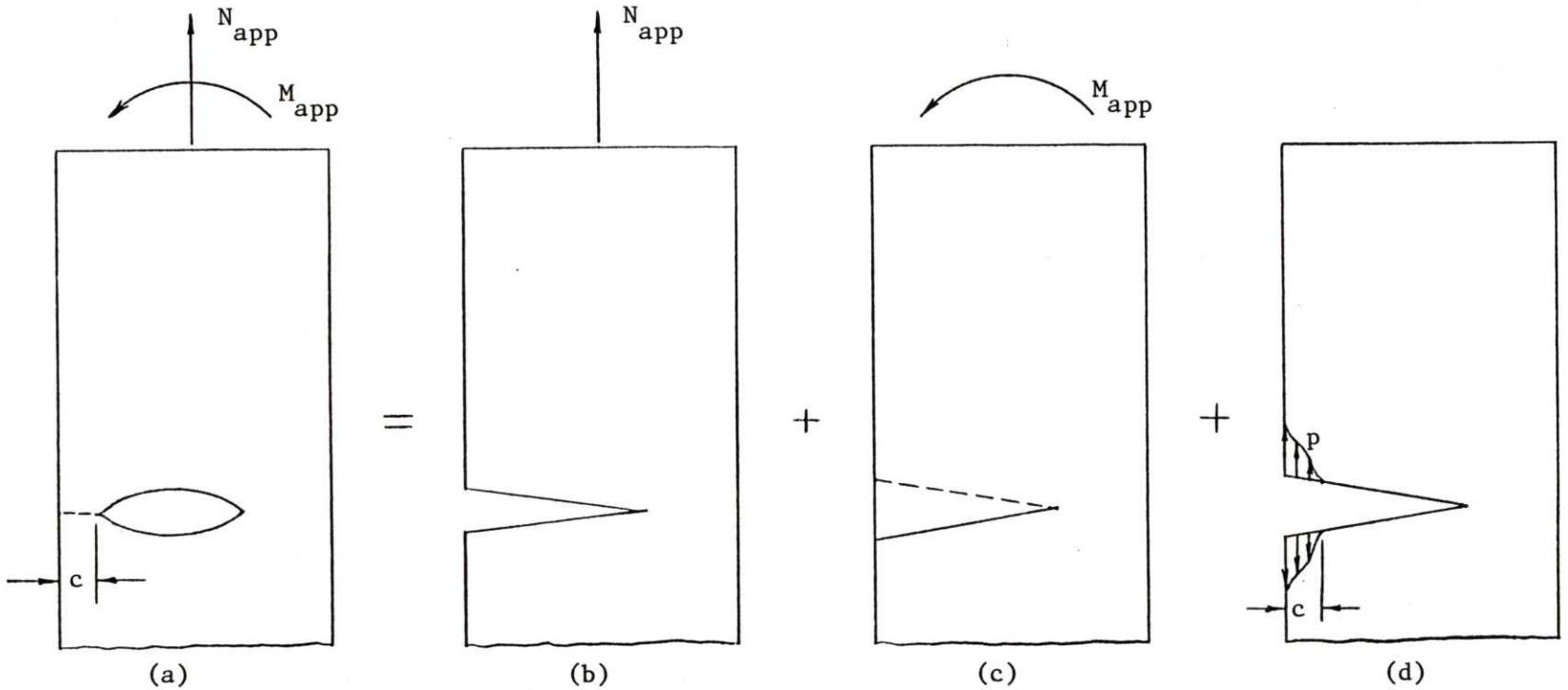

Figure 1.1-4

Superpositional Breakdown of a Partially-Closed Edge-Cracked Strip

(a) Equilibrium Configuration, (b) Membrane Force, (c) Reverse Bending and (d) Resultant Crack Surface Pressure Contributions

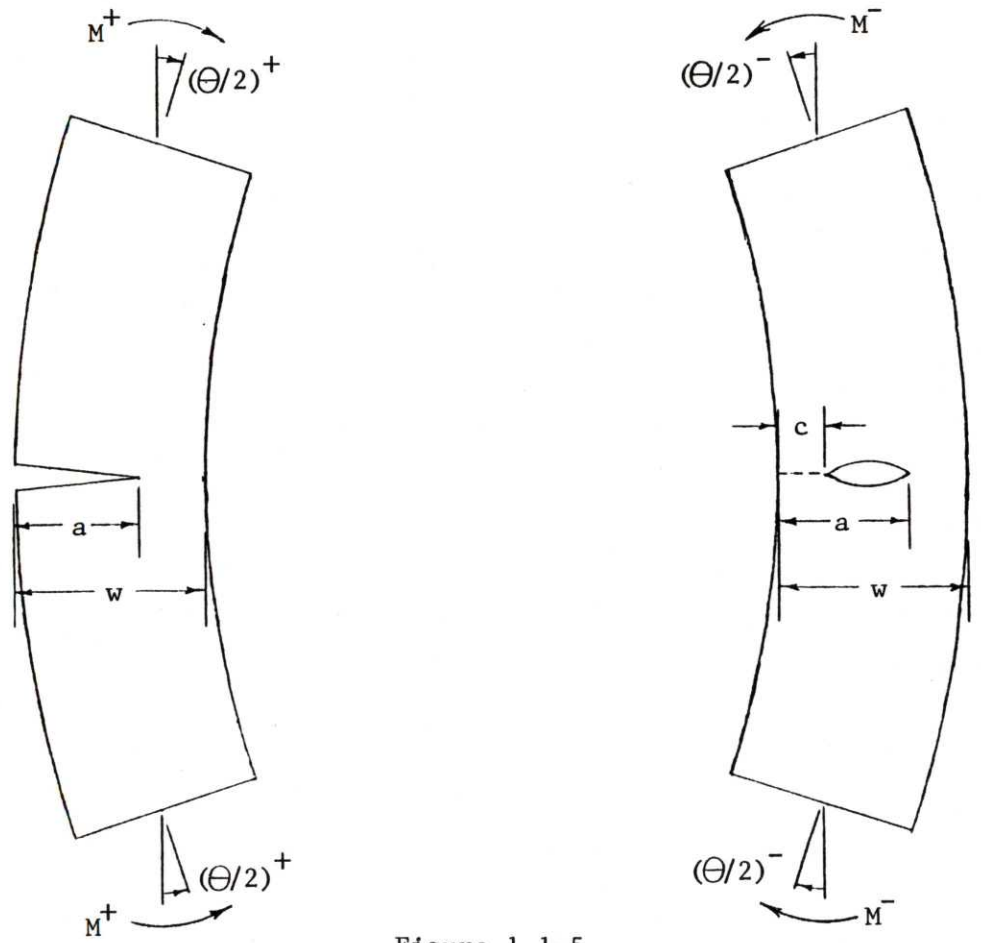

Figure 1.1-5

Pure Cyclic Reverse Bending of an Edge-Cracked Strip

the reversing moment is $\pm K_{IM}$ and for the pressure distribution, $+K_{Ip}$. By allowing overlap the range of the stress intensity factor is K_{IM} with a mean value of zero. By accounting for the crack surface contact the range of the SIF is $K_{I\ alt} = \pm (K_{IM} - \frac{1}{2}K_{Ip})$ with $K_{I\ mean} = +\frac{1}{2}K_{Ip}$. Therefore, the effect of the crack surface interference is to increase the mean applied stress intensity factor while decreasing its range.

1.2 Background

For fully three-dimensional crack configurations, partial closure has not been examined. The recent work of Mattheck et al [2,3] and Isida et al [22] is applicable only to the point at which closure begins. Theoretical and numerical examinations of two-dimensional crack configurations with partial closure date back to the late 1960's. Closed form solutions have been obtained for partially-closed Griffith cracks under a variety of loading conditions [9-11] and for the two-sided exterior crack [23]. Partial closure of edge-cracked strips subjected to pure reverse bending has been examined [12-15] with numerically calibrated relationships now available. To date partial closure of an edge-cracked strip subjected to combined tension and reverse bending has not been examined.

Burniston [9], Tweed [10] and Thresher and Smith [11] all, within a four year period, considered partial closure of a Griffith crack, albeit considering significantly different loading configurations and closure modes. Burniston applied the method of complex variables to the problem of a Griffith crack

subjected to biaxial tension, partially closed at its center by the application of concentrated forces at points located within the solid above and below the crack centerline. Using this approach closed form solutions were developed for the closure length and for the stress intensity factor. Tweed considered the Griffith crack loaded in biaxial tension and subjected to a symmetric system of body forces. Through application of a Fourier transform technique, formulae were derived for the crack opening displacement shape and the stress intensity factor. Finally, Thresher and Smith examined partial closure at one end of a Griffith crack subjected to an arbitrary polynomial loading function. By applying a potential formulation approach closed form solutions for the stress and displacement fields were developed as well as a criterion for determining the open length of the crack.

As far as partial closure of Griffith cracks are concerned, the work of Thresher and Smith appears to have the widest range of application. However, the work of Burniston has application in methods of crack (propagation) arrest.

Dundurs and Comninou [23] have considered the two-sided exterior crack configuration subjected to an arbitrary far-field load distribution. Using a formulation leading to singular integral equations, the possible closure regimes were defined in the "applied force / bending moment" plane and the resultant traction distribution in the neck was determined.

A fair amount of (non-closed form) analysis has been performed nearly simultaneously on partial closure of an edge-cracked strip under reversed bending. Bowie and Freese [12] considered the "overlapping" problem first for an arbitrary crack in a large plate subjected to bending. This solution was then modified and combined with numerical calculations to evaluate the closure characteristics and stress intensity factor of an internal crack in a finite width strip. At nearly the same time Paris and Tada [13] considered the effects of partial closure on the stress intensity factor of an edge-cracked strip subjected to load-controlled cyclic reversed bending. Empirical relations for the open (K^+) and closed (K^-) stress intensity factors were developed and the effect of closure on fatigue crack growth was discussed. Bowie and Freese [14] compared their previous work [12] to that of Paris and Tada [13] and noted some differences in stress intensity factor ratio (up to 20%) for deep cracks.[1] Gustafson [15] extended the work of Paris and Tada, evaluating the effects of partial closure on the stress intensity factor of an edge-cracked strip subjected to displacement-controlled cyclic reversed bending with some

---

1. The differences between the results of Paris and Tada [13] and those of Bowie and Freese [12] can be attributed at least in part to the fact that Paris and Tada actually considered a semi-infinite crack in an infinite plate subjected to reversed bending. A correction factor accounting for the finite width was applied; however, it was assumed to be equal to the tensile load correction factor for a center cracked finite width strip.

significantly different results. With reference to Figure 1.1-5, load-controlled cyclic bending is characterized by $M^+ = M^-$ and $\theta^+ \neq \theta^-$ while for deflection-controlled bending, $M^+ \neq M^-$ and $\theta^+ = \theta^-$.

In general the results and conclusions from past work on partial closure of an edge-cracked strip subjected to pure bending can be summarized as follows:

1. In analyzing partial closure of edge-cracked (finite width) strips some numerical computation is required (closed form solutions are not obtainable).
2. The classical solution for the stress intensity factor of an edge-cracked strip (allowing crack surface overlap) underestimates the SIF by 9-10% for a variety of crack depth ratios.
3. For load-controlled cyclic bending the SIF ratio is $K^-/K^+ = 5.4\%$ for crack depth ratios less than 0.8.
4. For deflection-controlled cyclic bending the SIF ratio can be significantly larger than for the load-controlled case; $K^-/K^+ = 6\%$ for crack depth ratio, $\zeta_a = 0.6$, $K^-/K^+ = 50\%$ for $\zeta_a = 0.80$. For deeper cracks, the SIF ratio increases further to $K^-/K^+ = 1.0$ for $\zeta_a = 0.88$ and rapidly to 4.5 for $\zeta_a = 0.95$.
5. For crack depth ratios less than 0.6 the effects of crack closure on fatigue crack growth is minimal. However, for deeper cracks under displacement-controlled bending the closure effects can be significant.

On the basis of the past work which has been performed on partial crack closure two major limitations become evident. First, the available solutions for pure reverse bending are valid only for crack depth ratios, $\xi_a \geq 0.5$. The reason is that for all smaller crack depths pure reverse bending causes full closure. Secondly, none of the available solutions for the edge-cracked strip combine the effects of tension loading and reverse bending. Even though the partially closed configuration (attributed to pure reverse bending) resembles an internally-cracked strip (for $\xi_a > 0.5$), the tensile stiffness of the closed portion of the crack is zero as is the stress intensity factor at the closed tip. Therefore, direct superposition of the stress intensity factor and related parameters from an internally-cracked strip in tension and an edge-cracked strip under pure reverse bending is not valid.

A final note is that the difference between the reverse stress intensity factors, K^- for load-controlled and deflection-controlled reverse bending [13 and 15] implies that the phenomenon of partial crack closure carries with it a significant stiffening effect. This appears to be especially true for deep cracks where the original total stiffness of the cracked specimen is very low relative to the uncracked stiffness. For a crack depth ratio of 0.8 there is an order of magnitude difference between the closed stress intensity factor, K^-, for deflection- and load-controlled cyclic bending. Combined with the increase in the effective uncracked ligament of the partially-closed case this necessitates a very large

M^-/M^+ for deflection-controlled cyclic reverse bending. These results indicate that K^- effects can have a significant influence on fatigue crack growth for sufficiently deep cracks subjected to deflection-controlled reverse bending (which, it should be noted, is more typical of thermal cycling).

2. LINE-SPRING MODEL WITH CLOSURE

Thus far the phenomenon of partial external closure of an edge-cracked strip has been discussed and past theoretical and numerical examinations have been summarized. With respect to the final objective, to incorporate partial closure capabilities into the line-spring model, the past work was not considered to contain sufficient definition over the entire range of crack depths to be conducive to the general nature of the finite element formulation. However, some of the past work can serve verification purposes.

The present approach is basically numerical, combining theoretical compliance relations with (polynomial interpolation of) discrete data from parametric two-dimensional finite element analyses. All required data are obtained from superposition of force and reverse bending solutions of an internally-cracked strip. The resulting finite element implementation introduces a nonlinear iterative (Newton-Raphson) scheme into the existing linear-elastic line-spring model. The resulting formulation allows for application of any combination of applied (mode I) loads and is capable of modeling all crack depth ratios through $\zeta_a = 0.8$.

The approach will be described in depth in the following sections beginning with an overview of the linear-elastic line-spring model formulation.

2.1 Linear-Elastic Line-Spring Model

The line-spring model of Rice and Levy [4] was introduced in 1972 and was originally used to estimate stress

intensity factors for part-through surface cracks in plates and shells subjected to membrane and bending loading. Further development of the line-spring concept by Parks et al [5-8,16] has extended its range of application to encompass linear-elastic and elastic-plastic configurations. Finite element implementation of the linear-elastic line-spring has been completed by Parks, Lockett and Brockenbrough [5] with plasticity capabilities incorporated by White [17].

In general, the existence of a crack in any structure decreases the overall stiffness of the structure. Herein lies one of the two basic features of the line-spring model; the introduction of an additional compliance into the cracked structure which, when combined with the compliance of the uncracked structure, fully characterizes the effects of the part-through surface crack. Consider the surface crack of length 2c' and variable thickness a(x) as shown in Figure 2.1-1(a). If the crack length is assumed to be much greater than the plate thickness then an idealized two-dimensional situation results in which the crack can be considered a one-dimensional crack of length 2c'. However, the traction-carrying capability of the uncracked ligament, w-a(x), must be retained. Therefore, in the line-spring model formulation, the part-through surface crack is replaced by a through crack of equal length with a generalized foundation between the crack faces as depicted in Figure 2.1-1(b). These generalized "line-springs" carry the membrane force, N, and bending moment, M, transmitted across the crack ligament.

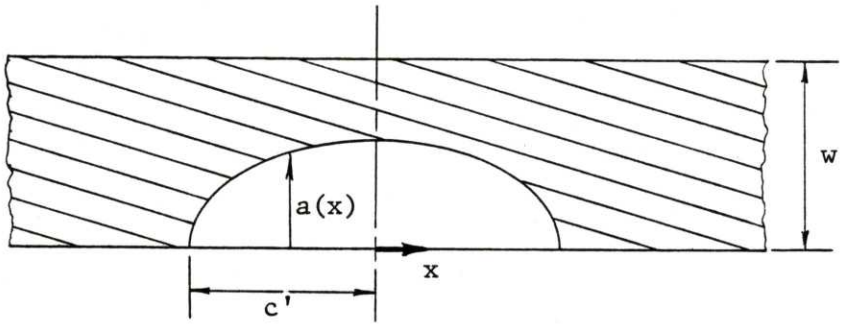

(a)

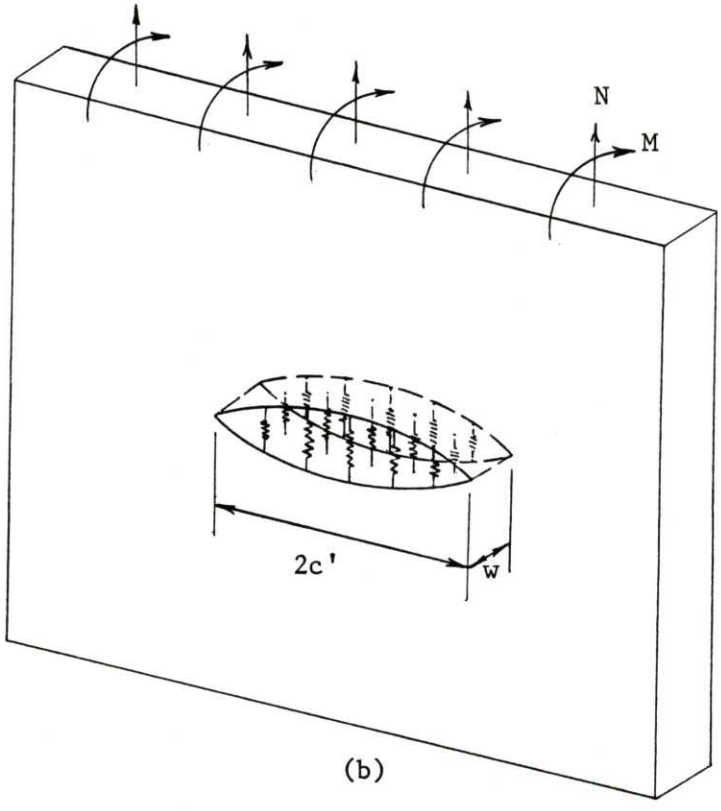

(b)

Figure 2.1-1

Line-Spring Representation of a
Part-Through Surface Crack

The stiffness of the line spring at any location x is related to the local uncracked ligament, w-a(x). With this information in hand, the general effects of the additional cracked compliance on the structure can be deduced. Consider the structure in the absence of a crack, a(x) = 0. In this case, there is no additional compliance. The tractions along the plane of the crack correspond to the far-field tractions and the displacements across the crack plane are zero. This corresponds to a zero displacement condition. Consider now a crack, a(x) = w, for which there is a (locally) infinite additional compliance. In this case the crack face tractions are zero and the displacements across the crack plane are discontinuous; a zero traction condition. For any crack depth profile, $0 < a(x) < w$ it can therefore be expected that the line-spring will result in a situation in between the zero traction and zero displacement conditions; i.e. some traction will be supported across the crack face and the displacements across the crack plane will be discontinuous.

As the stiffness of the line-spring model varies with crack depth it should be possible to examine the additional compliance introduced by the crack on a local basis. Herein lies the second basic feature of the line-spring model. Consider a section normal to both the plane of the shell and the plane of the crack at some location x. The resulting configuration reduces locally to that of an edge-cracked strip with crack depth "a" and loads "N" and "M" corresponding to

the local values: depth a(x) and loads, N(x) and M(x) transmitted across the cut (Figure 2.1-2).

All that now remains is to determine the local compliance of the cracked strip. To do this it is necessary to obtain a constitutive relation between the local (far-field) loads, N and M, and their local (far-field) work-conjugate displacements, δ and Θ. In general, this relation takes the form

$$\begin{bmatrix} \delta \\ \Theta \end{bmatrix} = \begin{bmatrix} C_{11t} & C_{12t} \\ C_{21t} & C_{22t} \end{bmatrix} \begin{bmatrix} N \\ M \end{bmatrix} = [C_t] \begin{bmatrix} N \\ M \end{bmatrix} \qquad (2.1\text{-}1)$$

where $[C_t]$ is the local total compliance matrix, related to the local total stiffness matrix by $[C_t] = [S_t]^{-1}$. The far-field displacements can be considered to consist of cracked and "no-cracked" contributions.

$$\begin{bmatrix} \delta \\ \Theta \end{bmatrix} = \begin{bmatrix} \delta_{nc} \\ \Theta_{nc} \end{bmatrix} + \begin{bmatrix} \delta_c \\ \Theta_c \end{bmatrix} \qquad (2.1\text{-}2)$$

The no-crack contribution is obtained from mechanics to be

$$\begin{bmatrix} \delta_{nc} \\ \Theta_{nc} \end{bmatrix} = \begin{bmatrix} 2l/E'w & 0 \\ 0 & 24l/E'w^3 \end{bmatrix} \begin{bmatrix} N \\ M \end{bmatrix} \qquad (2.1\text{-}3)$$

where E' is the plane strain modulus. The cracked displacements are a measure of the additional compliance introduced into the strip by the presence of the crack. Combining equations (2.1-1) through (2.1-3) gives

$$\begin{bmatrix} \delta_c \\ \Theta_c \end{bmatrix} = \begin{bmatrix} C_{11} & C_{12} \\ C_{21} & C_{22} \end{bmatrix} \begin{bmatrix} N \\ M \end{bmatrix} = [C] \begin{bmatrix} N \\ M \end{bmatrix} \qquad (2.1\text{-}4)$$

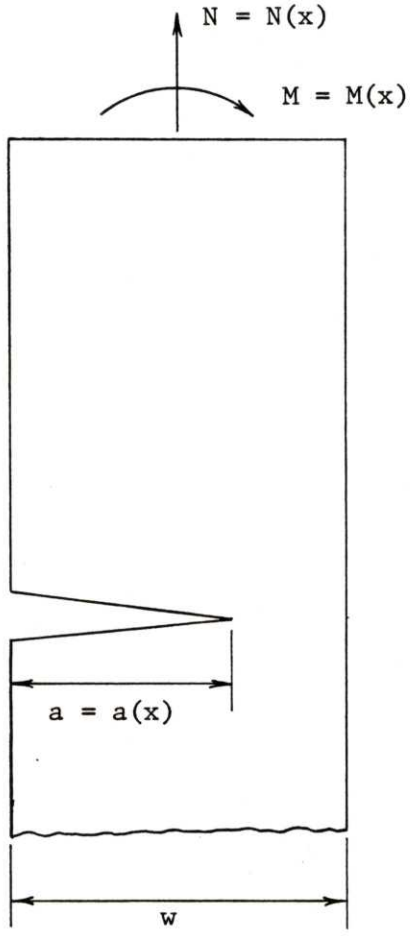

Figure 2.1-2

Cross-Section of a Part-Through Surface Crack at Location "x"
Resembling a Single Edge-Cracked Strip

where [C] is the local cracked compliance matrix. Note that these displacements are assumed to occur directly on the line of the crack and therefore represent discontinuities across the cut. From Rice's early work [18] the local compliances can be obtained from

$$\begin{aligned} C_{11} &= 2\pi\gamma'_{11}/E' \\ C_{12} &= C_{21} = 12\pi\gamma'_{12}/E'w \\ C_{22} &= 72\pi\gamma'_{22}/E'w^2 \end{aligned} \qquad (2.1\text{-}5)$$

$$\text{where} \quad \gamma'_{ij} = \int_0^{\xi_a} \bar{\xi} F_i(\bar{\xi}) F_j(\bar{\xi}) d\bar{\xi} \ . \qquad (2.1\text{-}6)$$

The functions F_1 and F_2 are K_I calibration factors from the single edge notched specimen:

$$K_I = (\pi a)^{\frac{1}{2}} [F_1(a/w)\ N/w + F_2(a/w)\ 6M/w^2] \ . \qquad (2.1\text{-}7)$$

The compliance aspects of the elastic line-spring model are now complete. The line-springs as defined by the above equations can now be distributed across a through crack representation of a surface cracked structure. The resulting equations can then be solved to obtain the displacement and generalized force solution across the crack. As a final step the local stress intensity factor can be estimated directly from equation (2.1-7).

2.2 Definition of Governing Parameters

Before proceeding with any analysis the parameters which govern the problem of edge cracks with partial closure must be ascertained and combined into appropriate dimensionless forms. The governing parameters can be obtained fairly directly from the geometric and the kinematic properties of the system. Geometrically the specimen thickness (w) and crack depth (a) are obvious choices (Figure 1.1-3(b)). The length dimension (l) from the crack plane to the "far-field" can be removed from consideration by assuring sufficiently large l/w (from Parmerter [19] et al, the far-field effects are minimal for $l/w \geq 2$). As partial closure of the crack is of interest the final geometric parameter is the closure length (c). For the kinematic parameters the only choices available are the far-field membrane force (N) and bending moment (M).

In dimensionless form the governing parameters are defined by

$\zeta_a = a/w$ - crack depth (ratio)

$\zeta_c = c/w$ - closure length (ratio)

$\bar{\lambda} = Nw/M$ - load ratio

Notice that the definition of the closure ratio limits the range of attainable values[1] to $0 \leq \zeta_c \leq \zeta_a$.

---

1. The choice of ζ_c relative to crack depth (a) rather than to thickness (w) is an alternative which gives a range of 0 to 1; however, in this way, to visualize the actual closure length the local crack depth must also be considered. The definition given above avoids this complication.

As was discussed earlier there are two possible closure modes, internal and external. Only the external closure mode is being examined here (internal closure is discussed in Appendix I). For the external closure mode a closing moment is required. As discussed in Section 1.1 the bending moment must therefore be negative relative to the crack face definition (i.e., a positive moment opens the crack). The membrane force can be tensile or compressive[1] so the range of the load ratio is $-\infty = \bar{\lambda} = +\infty$.

2.3 Limits of Closure

There are two critical situations between which the evaluation of partial closure is possible: the condition at which closure begins and the condition at which the crack is fully closed.

In general, the onset of closure can technically be defined as the point at which the stress intensity factor at, in general, either crack tip is zero (cusp). For any partially-closed cracked specimen the leading edge of the closure will always be defined by a cusp. Using logical reasoning this can be proven as follows:

Consider a crack tip formed by the closure of two crack

---

1. It will be shown that for full closure of cracks with $\xi_a > 0.5$ the force N must be compressive.

surfaces with an assumed $K_I > 0$. Locally the positive SIF indicates that a positive stress singularity exists at the crack tip. However, the two surfaces are independent and cannot support tensile load, therefore, the surfaces must separate (and the closure length will decrease). Consider now the opposite case with $K_I < 0$. On a local scale this implies an overlapping displacement field. As this cannot occur, the surface will separate and the closure length will increase. With respect to these two considerations the only closure length for which equilibrium is satisfied is that for which the stress intensity factor is zero. This deductive reasoning agrees with the findings of Thresher and Smith [11], who developed the further requirement that the slope of the crack opening profile also be zero at the cusp. Applying this reasoning to the edge-cracked specimen, the two critical situations mentioned above can be further defined as:

- Onset of Closure - outer edge of the crack surfaces (crack mouth) just contact (with zero load)
- Full Closure - K_I at each end of the crack is zero and its length is zero ($\xi_c = \xi_a$).

Before beginning the finite element analysis of the edge-cracked strip some preliminary calculations will be performed to define the load range over which partial closure applies as well as to serve as verification for the later modeling results.

Onset of Closure

Consider the condition where the crack is fully open and loaded as shown in Figure 2.3-1(a). By superposition the crack mouth opening displacement (CMOD) can be written as

$$CMOD = Nd_N + Md_M = 0. \tag{2.3-1}$$

With reference to Tada, Paris and Irwin [20]

$$d_N = \frac{4\,\xi_a}{E'}\left(\frac{1.46 + 3.42\,(1-\cos\phi)}{\cos^2\phi}\right)$$

and (2.3-2)

$$d_M = \frac{24\,\xi_a}{E'w}\left(0.8 - 1.7\,\xi_a + 2.4\,\xi_a^2 + \frac{0.66}{(1-\xi_a)^2}\right)$$

where $\phi = \pi\xi_a/2$. From the definition of the onset of closure, CMOD = 0, the critical load ratio becomes

$$\bar{\lambda}_{crit} = -6\cos^2\phi\left(\frac{0.8-1.7\xi_a+2.4\xi_a^2+0.66/(1-\xi_a)^2}{1.46+3.42(1-\cos\phi)}\right). \tag{2.3-3}$$

The critical load ratios given by this equation are presented in Table 2.3-1 for crack depth ratios $\xi_a \leq 0.80$. Notice that for all crack depths the critical load ratio is $\bar{\lambda}_{crit} < 0$. From the discussions in Chapter 1 and Appendix I, external closure occurs only for negative (closing) bending moments. Therefore, a tensile force and a closing moment are required for the onset of external closure.

Center-Cracked Strip

Consider the center-cracked strip as shown in Figure 2.3-1(b). In relation to the edge-cracked strip with partial closure this corresponds to a crack depth ξ_a with closure

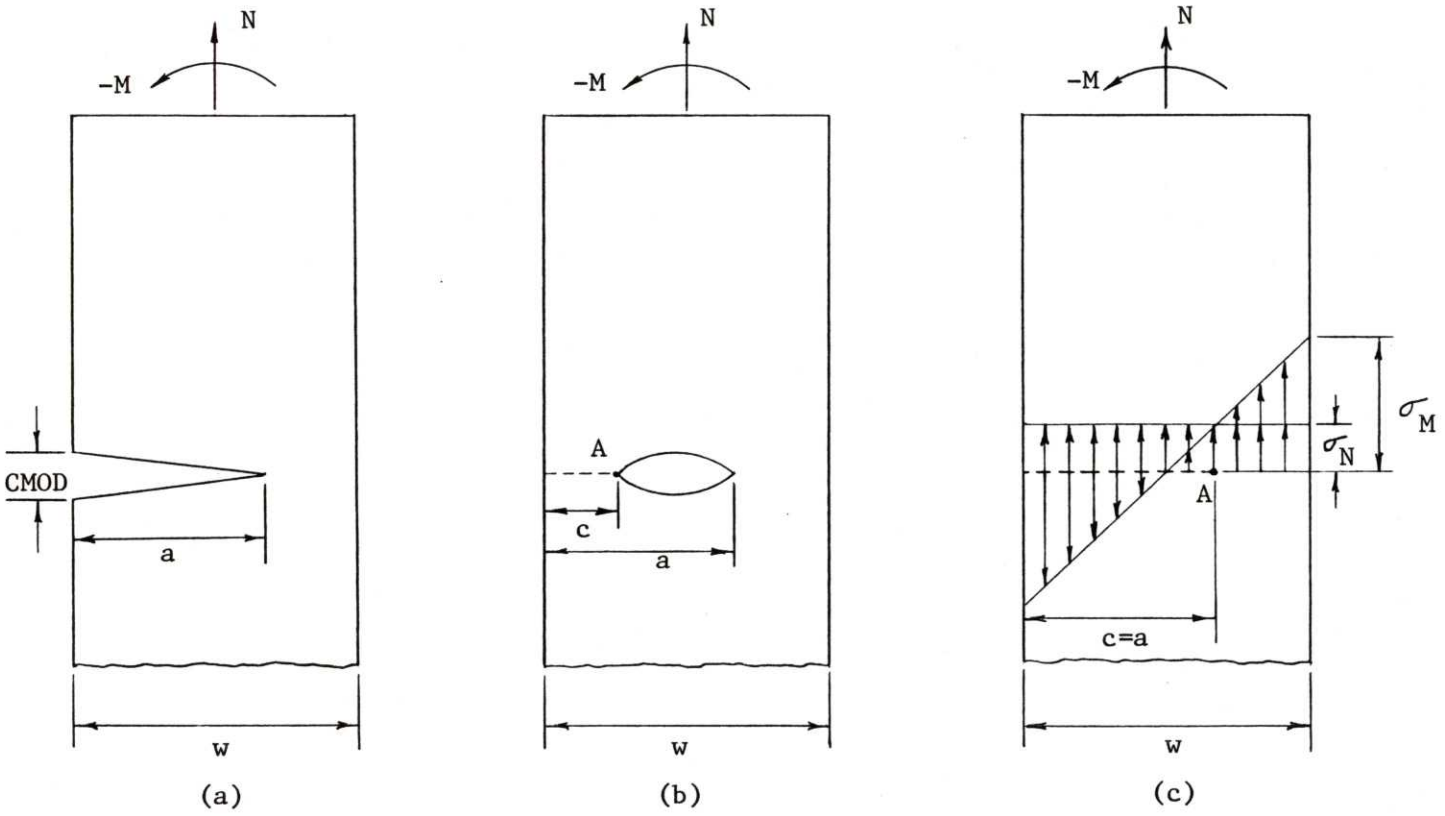

Figure 2.3-1

Partial Closure States for Which Theoretical Solutions Can Be Obtained (a) Fully Open Crack to Define the Onset, (b) Symmetrical Crack with K_I=0 at A, and c=w-a, and (c) Fully Closed with K_I=0 at A.

TABLE 2.3-1

THEORETICAL LOAD RATIO FOR SPECIFIC CLOSURE AMOUNTS

CRACK DEPTH (a/w)	LOAD RADIO		
	ONSET $\bar{\lambda}_{crit}$	SYMMETRIC $\bar{\lambda}_{symm}$	FULL $\bar{\lambda}_{cf}$
0.0	-6.0000	----	-6.0000
0.10	-5.7241	----	-4.8000
0.20	-5.2938	----	-3.6000
0.30	-4.8170	----	-2.4000
0.40	-4.3440	----	-1.2000
0.50	-3.8880	0.0	0.0
0.60	-3.4447	-0.5860	1.2000
0.70	-3.0175	-1.1004	2.4000
0.80	-2.6192	-1.5040	3.6000

length $\xi_c = 1 - \xi_a$. In this instance the closure length is defined by a cusp ($K_I = 0$) at point A. From superposition the stress intensity factor is then

$$K_I = Nk'_N + Mk'_M = 0 \ . \tag{2.3-4}$$

From Tada et al [20]

$$k'_N = \frac{\sqrt{\pi a'}}{2w'} F(\xi_a', 1/w' \sim \infty)$$

and (2.3-5)

$$k'_M = \frac{3\sqrt{\pi a'}}{2(w')^2} \frac{\sqrt{1-\xi_a'}}{(1-\xi_a'^3)} \xi_a' G(\xi_a')$$

where $w' = w/2$ and a' is the half length of the symmetrical crack. In these equations the function F is known in graphical form and G is an empirical relation. Combining equations (2.3-4) and (2.3-5) then gives the load ratio for the symmetric case

$$\bar{\lambda}_{symm} = \frac{6 \xi_a' G(\xi_a') \sqrt{1-\xi_a'}}{F(\xi_a', 1/w' \sim \infty)(1-\xi_a'^3)} . \tag{2.3-6}$$

Using the relations between ξ_a', ξ_c and ξ_a

$$\xi_a = \tfrac{1}{2}(\xi_a' + 1) \tag{2.3-7}$$

$$\xi_c = \tfrac{1}{2}(1 - \xi_a')$$

it can be seen that equation (2.3-6) applies only for $\xi_a \geq 0.5$ ($\xi_a' \geq 0.0$). The $\bar{\lambda}_{symm}$ is evaluated in Table 2.3-1.

Full Closure

The upper limit of the range of applicability of partial closure is that pertaining to full closure. Notice that once full closure has occurred the additional cracked compliance is zero

so an increase in the magnitude of the closing moment has no effect on the closure characteristics and the problem becomes linear. Upon decreasing the closing moment (or increasing the tensile load) a state of partial closure may again result. Full closure implies an effective crack length of zero and a stress intensity factor of zero at the "crack tip". This situation is demonstrated in Figure 2.3-1(c). At the "crack tip", A, the stress contributions are

$$\sigma_N = N/w$$

and (2.3-8)

$$\sigma_M = 6M\,(2\,\xi_a - 1)/w^2 \ .$$

For the stress intensity factor to be zero at the crack tip the net stress must also be zero so the critical load ratio for full closure is then

$$\bar{\lambda}_{fc} = 6(2\,\xi_a - 1) \ . \qquad (2.3\text{-}9)$$

This equation is also evaluated in Table 2.3-1. Notice that for crack depth ratios $\xi_a > 0.5$, $\bar{\lambda}_{fc}$ is positive. Therefore, since the moment is negative, a compressive force is required for full closure to occur.

2.4 Development of NonLinear Tangent Compliance Matrix

The final objective in the development of the line-spring model is the formulation of the corresponding compliance matrix. For the linear-elastic case, the compliance matrix is linear; dependent only upon the crack geometry as indicated by equations (2.1-5) and (2.1-6). The introduction of partial closure capabilities results in a nonlinear compliance matrix

which is dependent not only upon the crack geometry but also upon the crack closure length; which, in turn, is dependent on both the crack geometry and the applied loads. In these nonlinear situations it is far more convenient to formulate the local or tangent compliance matrix.

In the preceding section superposition of the membrane force and bending moment contribution of stress, crack mouth opening displacement and stress intensity factor was used to evaluate the load ratio at which specific closure "limits" would occur. Using the same approach the cracked displacements are

$$\begin{aligned} E' \delta_c &= N \delta_N + (M/w) \delta_M \\ E' \Theta_c &= (N/w) \Theta_N + (M/w^2) \Theta_M \end{aligned} \qquad (2.4\text{-}1)$$

where $\delta_{N,M}$ and $\Theta_{N,M}$ are the cracked displacement contributions on a per unit load, per unit thickness basis and, in general, are functions $f(\xi_c(\bar{\lambda}, \xi_a), \xi_a)$. For a given and constant crack depth (throughout the remaining work the term ratio will be implied when used with "crack depth" and "closure length") the cracked displacement contributions are dependent on the closure length which itself is uniquely defined by the load ratio, Nw/M (i.e., for a given load ratio with $M < 0$ there is one and only one corresponding closure length). Equations (2.4-1) can then be rewritten as

$$\begin{aligned} E' \delta_c &= (M/w)(\bar{\lambda} \delta_N + \delta_M) = (M/w) \delta^M \\ E' \Theta_c &= (M/w^2)(\bar{\lambda} \Theta_N + \Theta_M) = (M/w^2) \Theta^M \end{aligned} \qquad (2.4\text{-}2)$$

where δ^M, Θ^M are the total cracked displacements per unit bending moment, per unit thickness. Notice that the direct

effects of the membrane force have been explicitly removed from equation (2.4-2) by introducing the load ratio.

The compliance matrix relates the applied loads to their work-conjugate displacements such that

$$[C] = \begin{bmatrix} C_{11} & C_{12} \\ C_{21} & C_{22} \end{bmatrix} = \begin{bmatrix} \partial\delta_c/\partial N & \partial\delta_c/\partial M \\ \partial\Theta_c/\partial N & \partial\Theta_c/\partial M \end{bmatrix}. \qquad (2.4\text{-}3)$$

Combining equations (2.4-2) and (2.4-3) gives the tangent compliance matrix coefficients as

$$\begin{aligned} C_{11} &= (M/E'w)\left(\frac{\partial\bar{\lambda}}{\partial N}\delta_N + \frac{\partial\delta_N}{\partial N}\bar{\lambda} + \frac{\partial\delta_M}{\partial N}\right) \\ C_{12} &= (1/E'w)\,\delta^M + (M/E'w)\left(\frac{\partial\bar{\lambda}}{\partial M}\delta_N + \frac{\partial\delta_N}{\partial M}\bar{\lambda} + \frac{\partial\delta_M}{\partial M}\right) \\ C_{21} &= (M/E'w^2)\left(\frac{\partial\bar{\lambda}}{\partial N}\Theta_N + \frac{\partial\Theta_N}{\partial N}\bar{\lambda} + \frac{\partial\Theta_M}{\partial N}\right) \\ C_{22} &= (1/E'w^2)\,\Theta^M + (M/E'w^2)\left(\frac{\partial\bar{\lambda}}{\partial M}\Theta_N + \frac{\partial\Theta_N}{\partial M}\bar{\lambda} + \frac{\partial\Theta_M}{\partial M}\right). \end{aligned} \qquad (2.4\text{-}4)$$

From the definition of the load ratio it can be seen that

$$\partial\bar{\lambda}/\partial N = \bar{\lambda}/N \quad ; \quad \partial\bar{\lambda}/\partial M = -\bar{\lambda}/M \quad . \qquad (2.4\text{-}5)$$

Using the relationship

$$\partial\delta_N/\partial N = (\partial\delta_N/\partial\xi_c)(\partial\xi_c/\partial\bar{\lambda})(\partial\bar{\lambda}/\partial N) \quad , \qquad (2.4\text{-}6)$$

with similar expressions for the remaining terms, and equations (2.4-5) the tangent compliance matrix coefficients can be reduced to:

$$\begin{aligned} C_{11} &= (\delta_N + \alpha(\delta^M)')/E' \\ C_{12} &= (\delta_M - \alpha\bar{\lambda}(\delta^M)')/E'w \\ C_{21} &= (\Theta_N + \alpha(\Theta^M)')/E'w \\ C_{22} &= (\Theta_M - \alpha\bar{\lambda}(\Theta^M)')/E'w^2 \end{aligned} \qquad (2.4\text{-}7)$$

where the "prime" on the displacements δ^M and Θ^M represents differentiation with respect to closure length and $\alpha = \partial \xi_c / \partial \bar{\lambda}$.

At this point the formulation of the tangent compliance matrix is complete. What now remains is to determine the necessary functions; δ_N, δ_M, Θ_N, Θ_M, ξ_c such that the coefficients of equation (2.4-7) can be evaluated in terms of $\bar{\lambda}$ and ξ_a.

3. PARAMETRIC FINITE ELEMENT ANALYSIS

The data required to evaluate the tangent compliance matrix is obtained from a parametric finite element analyses of an edge-cracked strip and an internally-cracked strip. The discrete parametric results are then combined to satisfy the necessary conditions to define closure. This combination of discrete data then results in the parameters needed to evaluate the compliance matrix.

3.1 Model Description

The parametric analysis was performed using the ABAQUS © finite element program. The two-dimensional model of the cracked strip is presented in Figure 3.1-1. The model consists of 200 8-node biquadratic plane strain elements, CPE8 [21] with mesh refinement biased toward the crack plane. There are two active degrees of freedom per node (in-plane translation) and full 3 x 3 Gaussian integration was used.

Due to symmetry across the crack plane only one-half of the strip was modeled with a half-length to thickness ratio of 3:1 to the "far-field". For this l/w ratio, it is expected that interactions between the far-field and the crack will be negligible. To assure a unique evaluation of the far-field displacement and rotation the nodes along the top edge of the strip were required to remain in a straight line. Equation-defined connectors were used to relate the vertical displacement of each node to the center node (LP in Figure 3.1-2).

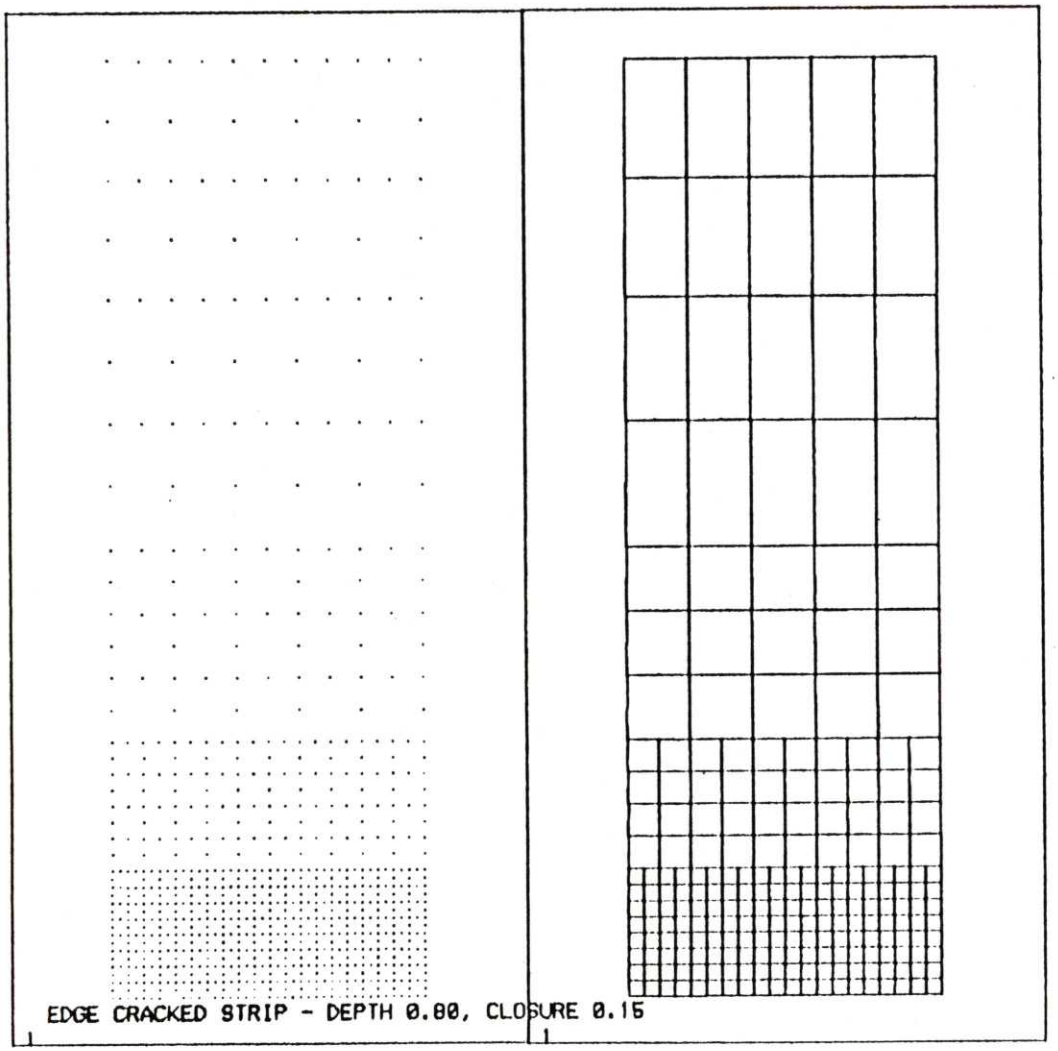

Figure 3.1-1

Finite Element Model of a Partially-Closed Edge-Cracked Strip
Used to Obtain Discrete Parametric Data

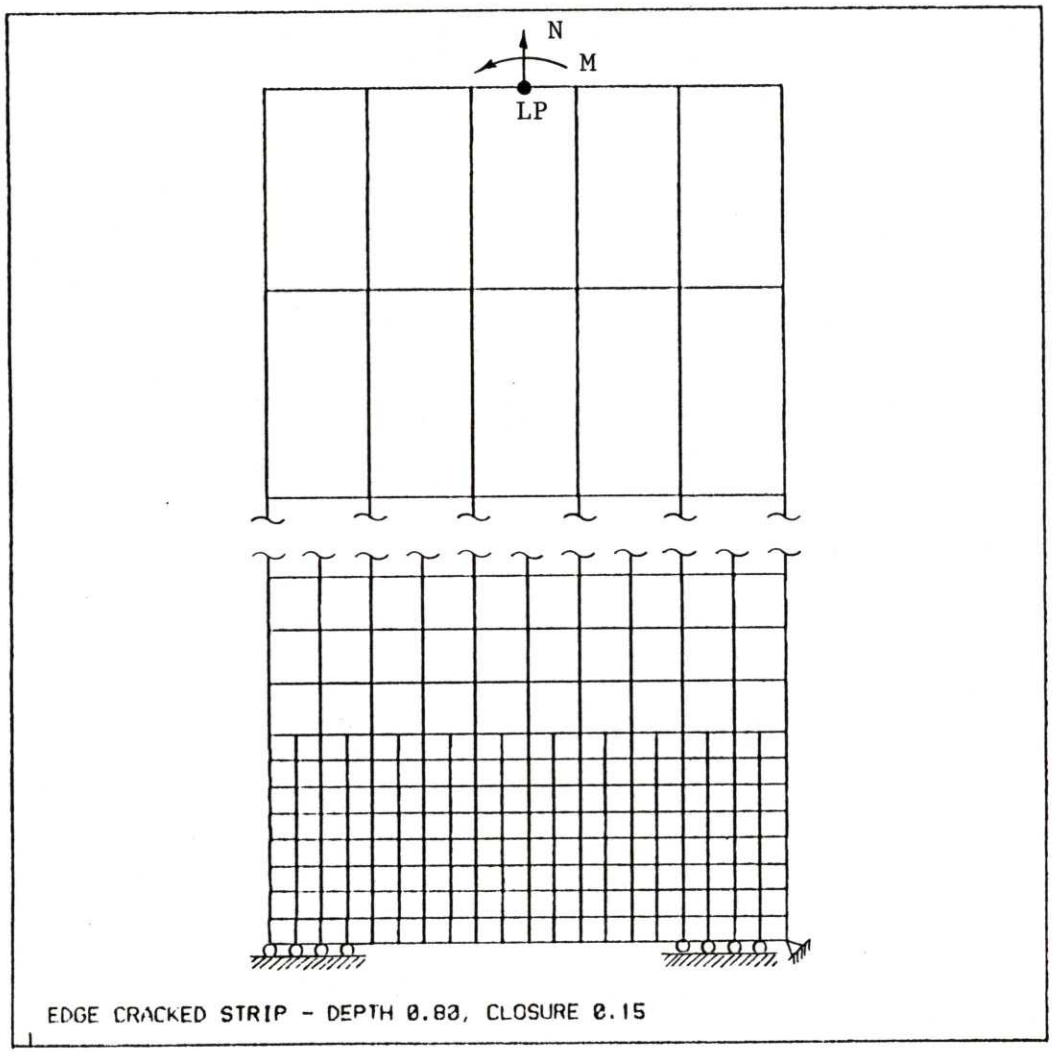

Figure 3.1-2

Boundary Conditions and Loading of the Partially-Closed Edge-Cracked Strip Model

A total of 20 uniformly sized elements were used along the plane of the crack. The crack depth was modeled by applying symmetry boundary conditions to those nodes corresponding to the remaining (uncracked) ligament. The closure length was modeled in the same way. In this way the model of the partially-closed edge-cracked strip more closely resembles an internally-cracked strip. However, by applying the far-field membrane force and bending moment independently, superposition can be used to assure that the required condition exists at the closed "crack tip" (i.e., a cusp is formed at the closed end with $K_I = 0$). The model as shown in Figure 3.1-2 represents a crack depth of 0.8 with a modeled closure length of 0.15.

J-integral estimation capabilities were applied at the crack tip node with up to 4 contour evaluations such that the effects of closure on crack tip stress intensity could be determined.

In obtaining the required data a crack depth (ratio) increment of 0.10 was used for depths up to 0.80. For each of these cases a closure length (ratio) from "fully open" to "fully closed" was examined in increments of 0.05. With the far-field force and moment applied independently, each pair of crack depth and closure length required two load steps to fully characterize the strip's behavior. A total of 144 steps were required to complete the entire behavior "matrix".

Each load step results in the evaluation of the following data

- total far-field displacements

- crack opening profile
- symmetry plane reaction forces (for the uncracked ligament and for the closed length)
- four J-integral estimations about the crack tip

which must be manipulated into a form more useful for evaluation of the tangent compliance matrix.

3.2 Evaluation of Load Ratio and Cracked Displacements

The first step in reducing the finite element results is to determine the closure length versus load ratio characteristics. This important step not only defines the range of loads over which partial closure applies but also serves as an initial comparison with accepted numerical solutions (see Section 2.3). The second step, to determine the characteristics of the cracked displacement contributions versus closure length, is required in conjunction with the first to numerically evaluate the tangent compliance matrix.

Before proceeding with the finite element data reduction several comments should be made:

1. The modeling of the cracked strip employed symmetry across the crack plane. The calculated far-field displacements therefore represent one-half of the actual work-conjugate displacements. The total work-conjugate displacements are used in the formulation of the tangent compliance matrix.
2. The calculated far-field displacements include contributions from both cracked and uncracked

cases. The cracked contributions are necessary for evaluation of the tangent compliance matrix and can be obtained as implied by equations (2.1-2) and (2.1-3).

3. All nodes along the open length of the crack deflect due to the application of the far-field loads. Under a tensile membrane force the opening profile corresponds to separation of the crack surfaces for all crack depths and closures. Under an "opening" bending moment, for sufficiently deep cracks ($\zeta_a >$ 0.5) the crack opening profile for some range of closure indicates that a portion of the open crack overlaps (Figure 3.2-1). Appropriate combination of the two loads is sufficient to eliminate this overlap.

4. The "closed" ligament will carry tractions under the application of the far-field membrane force and bending moment. Independently these tractions may be tensile, but after appropriately combining the loads the tractions must be compressive along the entire closure length. Physically the tractions occur continuously over the contact length. In the finite element formulation, however, the total traction is distributed among each node along the contact surface. Consider the schematic of an 8-node element as shown in Figure 3.2-2 with, for example, a lumped 1-4-1 nodal load distribution. The traction distribution shown in the figure becomes tensile near

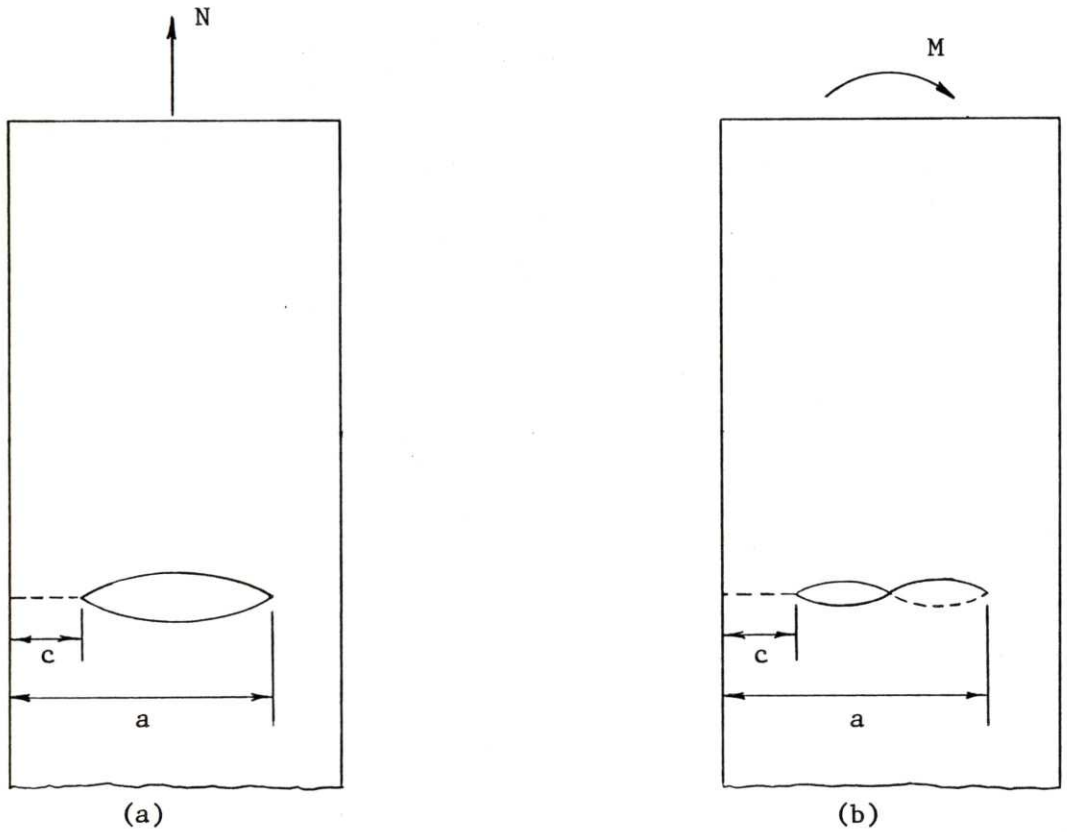

Figure 3.2-1

Crack Opening Profile of a Partially-Closed Edge-Cracked Strip due to (a) Membrane Force and (b) Bending Moment

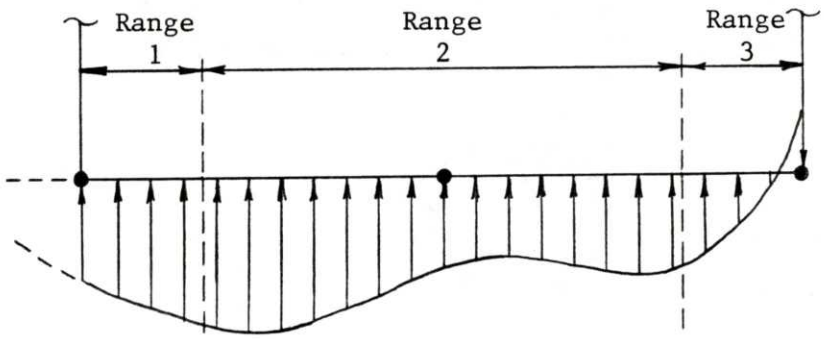

(a)

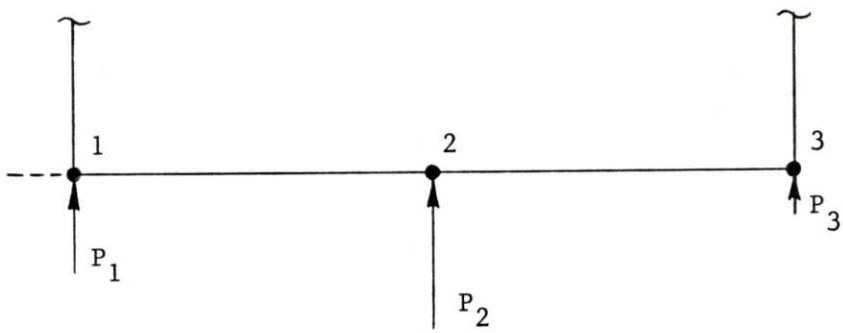

(b)

Figure 3.2-2

Possible Inconsistency Between Distributed Traction and Corresponding Nodal Distribution for an 8-Node Element (a) Continuous Distribution and (b) Discrete Nodal Distribution

node 3. In this situation the nodal load distribution results in a discrete compressive load at node 3. Therefore, the nodal tractions are not necessarily indicative of the actual continuous local traction distribution.

These comments will prove useful in the evaluation of the load ratio and the cracked displacement contributions.

In determining the load ratio corresponding to various closure lengths it is valuable to look more closely at the finite element model in the closed region. This is depicted in Figure 3.2-3 for a modeled closure length, $\zeta_{c,mod}$ at node i. The far-field tensile membrane force results in a reaction force, R_N at the closed tip (node i) and a separating displacement, COD_N at the first open crack node (node i+1). Similarly, the positive (opening) far-field bending moment introduces a reaction force, R_M and separating displacement, COD_M at the same nodes.

As was discussed in Section 2.3, the leading edge of closure is defined by a cusp (K_I=0). This also implies that the local reaction force (traction) is zero and that the crack surfaces are just in contact. Two methods of evaluating the load ratio now become evident; requiring a net zero reaction force at node i or requiring a net zero displacement at node i+1. From comment number 4 above, the former does not necessarily imply a cusp condition. Using the latter method as more suitable, the load ratio is determined to be

$$\bar{\lambda} = Nw/M = -COD_M/COD_N \ , \qquad (3.2\text{-}1)$$

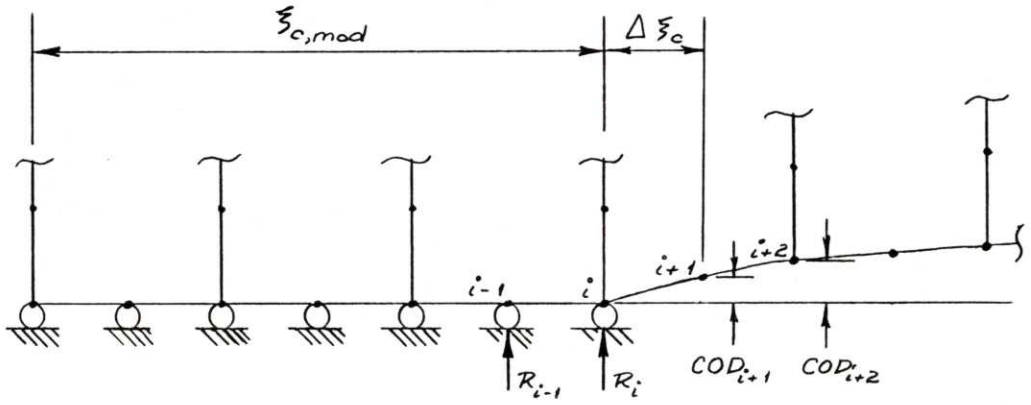

Figure 3.2-3

Finite Element Model in the Vicinity of the Modeled Closure Length

with a corresponding closure length of

$$\xi_c = \xi_{c,mod} + \Delta\xi_c \qquad (3.2\text{-}2)$$

where, $\Delta\xi_c = 0.025$ for the uniform finite element mesh used here. Equations (3.2-1) and (3.2-2) apply for all closure except for the onset. For this case

$$\bar{\lambda}_{crit} = -\,CMOD_M/CMOD_N \qquad (3.2\text{-}3)$$
$$\xi_c = 0.0^+$$

where CMOD is the crack mouth opening displacement for the fully open crack. The load ratios for the onset of closure and for symmetric closure are presented in Table 3.2-1 for all crack depths. The numerically accepted solutions from Table 2.3-1 are also included for comparative purposes. Over the entire range of crack depths the finite element analysis is seen to agree very well with the accepted numerical solutions. The closure length is plotted versus load ratio for all crack depths in Figure 3.2-4.

Several points can be made regarding the relationships between load ratio and closure length. For all crack depths the closure length asymptotically approaches the theoretical solution for full closure given by equation (2.3-9). As the theoretical solution is a straight line, the closure versus load ratio curves approach a constant slope at full closure. As a second point note that for crack depths greater than 0.5 a compressive membrane force is required for full closure to occur. This fact was noted earlier and is now verified by the finite element analysis.

TABLE 3.2-1

LOAD RATIO FOR ONSET OF CLOSURE AND SYMMETRIC CLOSURE

CRACK DEPTH (a/w)	LOAD RATIO (Nw/M) F.E.A	TABLE 2.3-1
Onset of Closure		
0.1	-5.647	-5.724
0.2	-5.247	-5.294
0.3	-4.811	-4.817
0.4	-4.353	-4.344
0.5	-3.892	-3.888
0.6	-3.446	-3.445
0.7	-3.032	-3.018
0.8	-2.655	-2.619
Symmetric Closure[1]		
0.6	-0.876 -0.437	-0.586
0.7	-1.366 -0.959	-1.100
0.8	-1.718 -1.355	-1.504

1. F.E.A. data for symmetric closure are calculated at ±0.025 from true symmetric closure length.

FIGURE 3.2-4
PARTIAL CRACK CLOSURE
CLOSURE LENGTH RATIO vs LOAD RATIO

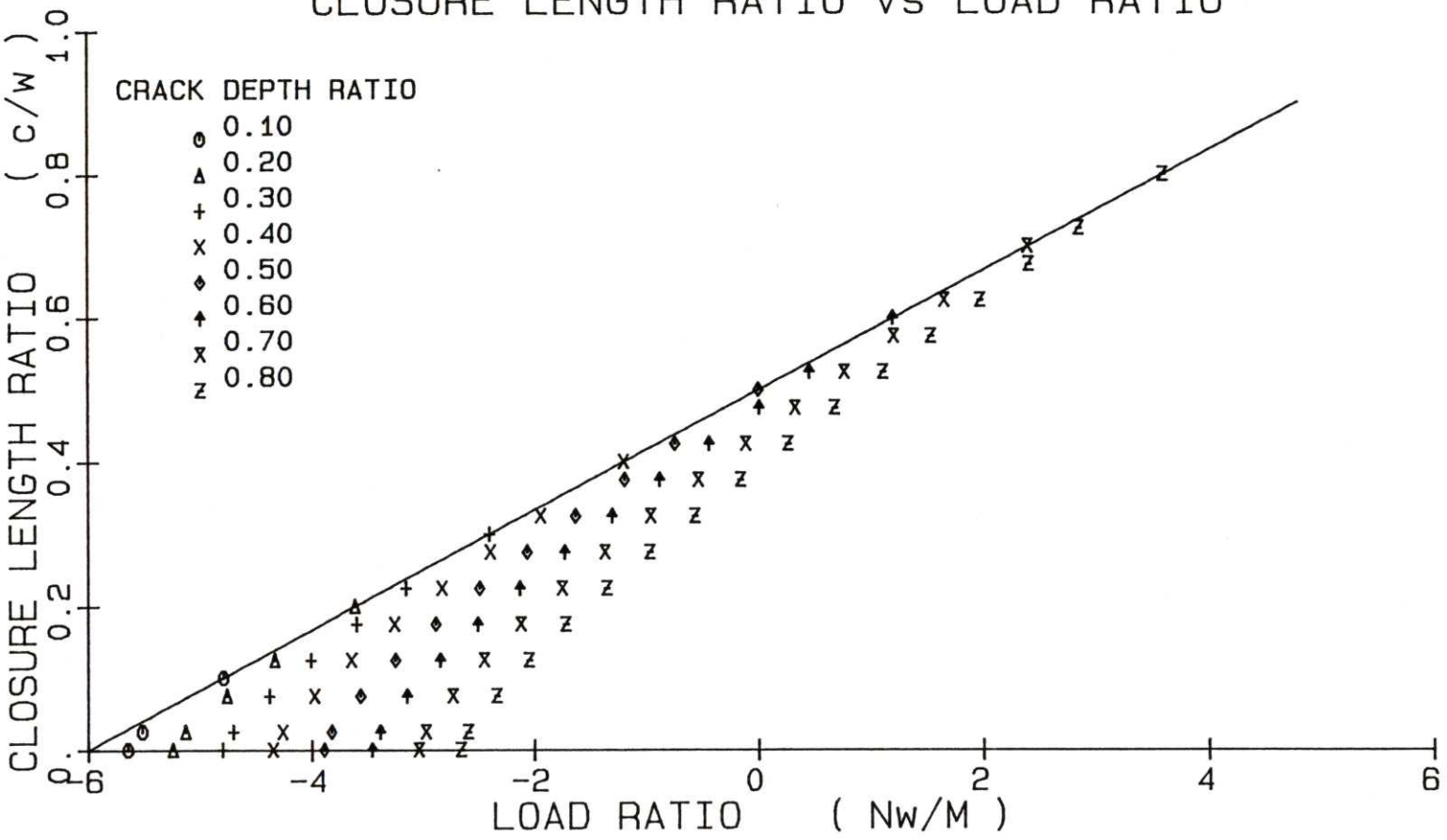

The cracked displacement contributions; δ_N, δ_M, Θ_N, Θ_M are obtained fairly directly from the finite element data by subtracting the uncracked far-field displacement contributions (equation 2.1-3) from the total calculated displacements. The resulting quantities (after appropriately accounting for the modulus of elasticity) are one-half of the actual work-conjugate displacements required for the tangent compliance matrix evaluation. The cracked displacement contributions are plotted against closure length in Figures 3.2-5 through 3.2-7. Again, several comments can be made regarding the figures. Because they are obtained under independent loads (force and moment not applied simultaneously), the displacement contributions actually correspond to the modeled closure lengths but are applied at the effective length defined by equation (3.2-2). Figure 3.2-6 presents the cracked displacement contribution due to a unit applied moment in the far-field (δ_M) and, because of reciprocity, it also represents the cracked rotation contribution due to a unit applied membrane force (Θ_N). Notice also that for symmetric modeled closure $\delta_M = \Theta_N = 0$ as is to be expected.

In the development of the tangent compliance matrix the total displacements per unit moment, δ^M and Θ^M were introduced. These terms combine the force and moment contributions corresponding to a given closure length (equation 2.4-2). These values are plotted versus closure length in Figures 3.2-8 and 3.2-9. In this case the values correspond to the actual closure lengths given by equation (3.2-2). The

FIGURE 3.2-5
PARTIAL CRACK CLOSURE
ONE-HALF CRACKED DISPLACEMENT (δ_N)
vs CLOSURE LENGTH RATIO

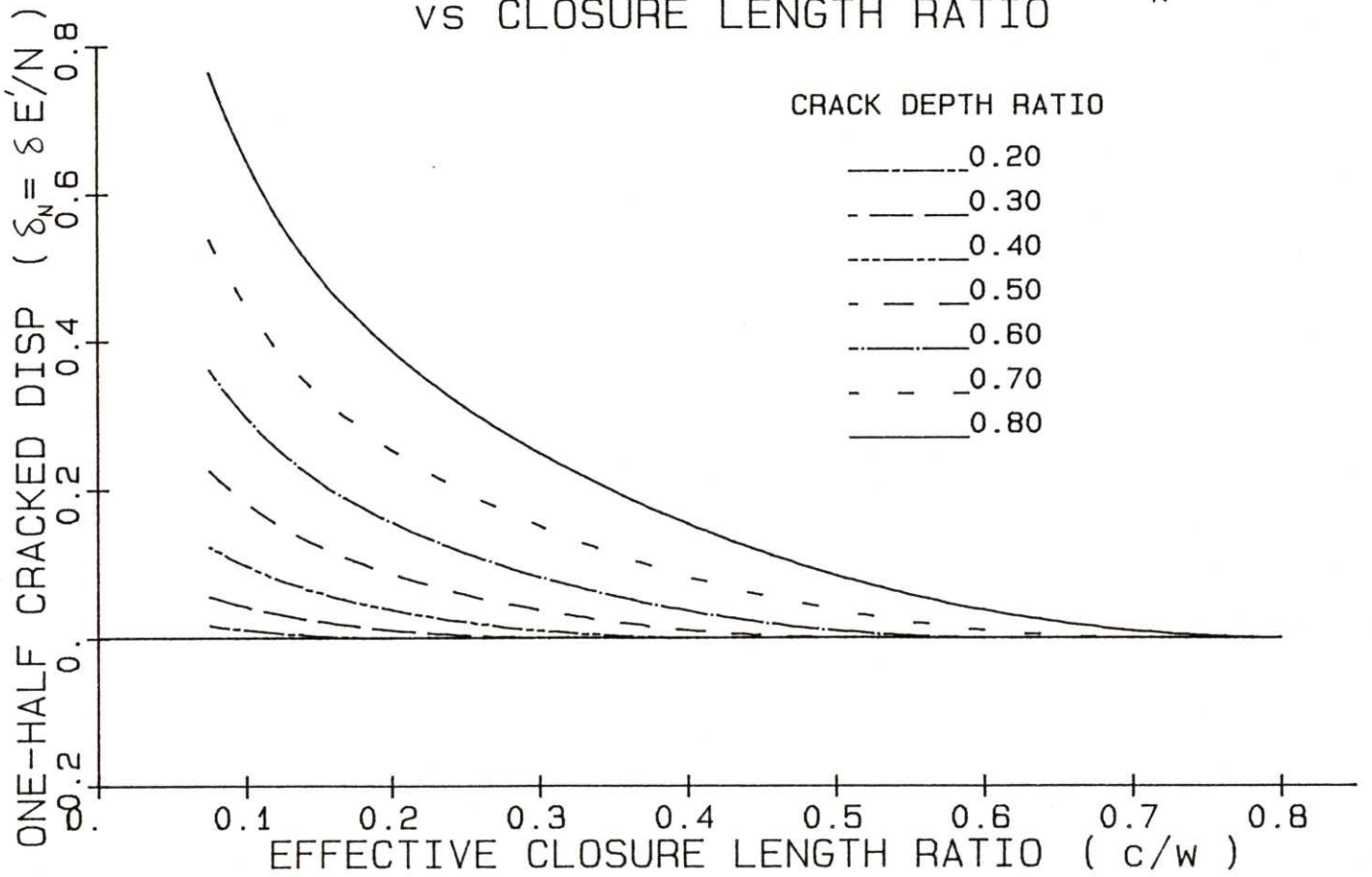

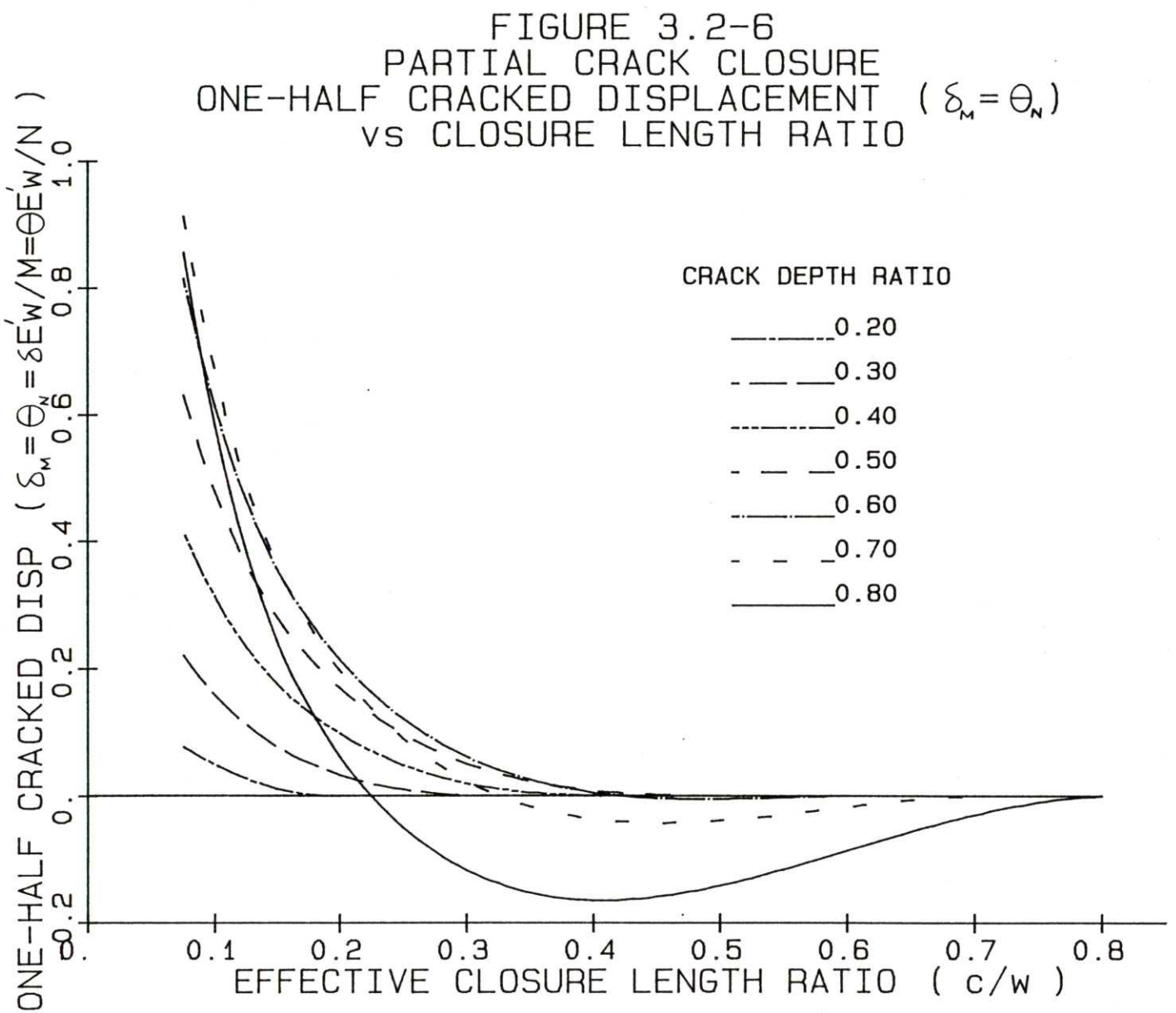
FIGURE 3.2-6
PARTIAL CRACK CLOSURE
ONE-HALF CRACKED DISPLACEMENT ($\delta_M = \Theta_N$)
vs CLOSURE LENGTH RATIO
CRACK DEPTH RATIO
0.20
0.30
0.40
0.50
0.60
0.70
0.80
ONE-HALF CRACKED DISP ($\delta_M = \Theta_N = \delta E'W/M = \Theta E'W/N$)
-0.2
0.
0.2
0.4
0.6
0.8
1.0
0.1
0.2
0.3
0.4
0.5
0.6
0.7
0.8
EFFECTIVE CLOSURE LENGTH RATIO (c/w)

FIGURE 3.2-7
PARTIAL CRACK CLOSURE
ONE-HALF CRACKED ROTATION (Θ_M)
vs CLOSURE LENGTH RATIO

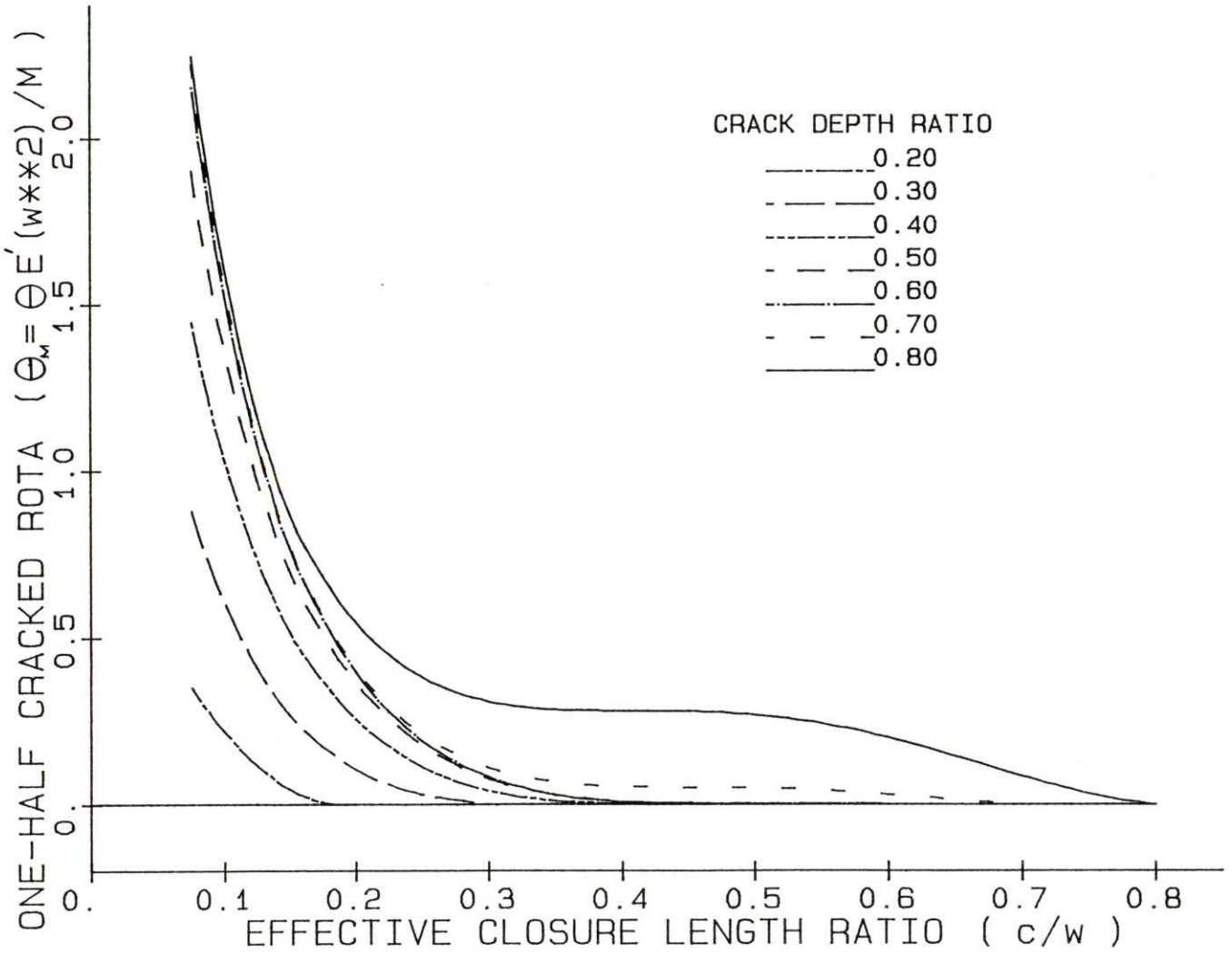

FIGURE 3.2-8
PARTIAL CRACK CLOSURE
ONE-HALF TOTAL CRACKED DISPLACMENT (δ^M)
vs CLOSURE LENGTH RATIO

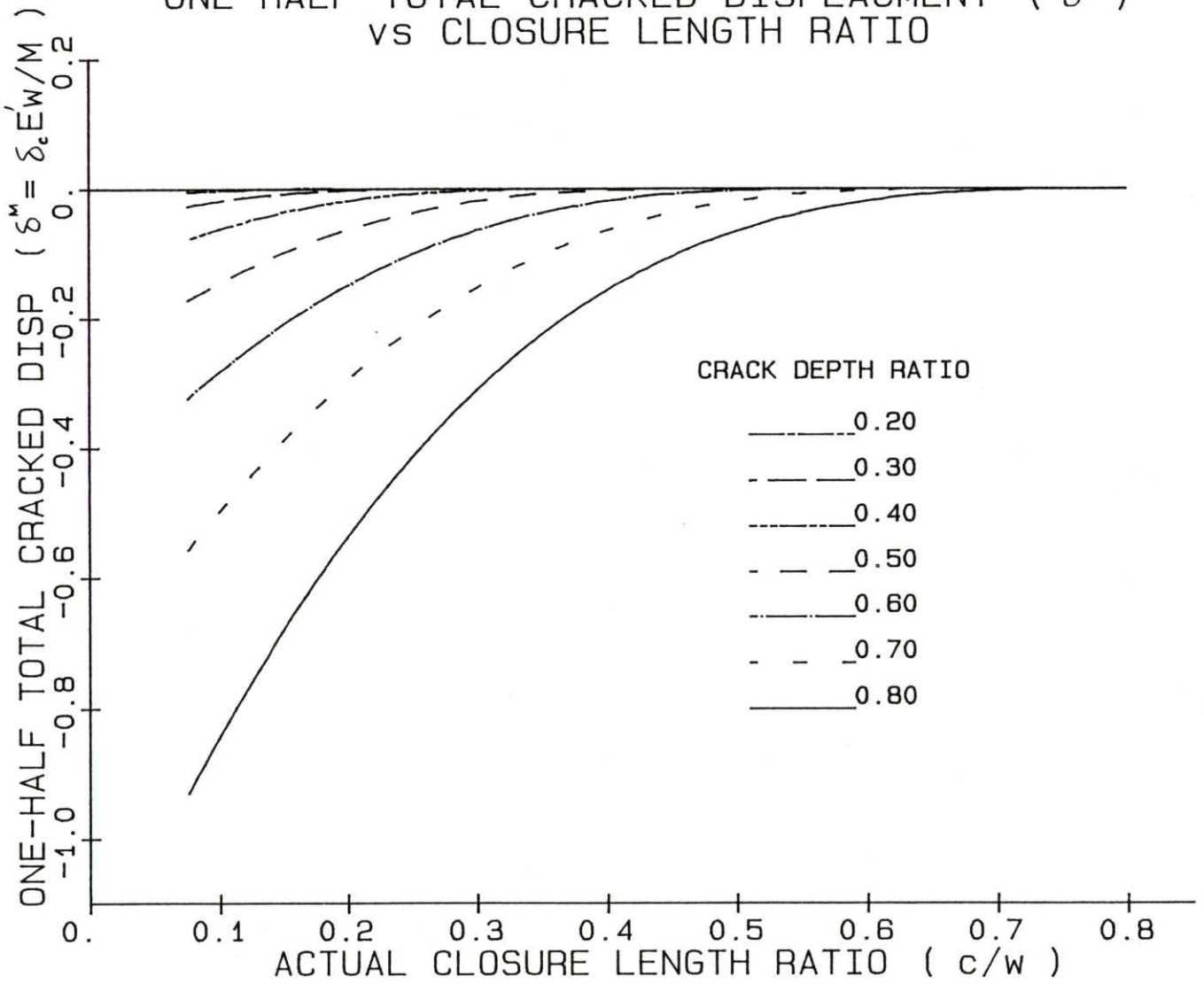

FIGURE 3.2-9
PARTIAL CRACK CLOSURE
ONE-HALF TOTAL CRACKED ROTATION (Θ^M)
vs CLOSURE LENGTH RATIO

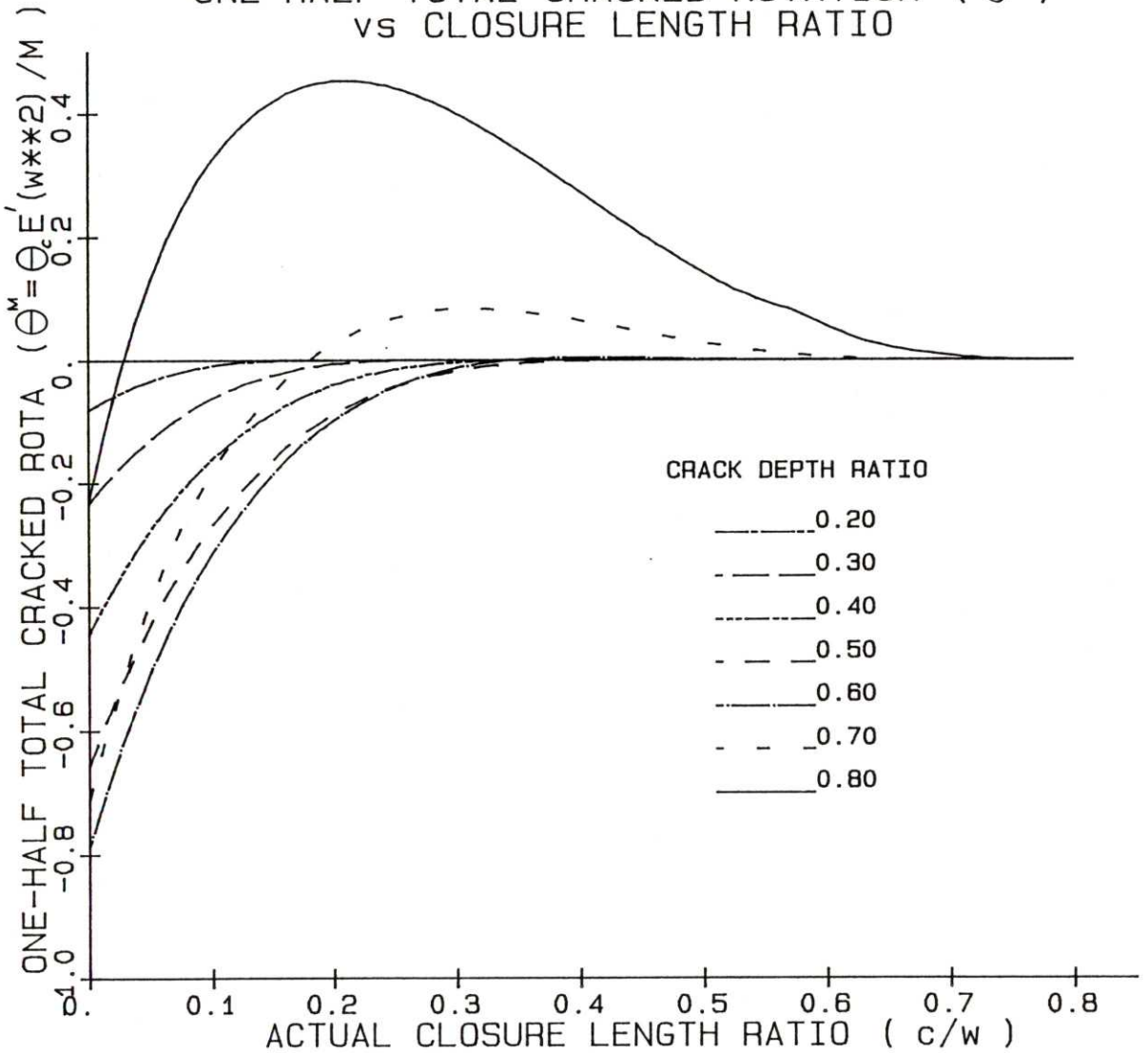

terms "effective" and "actual" closure length are discussed in more detail in Appendix II.

In all of the figures several of the small closure data points were not included due to their magnitudes relative to the remaining data. For completeness the remaining data are presented in Table 3.2-2. A sample of the data reduction is presented in Appendix II.

3.3 J-Integral and K_I Calibration

The final aspect of the finite element data reduction is the evaluation of the stress intensity factors for the partially-closed crack from the calculated J-integrals.

Four J-integral contour estimations were obtained about the crack tip for each load step. The appropriate J-integral for a given step was chosen on the basis of the convergence rate of the estimates from one contour to the next. For all crack depths the convergence characteristics followed a consistent trend. In general, for sufficiently large differences between crack depth and closure length convergence behavior was such that the 4th contour resulted in the best estimate. The sufficiently large difference was found to be satisfied when the 4th contour did not enclose both crack tips. Since each contour represents a normalized radius of 0.05 about the crack tip both tips were enclosed for $\xi_a - \xi_c = 0.20$. For the cases were both tips were enclosed the J-integral estimates begin to decrease; approaching the difference between the J-integral at the two tips. It should be noted that for very

TABLE 3.2-2

DISPLACEMENT DATA FOR SMALL CLOSURE

CRACK DEPTH	CLOSURE LENGTH[1]	$\delta_N/2$	$\delta_M/2$	$\Theta_M/2$	$\delta^M/2$	$\Theta^M/2$
0.10	0.000	0.019	0.104	0.576	-2.037E-3	-1.082E-2
	0.025	0.009	0.050	0.269	-0.896E-3	-0.463E-2
	0.100	0.0	0.0	0.0	0.0	0.0
0.20	0.000	0.092	0.466	2.366	-1.761E-2	
	0.025	0.048	0.234	1.149	-1.222E-2	
0.30	0.000	0.265	1.216	5.616	-6.023E-2	
	0.025	0.130	0.566	2.490	-4.720E-2	
0.40	0.000	0.640	2.645	11.07	-1.421E-1	
	0.025	0.273	1.044	4.10	-1.183E-1	
0.50	0.000	1.461	5.410	20.40	-2.753E-1	
	0.025	0.492	1.640	5.73	-2.380E-1	
0.60	0.000	3.374	11.15	37.65	-4.763E-1	
	0.025	0.798	2.27	7.05	-4.223E-1	
0.70	0.000	8.446	24.83	74.55	-7.761E-1	
	0.025	1.185	2.82	7.83	-7.006E-1	
0.80	0.000	25.70	66.98	177.6	-1.253	
	0.025	1.65	3.12	8.1	-1.145	

[1] For crack displacement contributions, this is the effective closure length.
For total cracked displacements, this is the actual closure length.

small open crack lengths ($\xi_a - \xi_c << 1$) and for symmetrical cracks the J-integral estimates approached zero as they should. To show these convergence trends the J-integral estimates for a crack depth of 0.4 subjected to far-field membrane force are presented in Table 3.3-1.

Once the appropriate J-integral was determined it was necessary to obtain the corresponding stress intensity factor. This can be obtained from

$$K_I = \sqrt{E' J} \quad . \tag{3.3-1}$$

For the fully open case the stress intensity factor due to the membrane force and due to the bending moment have been calculated from equation (3.3-1). These values compare very well to the accepted solutions [20] as presented in Table 3.3-2. The differences between the two were found to be of consistent magnitude for several other models of less mesh refinement about the crack plane; although the effect of using crack tip elements was not examined.

It was now necessary to determine the relationship between the stress intensity factor, the strip thickness and the applied load. The J-integral is equivalent to the energy release rate per unit crack growth,

$$J = \partial W_c / \partial c = \partial W_c / w \partial \xi_c \tag{3.3-2}$$

where

$$W_c = \tfrac{1}{2} [N \quad M] \begin{bmatrix} \delta_c \\ \theta_c \end{bmatrix} \quad . \tag{3.3-3}$$

TABLE 3.3-1

J-INTEGRAL ESTIMATES FOR CRACK DEPTH OF 0.40

DUE TO AN APPLIED MEMBRANE FORCE

EFFECTIVE CLOSURE LENGTH	J-INTEGRAL			
	CONTOUR 1	CONTOUR 2	CONTOUR 3	CONTOUR 4
0.0^-	1.610E-1	1.630E-1	1.631E-1	1.631E-1
0.0^+	5.341E-2	5.413E-2	5.417E-2	5.417E-2
0.05	2.514E-2	2.550E-2	2.552E-2	2.552E-2
0.10	1.762E-2	1.788E-2	1.789E-2	1.789E-2
0.15	1.304E-2	1.324E-2	1.325E-2	1.323E-2
0.20	9.624E-3	9.785E-3	9.779E-3	9.419E-3
0.25	6.794E-3	6.900E-3	6.654E-3	1.665E-4
0.30	4.220E-3	4.150E-3	7.280E-5	1.045E-5
0.35	1.745E-3	1.484E-5	5.567E-7	2.448E-7

TABLE 3.3-2

STRESS INTENSITY FACTOR CONTRIBUTIONS[1] FOR FULLY OPEN CRACKS

CRACK DEPTH	K_{IN}		K_{IM}	
(a/w)	FEA	Ref [20]	FEA	Ref [20]
0.1	0.6533	0.6702	3.4958	3.5003
0.2	1.0601	1.0833	4.9432	4.9248
0.3	1.5792	1.6068	6.4604	6.3946
0.4	2.3188	2.3630	8.3620	8.3030
0.5	3.4631	3.5426	11.080	11.094
0.6	5.3996	5.5511	15.461	15.637
0.7	9.1363	9.4545	23.625	24.169
0.8	18.146	19.012	42.782	44.463

[1] For unit thickness and unit applied load.

Rewriting equation (2.4-1) in the form

$$\begin{bmatrix} \delta_c \\ \theta_c \end{bmatrix} = 1/E' \begin{bmatrix} C_{11} & C_{12}/w \\ C_{21}/w & C_{22}/w^2 \end{bmatrix} \begin{bmatrix} N \\ M \end{bmatrix} \qquad (3.3\text{-}4)$$

and combining with equations (3.3-2) and (3.3-3) gives

$$J = (1/2E'w) \frac{\partial}{\partial \xi_c} (C_{11}N^2 + (C_{12}+C_{21})MN/w + C_{22}M^2/w^2) \quad . \qquad (3.3\text{-}5)$$

Since the force and moment have been applied independently, the J-integral contributions due to each become

$$J_N \propto N^2/E'w \; ; \quad J_M \propto M^2/E'w^3 \quad . \qquad (3.3\text{-}6)$$

From equation (3.3-1) the stress intensity factor contributions then become

$$\begin{aligned} K_{IN} &= \sqrt{E' J_N} \propto \sqrt{N^2/w} = k_N N/w^{\frac{1}{2}} \\ K_{IM} &= \sqrt{E' J_M} \propto \sqrt{M^2/w^3} = k_M M/w^{3/2} \end{aligned} \qquad (3.3\text{-}7)$$

where k_N, k_M include the necessary proportionality factors. By superposition the total stress intensity factor is

$$K_I = K_{IN} + K_{IM} = (k_N N + k_M M/w)/w^{\frac{1}{2}} \quad . \qquad (3.3\text{-}8)$$

As in equation (2.4-2) the effect of the membrane force can be eliminated resulting in

$$K_I = (\bar{\lambda} k_N + k_M) M/w^{3/2} = k^M M/w^{3/2} \qquad (3.3\text{-}9)$$

where k^M is the total stress intensity factor due to a unit bending moment with unit thickness. Note that since M is negative for all closures, k^M must also be negative. These values are plotted versus closure length in Figure 3.3-1.

FIGURE 3.3-1
PARTIAL CRACK CLOSURE
STRESS INTENSITY FACTOR (k^M)
vs CLOSURE LENGTH RATIO

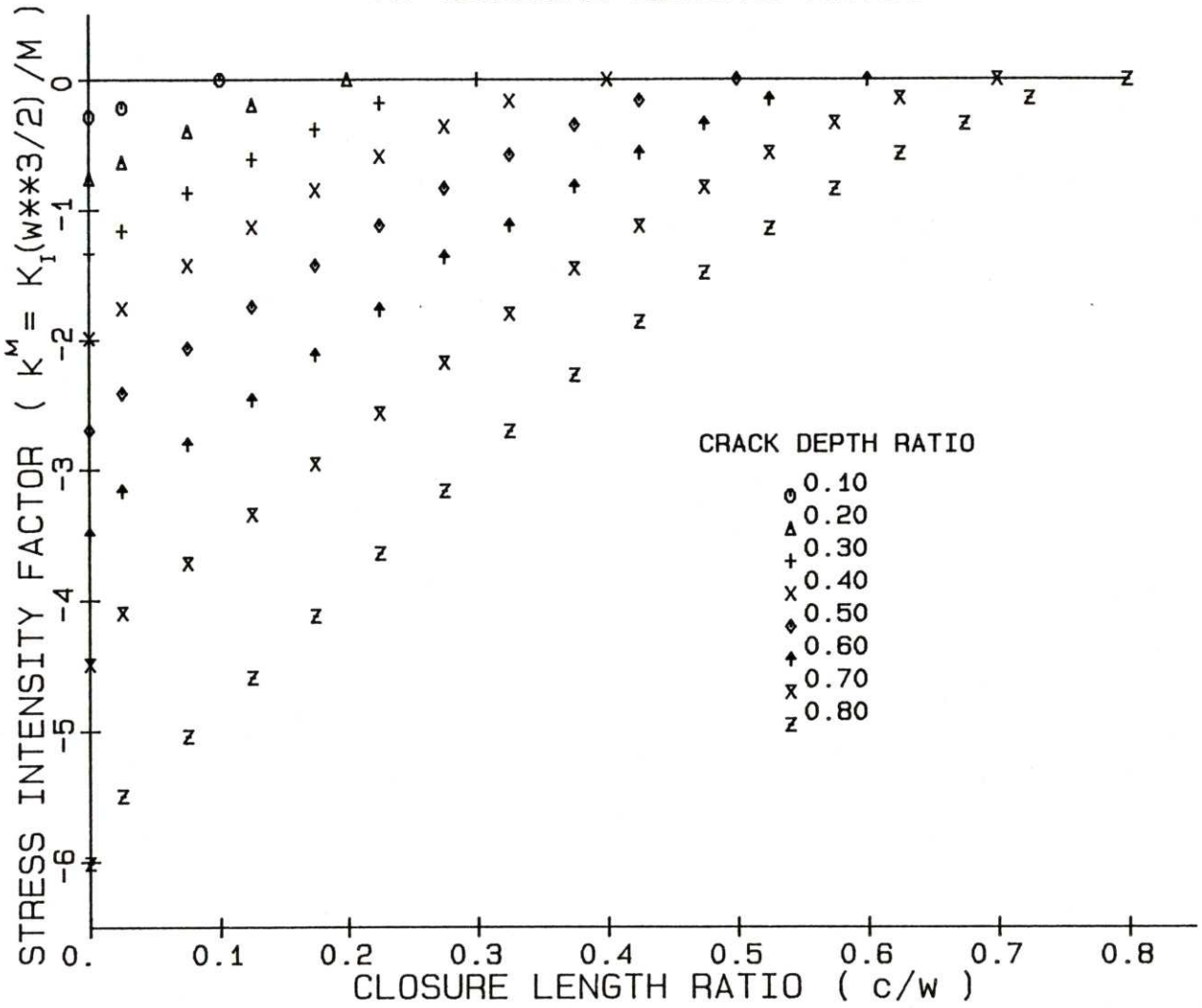

An interesting point should be made here regarding the stress intensity factor contributions of the negative bending moment. It is clear that K_{IN} will be positive for all closures. Similarly, for shallow cracks ($\zeta_a < 0.5$) the contribution due to the closing moment will be negative for all closure lengths. However, for crack lengths in excess of 0.5 there exists a closure length above which the SIF contribution due to the closing moment is positive. This can be visualized by considering a small (Griffith) crack located entirely within the tensile portion of a bending stress field (Figure 3.3-2), for which a positive SIF will exist at each end. Now remove the crack plane contact from the crack tip through the original compressive region (i.e., allow overlap). The stress field must redistribute resulting in a negative SIF at the crack tip. Clearly, somewhere between these two extremes the SIF contribution due to the moment must change from positive to negative. The FE results, being in the form of J-integral, are always positive so that this effect is more difficult to notice. In Figure 3.3-3 is presented a typical plot of J-integral versus modeled closure length due to an applied far-field bending moment. A curve through the data should reach J = 0 at some closure, increase (with a discontinuous but reflected slope) and gradually approach zero again at full closure. The contribution change-over occurs at the closure for which J = 0. A second method of estimating the change-over closure is to examine the crack opening profile in the vicinity of the crack tip. For a pure closing moment and no crack closure an

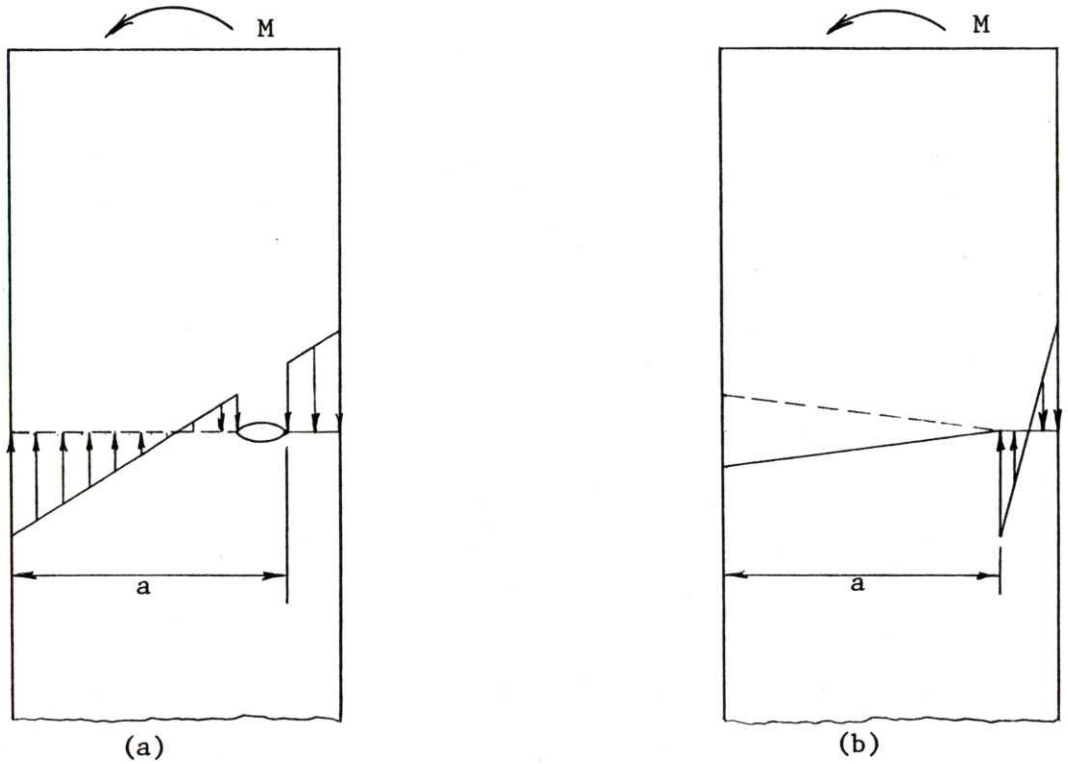

Figure 3.3-2

Approximate Bending Stress Distribution Along the Crack Plane
(a) Small Internal Crack Contained Entirely Within Tensile Field and (b) Deep Edge Crack

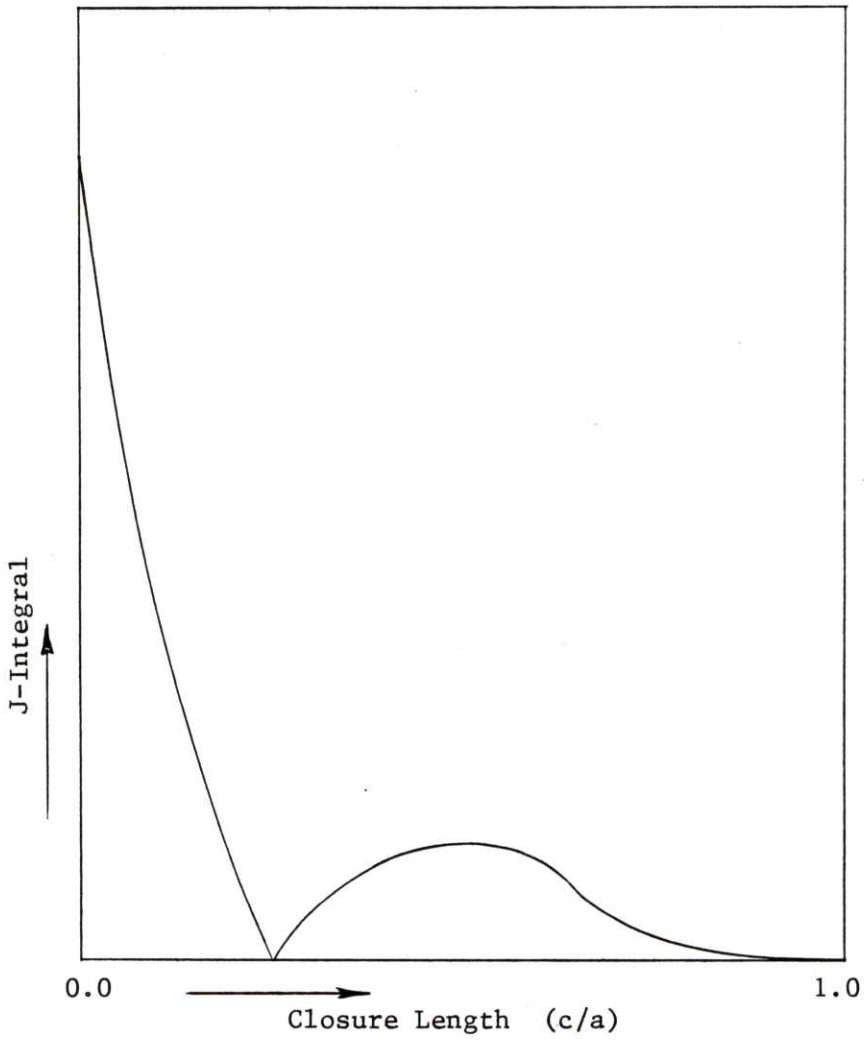

Figure 3.3-3

Typical Curve of J-Integral Versus Closure Length Due to Bending Moment for a Crack Depth Ratio < 0.5

overlapping crack opening profile is obtained. As the crack closure length is increased the crack opening profile changes, ultimately resulting in a positive crack opening profile at the tip. The closure length at which this occurs also signifies the contribution change-over.

Using both of these methods the range of the effective closure length in which the stress intensity factor contribution due to the applied moment reverses is

Crack Depth	Effective Closure Length
0.0	no reversal
↓	↓
0.5	no reversal
0.6	0.25 - 0.30
0.7	0.05 - 0.10
0.8	0.0^{+} - 0.05

As a final point, consider the stress intensity factors given in Table 3.3-2 for a crack depth ratio of 0.4. These values all correspond to the reference case N = M = w = 1 and therefore represent the stress intensity factor contributions, k_N and k_M of equations (3.3-7) through (3.3-9). Consider now an arbitrary load distribution: N = 20,000 lb, M = 4594.7 in-lb, with w = 1.0 in. The resulting load ratio is $\bar{\lambda} = -4.353 = \bar{\lambda}_{crit}$ for $\xi_a = 0.40$. Applying equation (3.3-8) with the FEA estimates, $k_N = 2.3188$ and $k_M = 8.3620$ gives a total stress intensity factor of $K_{I[FEA]} = 7.955$ ksi$\sqrt{in}$. Performing the same calculation with the estimates from reference [20], $k_N = 2.3630$ and $k_M = 8.3030$ gives $K_{I[20]} = 9.110$ ksi $\sqrt{in}$. Therefore, even though the individual errors are very small (1.9% on k_N, 0.5% on k_M) the combined error can be very

large at the onset of closure (12.7% in this case). As the estimates from reference [20] are the currently accepted solutions the finite element contributions [FEA] have been ratioed so as to satisfy continuity across the fully-open/ partially-closed interface.

The effects of both the reversal of the bending moment contribution and the error of the finite element estimates have been included in the evaluation of k^M from equation (3.3-9).

4. FINITE ELEMENT IMPLEMENTATION

The mathematical development of the nonlinear-elastic line-spring model with partial closure capabilities has been presented in Chapter 2. In Chapter 3 the parametric data necessary to employ the model in a generalized problem of crack closure was obtained and reduced. What remains is the topic of this chapter; to incorporate the partially-closed line-spring model into the ABAQUS © finite element program and to demonstrate its application to a specific problem.

For the type of problem to which the nonlinear-elastic line-spring model can be applied, the implementation of the partially-closed line-spring model results in a solution algorithm consisting of two iterative loops. The primary (or outer) loop represents the global iteration performed by the standard[1] ABAQUS © finite element code. In simplified form, the primary iteration algorithm, in conjunction with the partially-closed line-spring model, proceeds as follows:

Step 1 - Given an incremental tangent stiffness, the displacement and force distributions[2] are calculated.

---

1. The "standard" ABAQUS finite element code refers to the portion of the code which existed prior to the incorporation of the partially-closed line-spring model. Note that the operation of the "standard" portion is not affected by the new capabilities.

2. Unless otherwise noted, the displacement and force distributions which will be discussed in the following sections are those not of the entire structure but those of the line-spring element(s) only.

Step 2 - The displacement solution is applied to the partially-closed line-spring element and a new tangent compliance matrix and resultant force distribution are calculated.

Step 3 - Force distributions from steps 1 and 2 are compared. If convergence is not satisfied, the new tangent compliance from step 2 is input to step 1 for the next iteration.

The secondary (or inner) loop represents the iterations performed within the partial closure portion of the finite element code to obtain the incremental characteristics of the partially-closed line-spring model. This loop is completely contained within step 2 of the primary loop.

The implementation of the partially-closed line-spring model had associated with it three distinct parts:

1. Interface between the standard ABAQUS © code and the partial closure routines
2. Secondary iteration algorithm
3. Interpolation of the discrete parametric data

These topics are discussed in more detail in the following sections.

4.1 Interface Between Standard Code and Partial Closure Routines

Before proceeding with the discussion of the programming interface, a brief review of the terminology inherent in ABAQUS © multiple load case, nonlinear analyses is appropriate. In each ABAQUS © analysis a four level hierarchy exists which defines the solution state: step,

increment, attempt, and iteration. Each of these terms can be described as follows:

STEP - The largest division of the analysis. It represents a new set of applied loads, displacements, temperatures, etc.

INCREMENT - A fraction (≤ 1.0) of a step. Multiple increments form a step.

ATTEMPT - An effort to solve for the increment state. A reduction in increment size results if the effort is unsuccessful.

ITERATION - A single pass through the primary loop. Multiple iterations (may) form an attempt.

These four terms will be used throughout the remainder of this chapter.

The interface between the standard ABAQUS © finite element code and the programming required to analyze partial crack closure was developed with two major objectives:

1. Ensure minimal interaction between the standard code and the new routines.
2. Allow the partial closure routines to be accessed only when closure is predicted.

The standard configuration of the finite element implementation of the linear-elastic line-spring model consists of two primary routines, MATLSA and MATLS. To support the partial closure capability two additional primary routines have been introduced, PRTCLL and PART, and minor modifications

have been made to MATLS. With respect to the first objective above, the interface between the standard code and the partial closure routines is contained entirely within routine MATLS. The modifications which have been made to this routine serve three purposes; initialization of fixed data and storage locations, updating storage locations, and evaluation of closure. Each of these will be discussed in more detail below.

During execution, upon entering routine MATLS the standard code retains only the displacement and force distributions for the last converged increment and, in general, a current incremental displacement distribution estimate. For reasons to be discussed later, the solution algorithm for the partially-closed line-spring requires a significant amount of intermediate data to be carried from iteration to iteration prior to incremental convergence. The majority of the data and storage location initialization and updating is performed within the supporting partial closure routines and, as such, are not affected by the operation of the standard code. Data initialization consists basically of reading the discrete parametric data into a common array for use by all routines. This operation is performed once per analysis within routine MATLS. Intermediate data updates are performed once per iteration within the support routines INIT, INIT1 and ICOUNT. Appendix III contains the listing of the modified MATLS routine with each area of modification indicated and described.

The evaluation of closure is, of course, the final objective of the implementation of the partial closure routines. The

entire solution for the partially-closed line-spring model is obtained in routine PART, as will be discussed in the following section. Prior to the evaluation of closure two other operations must be considered; checking to see if closure is predicted and, if so, ensuring that the correct intermediate data are input to routine PART. The first of these is performed in a manner similar to that by which a structure is found to be stressed above its yield limit. An incremental displacement distribution (step 1 of the primary iteration loop) is applied to the fully open (linear-elastic) line-spring element. The resulting work-conjugate force distribution is determined in the form of the load ratio, $\bar{\lambda}$. A load ratio exceeding the critical load ratio required for closure to occur (Table 3.2.1) indicates that the line-spring element is no longer linear; the closure has introduced nonlinearities. In conjunction with objective 2, should closure not be obtained the partial closure routines are bypassed (with the exception of storage updating routines) and the standard solution algorithm is followed.

In the event that closure has occurred the data which must be input to the partial closure routines (step 2 of the primary iteration loop) can be of several forms. Consider the diagrams of Figure 4.1-1 which represent different primary iteration step 2 procedures between the same solutions. In the first, Figure 4.1-1(a) the procedure is stationary, always proceeding from the previously converged increment. The second diagram, Figure 4.1-1(b), shows a progressive procedure in which the previously converged iteration or

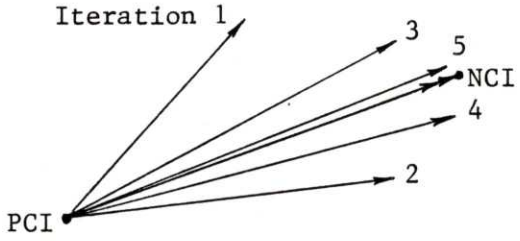

(a)

PCI = Previous Converged Increment
NCI = New Converged Increment

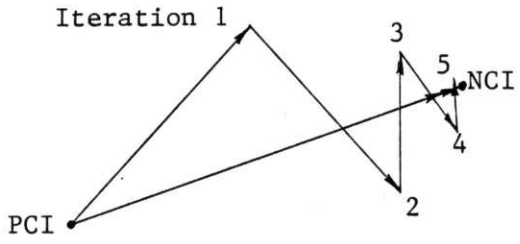

(b)

Figure 4.1-1

Schematics of Different
Primary Iteration Procedures
(a) Stationary and (b) Progressive

increment is used as input for the next iteration. In other words, the "base" for the stationary procedure does not change until incremental convergence is obtained. The "base" for the progressive procedure progresses with the solution. Notice that for both iteration procedures a previously converged solution is required to determine the solution state of the partially-closed crack. This restriction is satisfied only when a linear (fully open crack) solution has been obtained. Therefore, a linear solution must be performed prior to the existence of closure. Intuitively it is expected that the progressive procedure should have better inherent convergence characteristics than the stationary procedure. For this reason the progressive solution procedure was selected for step 2 of the primary iteration loop with the following exceptions:

1. Consider a situation with a very large increment size and increasing closure length. Due to the large increase in line-spring element stiffness with increasing closure, the work-conjugate force distribution may be very large (Figure 4.1-2(a)). This occurs because the current incremental displacement estimate corresponds to the previous, lower stiffness solution. If this progressive solution is input to the partial closure routines the secondary iteration loop may become unstable. To avoid this possibility, the stationary procedure is applied in these situations.

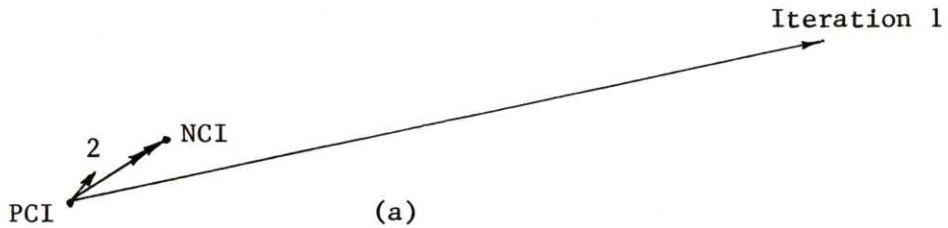

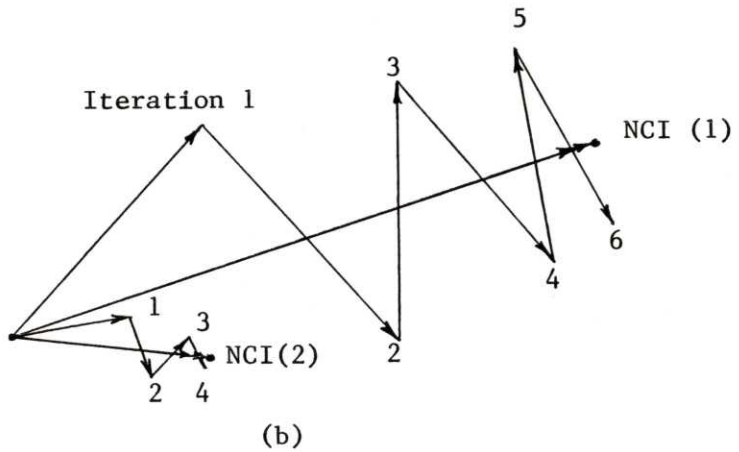

Figure 4.1-2

Exceptions to Progressive Iteration Procedure
(a) Excessive Step Size and (b) Non-Convergence

2. If convergence is not obtained after a sufficient number of iterations, the increment size is decreased by the standard ABAQUS © code. For the first iteration of the new attempt the progressive solution procedure is started from the previously converged increment rather than continuing from the previous iteration (Figure 4.1-2(b)).

At this point the reason for requiring storage of intermediate data becomes evident. As mentioned earlier, the standard code retains only the displacement and force distributions from the previous increment and the current incremental displacements. To input the data from the previous iteration into the partial closure routines requires intermediate results from that iteration as well as, for the exceptions noted above, results from the previous converged increment.

4.2 Secondary Iteration Algorithm

The partial closure portion of the total finite element program consists of 18 subroutines. As discussed in the previous section, the interface between the standard code and the partial closure portion is performed entirely within routine MATLS. Direct access is made by MATLS to six of the subroutines. The subroutine hierarchy and access paths are presented diagramatically in Figure 4.2-1. A description and listing of each of the partial closure routines is presented in Appendix IV.

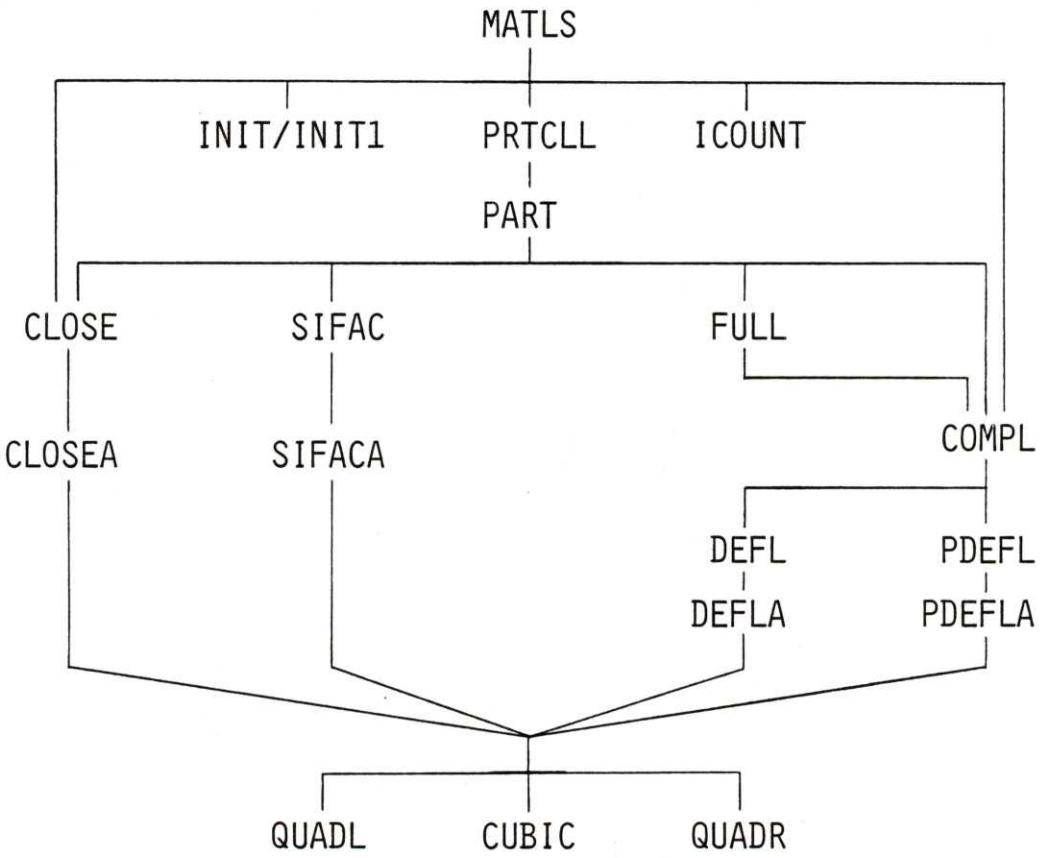

Figure 4.2-1

Hierarchy of Partial Closure Subroutines

In general, the objective of the partial closure routines can be described as follows: given the force and displacement distribution from a previous solution state and a current displacement increment, determine the corresponding partially-closed crack characteristics. The crack characteristics consist of the resultant force distribution and tangent stiffness (or compliance) matrix, the closure length ratio, and the stress intensity factor. The previous solution state may be either the previously converged increment or the last iteration as discussed in Section 4.1. Routine PRTCLL is the primary interface between the standard code and the remaining partial closure routines. The data input to the closure routines is controlled by PRTCLL and the other storage initialization and updating routines.

The secondary iteration is performed entirely within subroutine PART. A Newton-Raphson scheme is employed and is described briefly below:

Step 1 - Use the incoming force distribution to evaluate a new tangent compliance matrix.

Step 2 - Use the incremental displacements and the new tangent compliance to determine the load increments.

Step 3 - Use the total load estimate and total compliance to calculate the total displacement estimate.

Step 4 - Compute the error in the total displacement from the incoming displacement. If convergence is not satisfied, return to step 1 replacing the

incoming force distribution with the total load estimate and replacing the incremental displacements (step 2) with the displacement error.

The steps outlined above comprise primary iteration step 2 with the results being used for comparative purposes in primary iteration step 3. The actual secondary iteration algorithm is discussed in more detail in Appendix V.

A significant aspect of the partial closure algorithm deals with the stiffness mismatch across the fully-open/ partially-closed interface. At this interface, the onset of closure, the fully-open and the partially-closed line-spring stiffnesses should be equal. Due to the different calculation procedures (Sections 2.1 and 2.4) this is not the case. The resulting stiffness discontinuity is unacceptable as convergence will never be obtained in the small closure range. To avoid this inconsistency, factors are calculated within routine MATLS to relate the fully-open and the partially-closed line-spring stiffnesses at the onset of closure. The factors may be greater or less than 1.0 and are applied the partially-closed stiffnesses at each step of the secondary iteration loop (within routine PART). The rationale behind applying the factors to the closed stiffnesses is relatively simple. The stiffness calculation as discussed in Section 2.4 requires a significant amount of interpolation and slope evaluation of discrete data "curves" (Section 4.3). It is to be expected that some error will be introduced due to the interpolation, predominantly in

the small closure range where the most severe gradients occur. Therefore, to minimize the effects of the interpolation errors, the factors are applied to the partially-closed stiffnesses. However, beyond the small closure range the discrete data "curves" tend to be more well behaved. In this range it is expected that the partially-closed equations (equations 2.4-7) yield relatively good stiffness estimates. Therefore, the factors should be "reduced" to a value of 1.0 at some point in the closure range. The method by which this reduction is performed has a significant effect on the convergence characteristics of the partially-closed line-spring model. This will be discussed in more detail later. In routine PART, presented in Appendix IV, the reduction occurs linearly over the range $0 \leq \xi_c \leq \xi_a$.

4.3 Interpolation of Discrete Parametric Data

The description of the parametric data necessary to characterize partial closure of external cracks has been presented in Chapter 3. It should be noted that although the data was obtained at discrete values of crack depth and closure length, the final objective this study is to apply the analytical technique to all cracks with depths $\xi_a \leq 0.8$. Therefore, an interpolation scheme was required which would allow continuous evaluation of the parametric data. Of itself this presents little difficulty as a linear interpolation scheme would satisfy the requirement. However, to evaluate the tangent compliance matrix coefficients (equations 2.4-7) the

slopes of the discrete data "curves" must be known. A further requirement then becomes that slope continuity must be satisfied by the interpolation scheme.

Each parametric data set must be interpolated with respect to two variables; closure length, for displacement and stress intensity factor contributions, and crack depth. The closure length must be interpolated with respect to load ratio and crack depth.

Interpolation with respect to closure length (and load ratio) was performed using a cubic spline curve through two consecutive data points with known slopes. As indicated in Figure 4.3-1 the slopes were evaluated by a weighted central difference approximation. This approach is sufficient to satisfy the continuity requirements described above. This interpolation scheme has been applied to all data ranges with the following exceptions:

1. For the first range of the stress intensity factor contribution ($0 \leq \zeta_c \leq 0.025$) the left-side slope is unknown. In this range a quadratic interpolation scheme is used (QUADR). The situation is similar at the final SIF range ($\zeta_a - 0.075 \leq \zeta_c \leq \zeta_a$) and for the first closure length (vs. load ratio) range where quadratic interpolation was used (QUADL and QUADR, respectively).
2. For the first two ranges of the displacement contribution ($0 \leq \zeta_c \leq 0.025$ and $0.025 \leq \zeta_c \leq 0.075$, Figures 3.2-5 through 3.2-7) the situation is

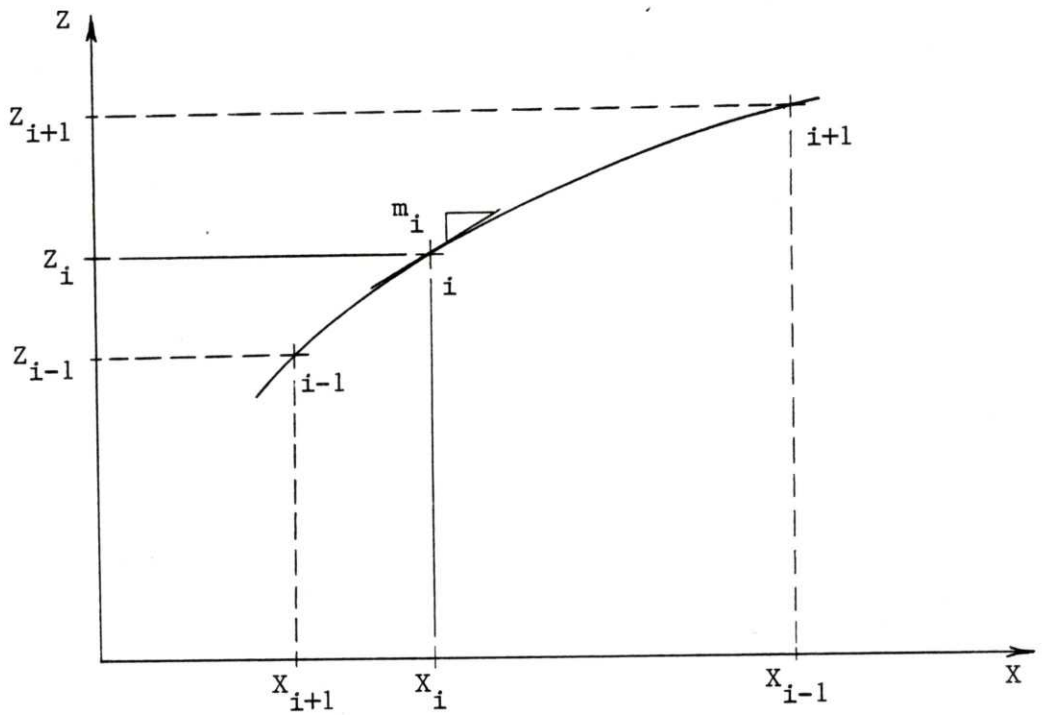

$$m_i = \frac{Z_i - Z_{i-1}}{X_i - X_{i-1}} \frac{X_{i+1} - X_i}{X_{i+1} - X_{i-1}} + \frac{Z_{i+1} - Z_i}{X_{i+1} - X_i} \frac{X_i - X_{i-1}}{X_{i+1} - X_{i-1}}$$

Figure 4.3-1

Slope Evaluation Using Weighted Central Difference Approximation

somewhat different. As illustrated in Figure 4.3-2 the gradient of the displacement contributions are very large at the onset of closure. Direct use of the weighted central difference approximation for the slope at data point 2 (ξ_c = 0.025) resulted in a non-monotonic displacement curve (cubic spline) between data points 2 and 3 as shown (cubic/quadratic). To avoid this, multiple quadratic interpolation is performed; first using routine QUADR between points 2 and 3 and then, with the slope calculated at point 2, using QUADR again between points 1 and 2 (double quadratic). The resulting "curve" satisfies the continuity requirements, as well as the monotonic expectations. Note that at the full closure end of the data (final range) the slopes of the displacement vs. closure length and the closure length vs. load ratio curves are known. Therefore, cubic spline interpolation is applicable in the final data range.

As no differentiation with respect to crack depth is required a linear interpolation scheme in ξ_a was deemed sufficient. Although this represents the most direct type of interpolation several aspects of it should be noted. Figure 4.3-3 shows a 3-D representation of a typical crack closure length versus load ratio curve for two discrete crack depths, ξ_{a1} and $\xi_{a2} = \xi_{a1} + 0.1$. As can be seen in the figure both curves are not defined over the same total data range. The curves for ξ_{a2} and ξ_{a1} are undefined in regions I and III,

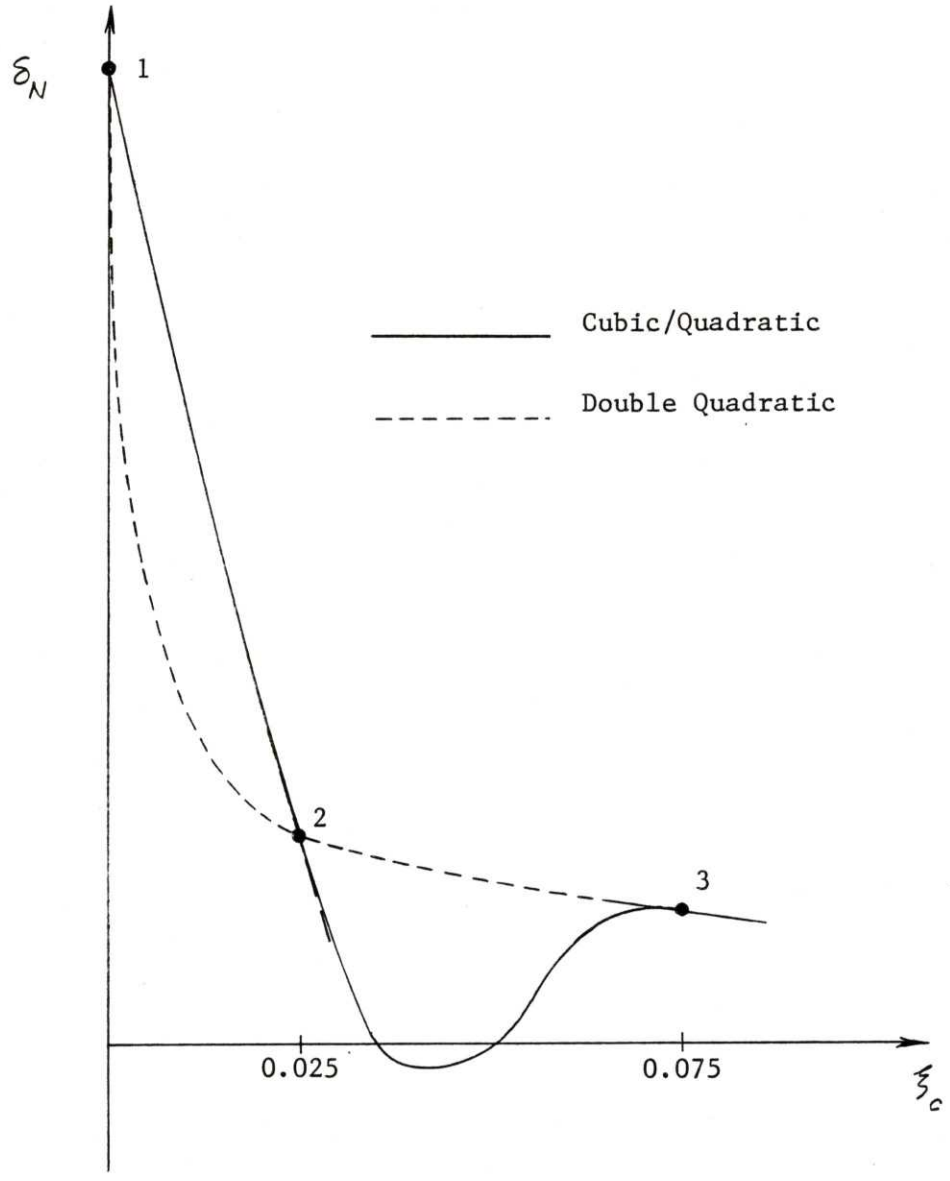

Figure 4.3-2

Interpolation Scheme in First Two Ranges of Displacement Contribution Curves

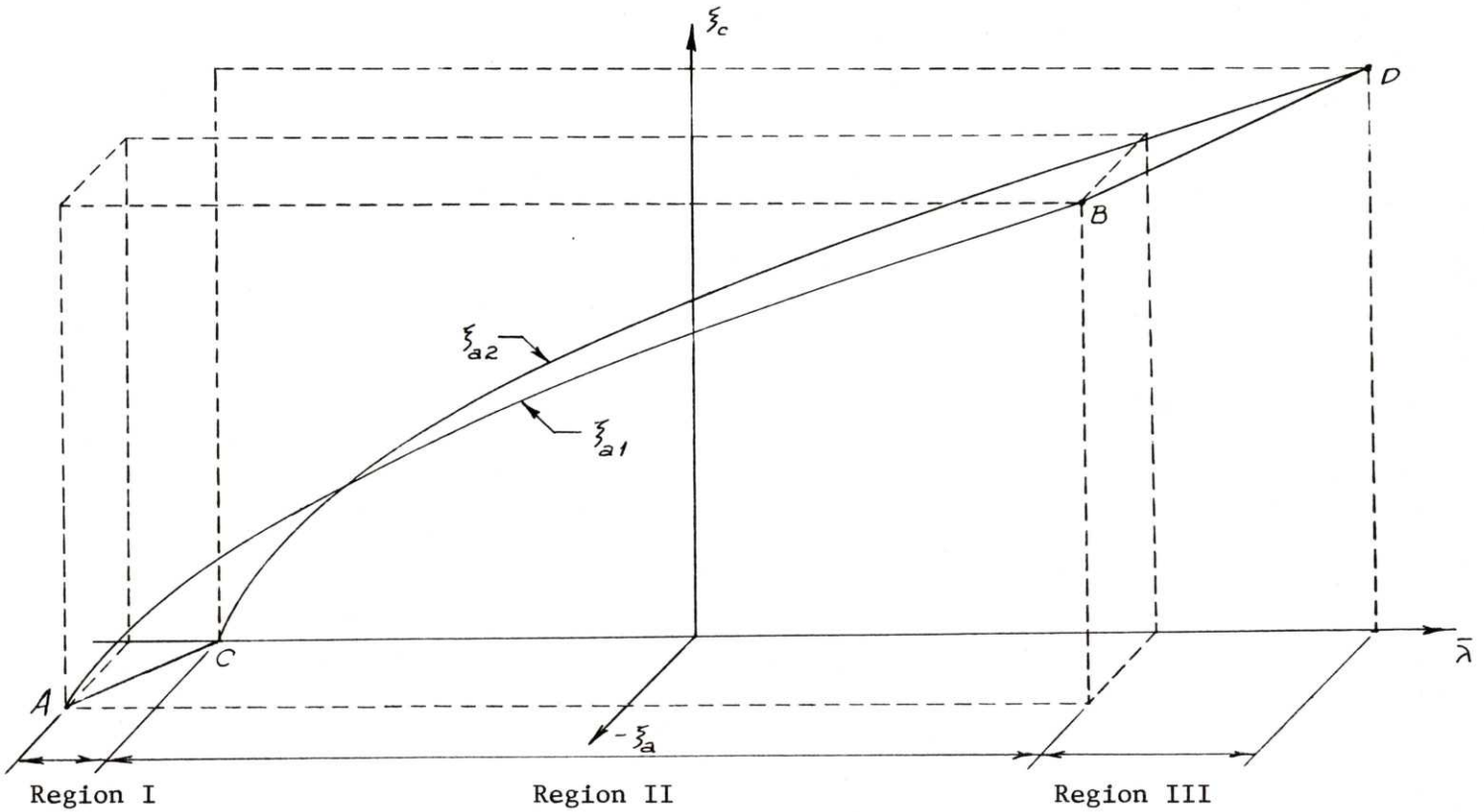

Figure 4.3-3

Linear Interpolation Regions of Closure Length versus Load Ratio Curves

respectively. In region II both curves are defined and the interpolation can be performed directly. In region III, line BD defines the load ratio for full closure for crack depths between ζ_{a1} and ζ_{a2}. The data and slopes along this line are known (equation 2.3-9) so the interpolation can be performed between the curve for ζ_{a2} and a point on the (known) line BD. In region I, line AC defines the approximate onset of closure. In this region the data and slopes are not known and must first be interpolated (linearly) along the line between points A and C. The interpolation in ζ_a can then be performed between this point and the curve for ζ_{a1}. These same types of considerations are required at the full closure end of the displacement and SIF contribution curves.

4.4 Application of the Partially-Closed Line-Spring Model

A crack configuration which is of value due to both its generality and its relative simplicity is that of a cylindrical pressure vessel containing two long, axial, internal surface cracks located diametrally opposite each other. Accepted solutions for partial closure of surface cracks subjected to an arbitrary membrane force/bending moment combination are not available. Therefore, the verification of the partially-closed line-spring model implementation is performed by examining the cracked cylinder in two ways: one using gap elements to define the crack face and the other using the line-spring model. A comparison of the results of the two examinations is presented in the next chapter.

The crack configuration and loading is presented in Figure 4.4-1. The long axial cracks (i.e., $2c' >> w$) are approximated by plane strain edge cracks. Due to the presence of the cracks, the internal pressure results in a tensile membrane force and a small closing bending moment applied to each crack. For closure to occur the cylinder is also "pinched" by concentrated compressive loads applied normal to the plane of the cracks. The geometric parameters defining the configuration are:

cylinder average radius, $R = (R_o+R_i)/2 = 21.0$ in.,

cylinder thickness, $w = 2.0$ in.,

crack depth ratio, $a/w = 0.4$.

The internal pressure, p, is held constant in both analyses with the resulting membrane force due to the pressure, being equal. Recall that the partial closure routines require a linear solution to be available prior to the onset of closure. To satisfy this requirement the compressive load, F, is applied incrementally; beginning at a small value for which closure will not occur and increasing such that partial closure is obtained. Crack face pressurization is not considered.

The plane strain crack configuration contains two planes of symmetry, thereby allowing only one-quarter of the geometry to be modeled.

In the first analysis the cylinder is modeled using 336 8-node plane strain elements (CPE8R). The crack face is defined by 16 gap elements. This model will be referred to as the "gap" model and is shown in Figure 4.4-2.

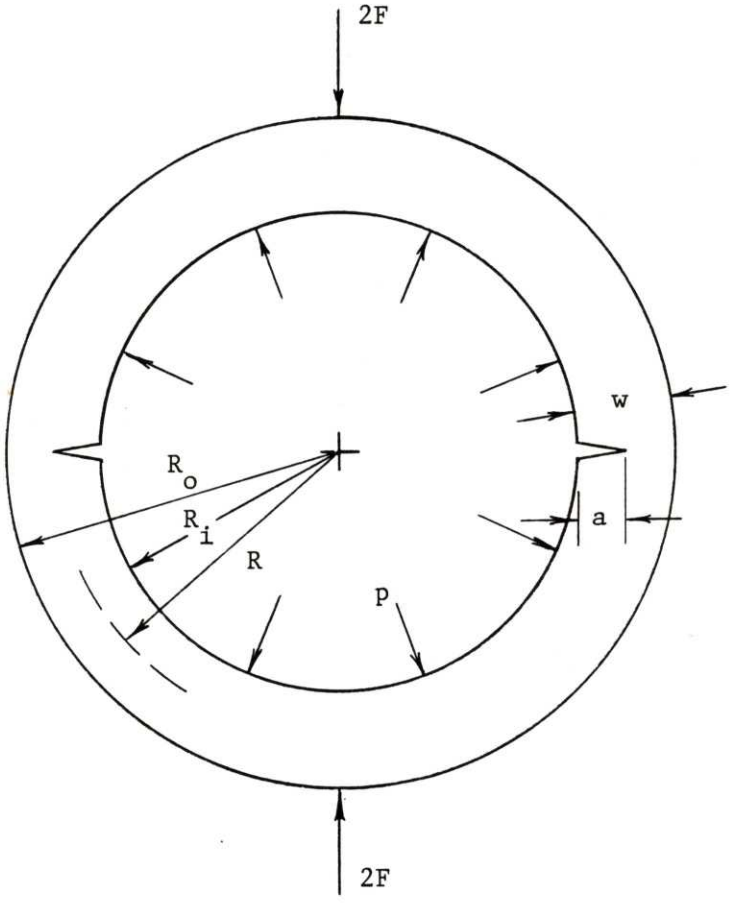

Figure 4.4-1

Axially-Cracked Pressurized Cylinder
Analyzed Using the Partially-Closed
Line-Spring Model

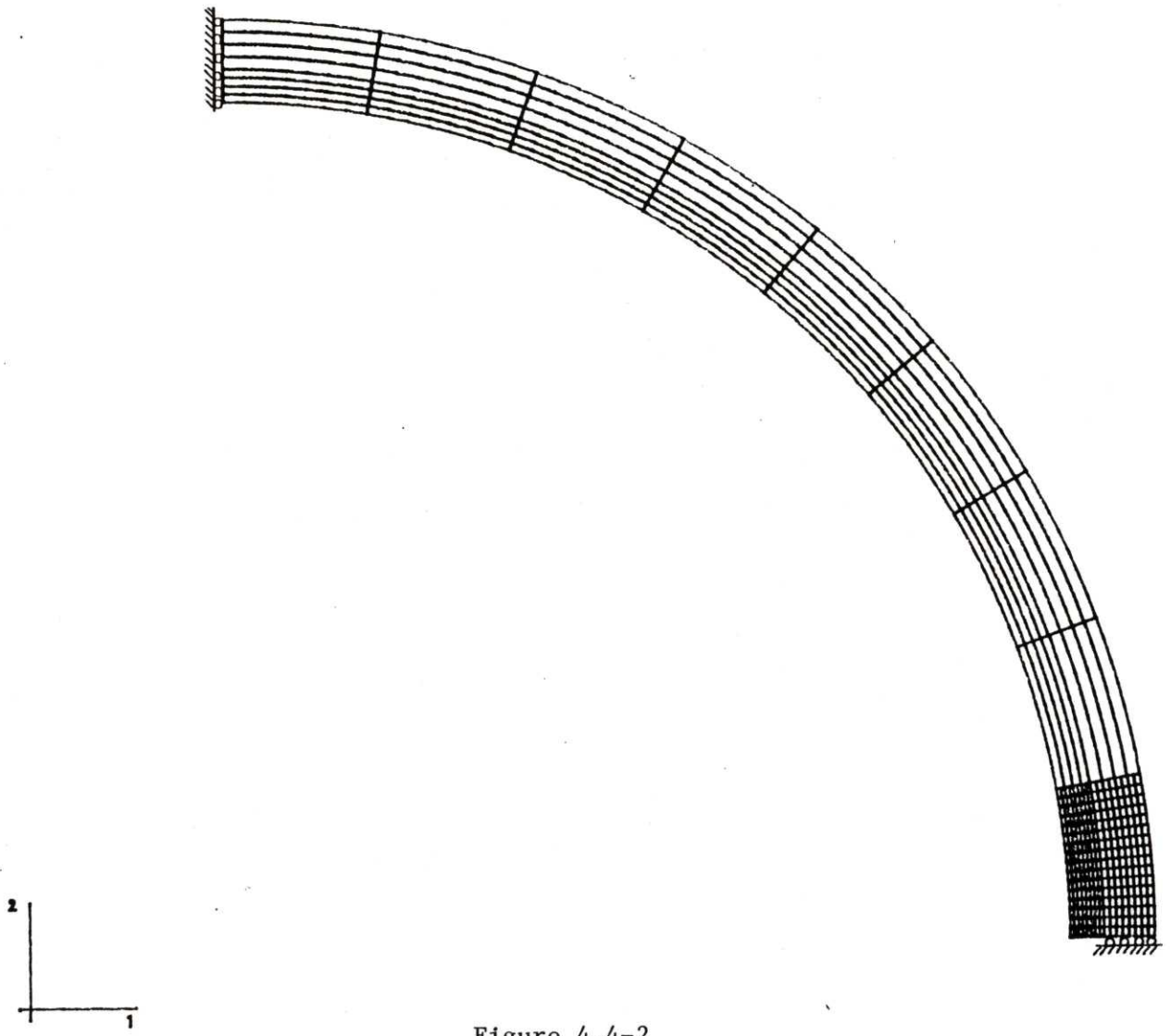

Figure 4.4-2

Plane Strain and Gap Finite Element Model of
the Axially-Cracked Pressurized Cylinder

In the second analysis, the cracked cylinder is modeled with 6 8-node shell elements (S8R) and one 3-node line-spring element (LS3S). Convergence tolerance limits of 1-2% of the resultant line-spring force distributions at the onset of closure were used. This "shell" model is presented in Figure 4.4-3.

Several points should be noted with respect to the analyses. As was mentioned, the internal pressure was held constant in each analysis. However, the actual pressures are not the same. For the gap model the pressure, p_g, acts over the inner surface (radius R_i). For the shell model the elements are located at the average radius, R, so the pressure, p_s, effectively acts over a larger area. Therefore, the pressure for the shell model must be

$$p_s = p_g \, R_i/R \qquad (4.4\text{-}1)$$

to result in the constant crack plane membrane force due to pressure in the two analyses.

For the shell model, the partial closure routines as presented in Appendices III and IV are used. In Appendix III the variables FC1, FC2, and FC3 are introduced. As described in Section 4.2 these factors are used to multiply the stiffnesses obtained from the partial closure routines such that at the onset of closure the "fully-open" and the "partially-closed" stiffnesses are equal (i.e., assure continuity across the open/closed interface). These factors must be "reduced" to 1.0 at some closure length $\xi_c = \xi_a$. For the

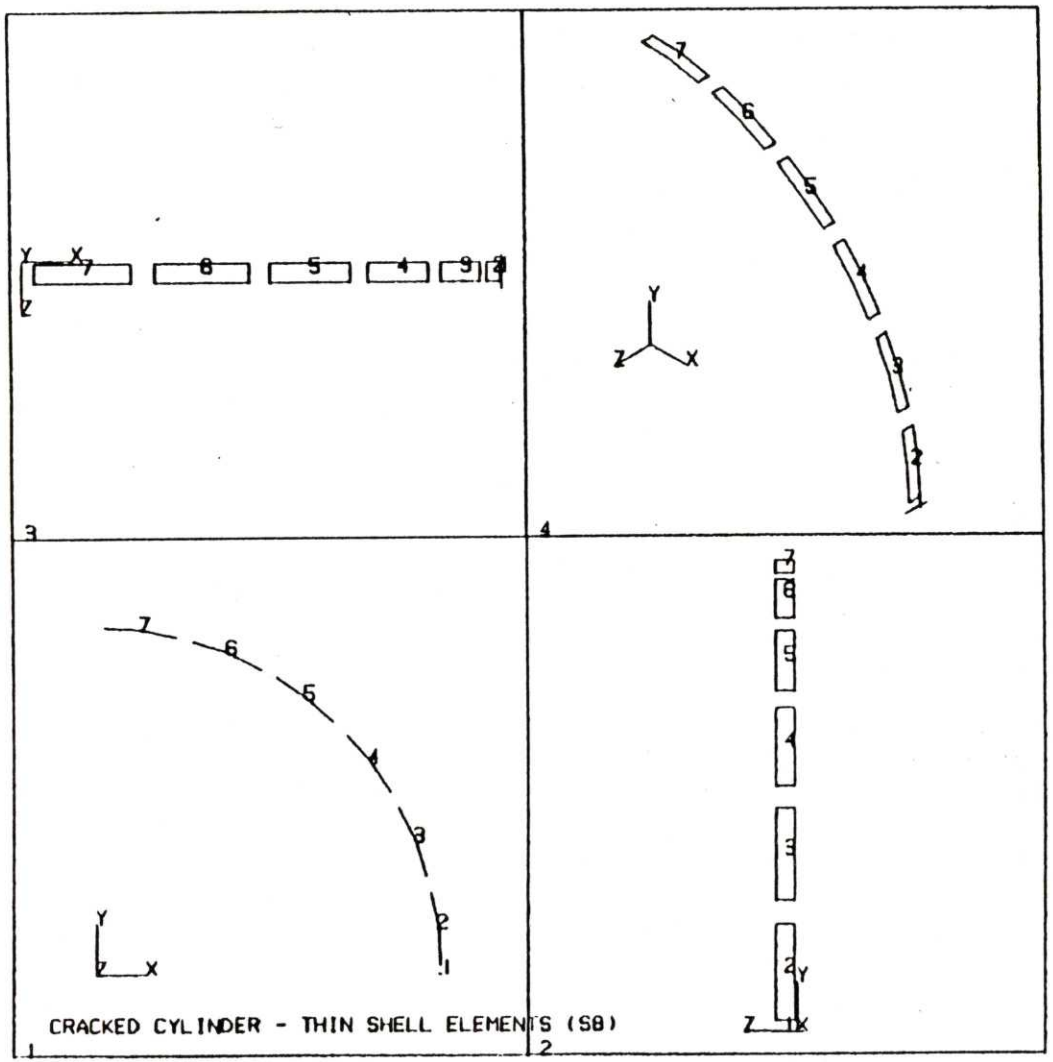

Figure 4.4-3

Shell and Line-Spring Finite Element Model of
the Axially-Cracked Pressurized Cylinder

shell model this reduction is performed linearly over the total crack depth.

5. RESULTS OF AN AXIALLY-CRACKED CYLINDER

Of primary interest in the linear-elastic analysis of cracked structures is the crack tip stress intensity. With the introduction of partial crack closure a second parameter becomes of interest, the crack closure length. Figure 5-1 presents the closure length ratio, ξ_c, versus normalized compressive force, F/F_{fc}, for the axially-cracked pressurized cylinder described in the previous section. The normalizing force, F_{fc}, corresponds to the force required for full closure to occur. From previous discussion, full closure is representative of an uncracked structure with zero stress at the location of the crack tip. From reference [24], the force which satisfies this requirement for the axially cracked cylinder is

$$F_{fc} = pRw/(w-0.3634\ R\bar{\lambda}_{fc}) \qquad (5\text{-}1)$$

where $\bar{\lambda}_{fc}$ is the load ratio at full closure from Table 3.2-1.

In general, the two solutions agree quite well. It should be noted that the shell model allows for a pseudo-continuous evaluation of the closure length (i.e., although a unique value of closure length is obtained, a range of values exist for which convergence criteria are satisfied). The closure length estimates for the gap model are known only as a range of values which are governed by the mesh refinement of the model. This closure range is plotted in the figure. The actual closure length falls within the defined range for the gap model. For the shell model the range is unknown as is the location of the estimated closure length within the range. In general, the accuracy of the estimated closure length is governed

FIGURE 5-1
AXIALLY-CRACKED PRESSURIZED CYLINDER
R = 21.0 in, w = 2.0 in, a = 0.8 in
CRACK CLOSURE LENGTH vs COMPRESSIVE LOAD

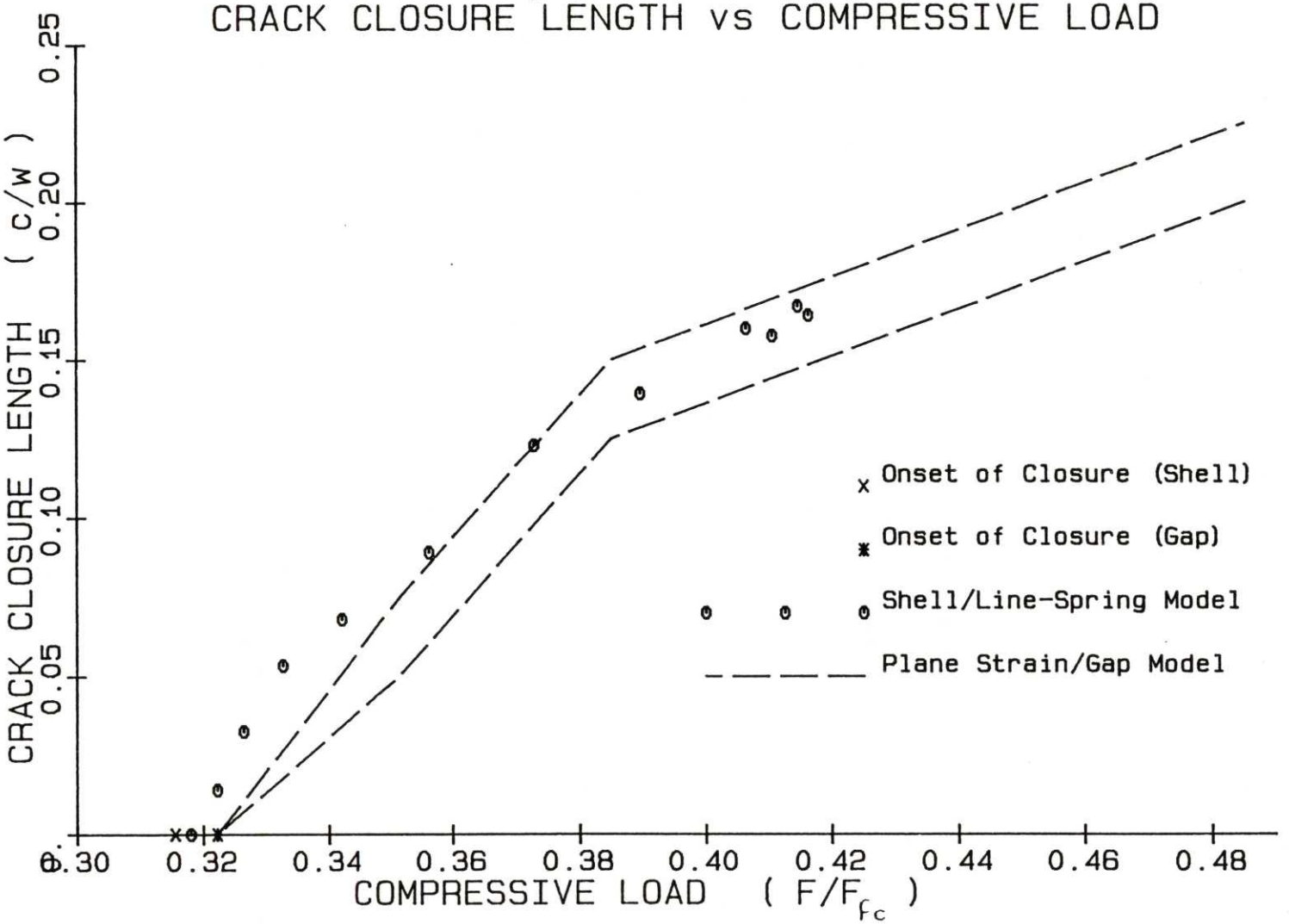

by the convergence tolerance limits for line-spring elements and by the mesh refinement for gap models.

Both models have been analyzed for two linear (fully open) load cases such that the linear trends could be examined. For the shell model, the following relationships were obtained between the generalized forces, N and M, and the applied loads,

$$N = pR - F$$
$$M = -0.02588\ pR - 7.204\ F \qquad (5\text{-}2)$$

where F is positive as shown in Figure 4.4-1. From the definition of the load ratio, the onset of closure is found to occur at F_{crit}/F_{fc} = 0.316. Similar development for the gap model, using the crack mouth opening displacements rather than the generalized crack plane tractions, yields

$$CMOD = (7.39E\text{-}8)\ pR - (1.280E\text{-}6)\ F \qquad (5\text{-}3)$$

for a critical force of F_{crit}/F_{fc} = 0.322. Both of these critical load points are indicated in the figure.

Figure 5-2 presents the second and final comparison between the two solutions; the normalized crack tip stress intensity, $K_I/(pR\sqrt{\pi a}/w)$, versus normalized compressive force. Again, the two solutions agree very well over the applicable range of closure. The linear solutions from each analysis have been combined, resulting in the following relationships between K_I and the applied loads:

$$K_I = 1.5952\ pR - 22.823\ F \qquad (5\text{-}4)$$

for the shell model and

FIGURE 5-2
AXIALLY-CRACKED PRESSURIZED CYLINDER
R = 21.0 in, w = 2.0 in, a = 0.8 in
STRESS INTENSITY FACTOR vs COMPRESSIVE LOAD

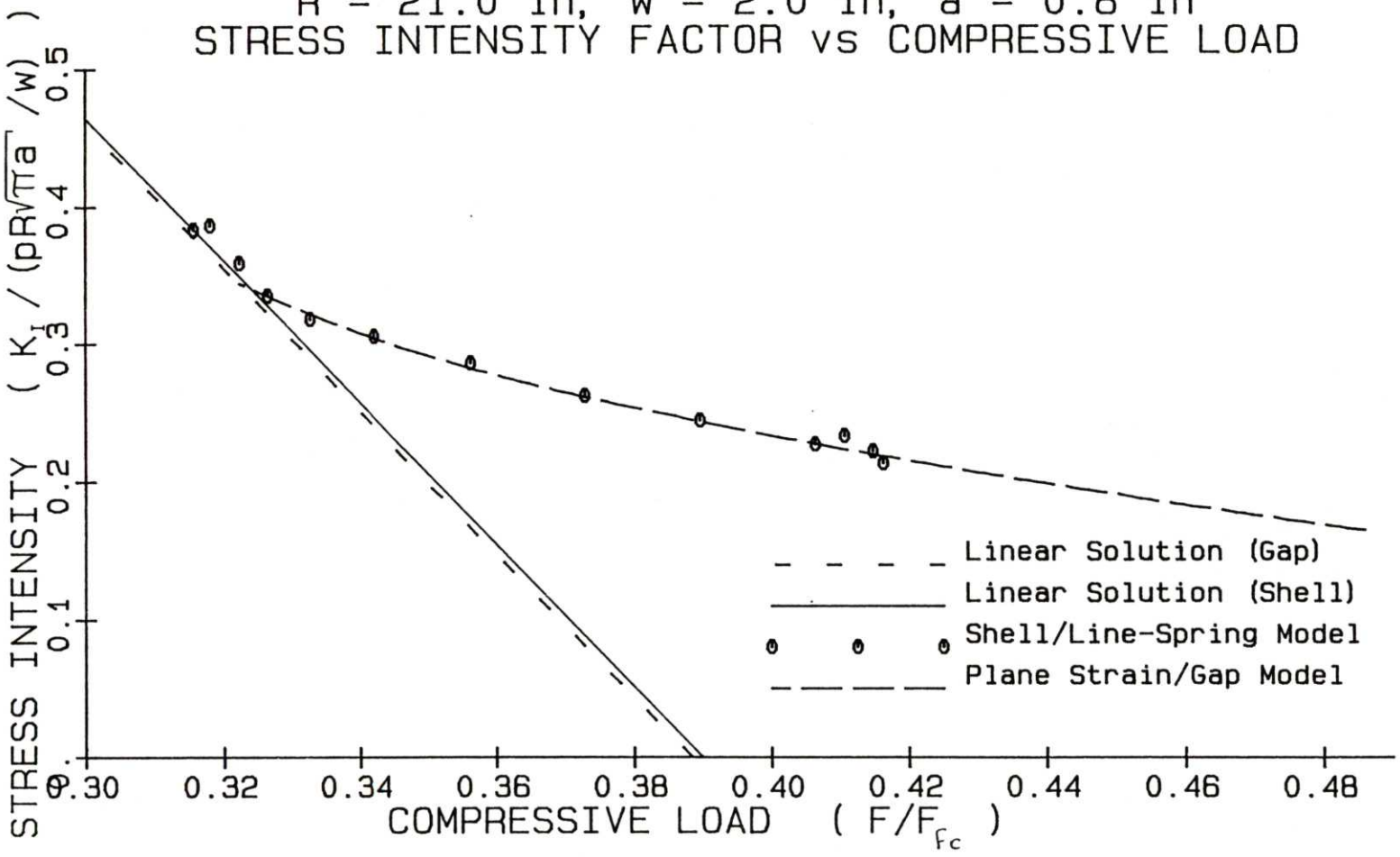

$$K_I = 1.6005\ pR - 22.9877\ F \qquad (5\text{-}5)$$

for the gap model. These linear solutions are also plotted in Figure 5-2. The effects of partial crack closure on the stress intensity factor are dramatically shown. From equations (5-4), the linear stress intensity factor is zero at $F/F_{fc} = 0.390$. However, both solutions indicate that at this load point the stress intensity factor has decreased only by ~33% from the fully open case (the onset of closure).

It should be noted that the curves presented in Figures 5-1 and 5-2 are applicable only for the geometry modeled (i.e., R = 21 in, w = 2 in, a = 0.8 in). However, since the closure length ratio is purely geometric and the applied force and the stress intensity factor are normalized with respect to the internal pressure, the effects of kinematic variations are implicitly included.

Notice also that the agreement between the stress intensity factors is better than that between the closure lengths. This is expected to be the case in general because a larger closure length implies greater stiffness which, for a given displacement field, results in a greater bending moment. Simultaneously, Figure 3.3-1 shows that the increased closure length corresponds to a lower stress intensity factor calibration. The increase in the moment is therefore offset by the decrease in the SIF calibration resulting in a more well behaved SIF.

Also, in both figures it can be seen that the shell model solution is applicable over a limited range of closure. This topic will be discussed in the following chapter. For the present, let it suffice to say that over the applicable range, the very good

agreement between the two solutions suggests that the nonlinear-elastic line-spring model formulation provides the analytical capability of much more complex finite element models.

6. DISCUSSION

The objective of this work has been the development and implementation of the nonlinear-elastic line-spring model to be applied in the analysis of partially-closed surface cracks in plates and shells. The results of an axially-cracked pressurized cylinder have been presented, indicating that the newly developed model is capable of analyzing surface-cracked structures to the same extent as much more complex finite element models. It has been noted that the nonlinear-elastic line-spring model solution is applicable over a limited range of closure. Some of the factors which control this range are now considered.

The primary factor contributing to the limited solution range is considered to be the lack of parametric data available for interpolation. This lack of data appears to be most severe in the small closure range. Recalling Figures 3.2-4 through 3.2-9, the most extreme variations in displacement contributions versus closure length and closure length versus load ratio occur at and just beyond the onset of closure. As discussed in Section 4.3, a significant amount of interpolation is performed on all of the parametric displacement data to evaluate the compliance matrix coefficients. The large variations in the data in the small closure range represent a challenge to the interpolation technique, especially with very few data points defining the curves. The importance of this area increases when considering that the fully-open and the partially-closed stiffnesses must be equal at the onset of closure to satisfy convergence requirements. To satisfy this requirement, stiffness factors are applied to the partially-closed

stiffnesses as discussed in Section 4.2. The stiffness factor reduction technique (i.e., linear, quadratic, etc. and the range over which it is applied) serves to shift the effect of insufficint data to a different closure range.

A significant number of trial analyses of the axially-cracked cylinder were performed to examine the effects of convergence tolerance limits, iteration procedure, and stiffness factor reduction techniques on the nonlinear-elastic line-spring model characteristics.

The effects of the tolerance limits on the convergence characteristics of the line-spring model have a relatively predictable trend. In general, the larger the tolerance limit, the quicker the convergence; the smaller the limit, the longer the solution time. The accuracy of the line-spring model solution is governed by the tolerance limits defined in the analysis. Therefore, a better solution is expected if small tolerance limits are defined. Unfortunately, as is typically the case, there exist advantages and disadvantages to both small and large tolerance limits. As can be seen in Figures 5-1 and 5-2, at the upper limit of applicability of the shell model the increment size decreases and both the closure length and the stress intensity factor solutions begin to oscillate. At the maximum increment size allowed in the analysis of the axially-cracked cylinder, the increment in applied load, F, was 60 lb. The resulting linear increments in the generalized forces, N and M, were 60 lb and 430 in-lb, respectively, versus a tolerance limit of 150 lb and 150 in-lb. This indicates that if the increment size is decreased by a factor of 3 in the linear regime the incremental generalized forces will be less than the tolerance limit.

Due to the nonlinearities which develop with crack closure, these incremental forces will change. However, it can be expected that a sufficiently small increment size exists, and has been attained, for which the incremental generalized forces are less than the tolerance limits. A second effect of the tolerance limit demonstrates the sensitivity of the nonlinear line-spring model solution to the "ligament" tractions. A relatively small variation in the generalized force or moment (or load ratio) can have a significant effect on the solution. Closure length differences of up to 20% were obtained for the same load state with maximum residuals in the upper (+150) versus the lower (-150) portion of the tolerance range. The effect on the stress intensity factor is somewhat less severe. Both of these situations have been found to contribute to the solution behavior at the upper limit of applicability.

From this it appears that very small tolerance limits are desirable. However, the solution time required to converge to very small tolerances may be restrictive. In general, the larger tolerances will yield good results for sufficiently large increment sizes, smaller tolerances may require smaller increments and correspondingly greater solution times. One further effect of the tolerance limit can be seen at the onset of closure. From Figure 5-1, the first solution point within the closure range predicted zero closure. The reason is that the nonlinear stiffnesses associated with closure resulted in an incremental displacement estimate which corresponded to a fully open crack configuration. The resulting residual forces were small enough to satisfy convergence requirements. A smaller tolerance limit will minimize the range of

closure length over which this can occur but it will not remove the possibility of occurence.

The stationary and progressive iteration schemes have been described in Section 4.2. Several analyses comparing the convergence characteristics of the two procedures have been performed. In each case, the convergence characteristics of the progressive iteration scheme exceeded those of the stationary scheme. Although the amount varied with the tolerance limit and the stiffness factor reduction technique, the progressive precedure resulted in consistently better convergence.

By far, the stiffness factor reduction technique was found to have the greatest impact on the line-spring model characteristics. In light of this, a significant number of reduction techniques have been considered as summarized below:

STIFFNESS FACTOR REDUCTION TECHNIQUE

Linear	to	$\zeta_c = 0.075$
"	to	$\zeta_c = 0.100$
"	to	$\zeta_c = \zeta_a$
Quadratic	to	$\zeta_c = 0.075$
"	to	$\zeta_c = \zeta_a$

In addition, constant factors were applied (no reduction) and the partially-closed stiffnesses were used directly. There was no clear effect of the factor reduction technique. In the example considered, linear reduction was applied over the total crack depth. For the same model, no reduction and quadratic reduction over the crack depth resulted in very different convergence behavior. Applying the partially-closed stiffnesses directly (i.e., a constant

factor of 1.0) had a second effect; the load at which closure began changed due to the difference between the fully-open and the partially-closed crack stiffness. However, it should be noted that over the applicable closure range for each reduction technique, the closure length estimate for the same load state were somewhat different. This difference is due in part to the increased or decreased effects of the tolerance limits and to the stiffness differences obtained by the reduction technique.

The effects of the three primary aspects of the partial crack closure implementation on the convergence characteristics of the nonlinear-elastic line-spring model can be summarized as follows:

- Large tolerance limits in conjunction with small increment sizes can result in oscillatory solution behavior.
- Progressive iteration is more advantageous than stationary iteration.
- The stiffness factor reduction technique has the most significant effect on convergence.
- The calculated closure length is affected more than the corresponding stress intensity factor.

A comparison of the gap model and shell model results presented in Figures 5-1 and 5-2 indicate that over the applicable range the two solutions give effectively the same results, especially for the stress intensity factor. The most dramatic difference between the two analyses is that of model complexity (Figures 4.4-2 and 4.4-3). The gap model consists of a relatively large number of 8-node plane strain elements in comparison to the shell model which consists of 6 8-node shell elements. The shell elements were chosen

because of their suitability in modeling cylindrical structures. Another advantage of the shell elements is that the nodal degrees of freedom are the same as for the line-spring element allowing for a simple and direct connection. A model consisting of plane strain elements and a line-spring element would require additional modeling effort associated with a larger number of elements necessary to model the cylinder and the definition of constraint equation connections between the line-spring element and the lower order palne strain elements. A caution associated with the shell elements is that the cylinder centerline is modeled such that the internal pressure must be modified to account for the actual pressure area. For very large radius to thickness cylinders this pressure load variation is not significant. However, for the example performed here the 5% difference could have a major influence considering the impact of the other factors already considered.

It was originally expected that the most significant gradients of the data would occur in the range of full closure as the cracked compliances must decrease to zero (and the stiffnesses must become infinite). As evidenced by the parametric data curves, Figures 3.2-4 through 3.2-9, the reverse is true; all curves show very smooth trends as full closure is approached. For the most part, the presence of the stiffness factor is due to the lack of parametric data available for interpolation in the small closure range. The evaluation of the partially-closed compliance matrix coefficients (equations 2.4-7) requires estimation of slopes and displacements of the parametric data curves. With reference to Figure 4.3-2, a very different displacement can be obtained depending on which

interpolation procedure is used. Similarly, slope estimates can be widely varied. The interpolation method used can result in a very different compliance matrix in this closure range. The differences decrease with increasing closure because of the smoother data curves obtained.

The results from the cases which have been examined by modifying the stiffness factor reduction technique, the iteration procedure and the tolerance limits indicate that the interpolation of the parametric data governs the convergence characteristics of the nonlinear-elastic line-spring model. The interpolation is most severly tested in the range of small closure where the parametric data curves are not well defined.

When the partially-closed stiffnesses are used throughout the analysis, a difference will exist in the load required to cause closure. For this reason it is advantageous to apply the stiffness factor. It is expected that additional small closure data will result in a more accurate estimate of the partially-closed stiffnesses and will minimize the effect of the stiffness factor. However, unless the partially-closed stiffness is to be applied at all time (i.e., the 0.0 closure stiffnesses apply for the fully-open crack as well), the stiffness factor will be necessary to assure continuity across the fully-open/partially-closed interface.

The implementation of additional parametric data or modifications in the stiffness factor reduction technique, should follow the procedure discussed in Appendix VI.

7. CONCLUSIONS

In this study, the linear-elastic line-spring model has been extended to include nonlinear-elastic response resulting from partial external closure of surface cracks. This enhanced model has been incorporated into the ABAQUS © finite element program. From the comparisons and discussion presented, the following conclusions are drawn.

1. Partial closure of an axially-cracked cylinder has been analyzed using both a highly detailed model consisting of plane strain elements and gap elements and a very simple model consisting of several shell elements and a single nonlinear-elastic line-spring. The two methods result in essentially the same variations in closure length and stress intensity factor with variations in the applied loads.
2. A progressive iteration scheme requires storage of intermediate displacements, forces and stiffnesses. Despite this increased recordkeeping, progressive iteration is more advantageous than stationary iteration due to its inherently better convergence characteristics.
3. The effect of crack closure on the stress intensity factor is dramatic. An order of magnitude difference in the stress intensity factor between the linear and the nonlinear solutions can be obtained within a closure length equal to 1/3 of the crack depth.
4. The nonlinear-elastic line-spring model is applicable over a limited range of closure. The actual range varies with

several factors. However, the primary cause is considered to be the lack of parametric data available for interpolation. The lack of data is most severe in the small closure range where the largest variations in the displacement contributions occur.

In general, the newly developed nonlinear-elastic line-spring model is a viable alternative to highly detailed finite element models in analyzing partial external closure of surface cracks in plates and shells.

For future consideration it is expected that additional parametric data is required, primarily in the small closure range, to fully utilize the nonlinear-elastic line-spring model.

REFERENCES

1. Bueckner, H.F., "Weight Functions for the Notched Bar", General Electric Company, Large Steam Turbine-Generator Department, Technical Report 69-LS-45, May 12, 1969.

2. Mattheck, C., Munz, D., and Stamm, H., "Stress Intensity Factor for Semi-Elliptical Surface Cracks Loaded by Stress Gradients", submitted to Engineering, Fracture Mechanics, 1982.

3. Mattheck, C., Morawietz, P. and Munz, D., "Stress Intensity Factor of Semi-Elliptical Surface Crack in Plates Exposed to Stress Gradients", submitted to International Journal of Fracture, 1982.

4. Rice, J.R., and Levy, N., "The Part-Through Surface Crack in an Elastic Plate", Journal of Applied Mechanics, V. 39, 1972, pp 185-194.

5. Parks, D.M., Lockett, R.R., and Brokenbrough, J.R., "Stress Intensity Factors for Surface-Cracked Plates and Cylindrical Shells Using Line-Spring Finite Elements", in 1981 Advances in Aerospace Structures and Materials, AD-01, Eds. S.S. Wang and W.J. Renton, American Society of Mechanical Engineers, 1981, pp. 279-285.

6. Parks, D.M., "The Inelastic Line-Spring: Estimates of Elastic-Plastic Fracture Mechanics Parameters for Surface-Cracked Plates and Shells", Journal of Pressure Vessel Technology, V. 103, 1981, pp 246-264.

7. Parks, D.M., and White, C.S., "Elastic-Plastic Line-Spring Finite Elements for Surface-Cracked Plates and Shells", Journal of Pressure Vessel Technology, V. 104, 1982, pp. 287-292.

8. Parks, D.M., "The Inelastic Line-Spring", in Proceedings of the Ninth U.S. National Congress of Theoretical and Applied Mechanics, Ed. Y.H. Pao et. al., ASME, 1982, pp 135-142.

9. Burniston, E.E., "An Example of a Partially Closed Griffith Crack", International Journal of Fracture Mechanics, Vol. 5, March, 1969, pp. 17-24.

10. Tweed, J., "The Determination of the Stress Intensity Factor of a Partially Closed Griffith Crack", International Journal of Engineering Sciences, Vol. 8, 1970 pp 792-803.

11. Thresher, R.W. and Smith, F.W., "The Partially Closed Griffith Crack", International Journal of Fracture, Vol. 9, March, 1973, pp. 33-41.

12. Bowie, O.L. and Freese, C.E., "On the 'Overlapping' Problem in Crack Analysis", Engineering Fracture Mechanics, Vol. 8, 1976. pp 373-379.

13. Paris, P.C. and Tada, H., "The Stress Intensity Factors for Cyclic Reversed Bending of a Single Edge Cracked Strip Including Crack Surface Interference", International Journal of Fracture, Vol. 11, 1975, pp. 1070-1072.

14. Bowie, O.L. and Freese, C.E., "A Note on the Bending of a Cracked Strip Including Crack Surface Interference", International Journal of Fracture, Vol. 12, 1976, pp. 457-459.

15. Gustafson, C.G., "Discussion: 'The Stress Intensity Factors for Cyclic Reversed Bending of a Single Edge Cracked Strip Including Crack Surfaces Interference', P.C. Paris and H. Tada", International Journal of Engineering Sciences, Vol. 8 1979 pp. 793-803.

16. Chen, B.S., "The Effects of Residual Stresses on Stress Intensity Factors Using the Line-Spring Model", BSME Degree Thesis, MIT, 1982.

17. White, C.S., "Elastic-Plastic Analysis of Surface Cracks", MSME Degree Thesis, MIT Department of Mechanical Engineering, 1982.

18. Rice, J.R., "Some Remarks on Elastic Crack Tip Fields", International Journal of Solids and Structures, Vol, 8, 1972, pp. 751-758.

19. Parmerter, R. Reid, and Mukherji, B., "Stress Intensity Factors for an Edge-Cracked Strip in Bending", International Journal of Fracture, Vol 10, 1974, pp 441-444.

20. Tada, H., Paris, P., and Irwin, G.R.. "The Stress Analysis of Cracks Handbook", Del Research Corporation, Bethlehem, 1973.

21. ABAQUS User's Manual, Hibbitt, Karlsson and Sorensen, Providence, RI, July, 1982.

22. Isida, M., Noguchi, H., and Yoshida, T., "Tension and Bending of Finite Thickness Plates with a Semi-Elliptical Surface Crack", International Journal of Fracture, Vol. 26, 1984, pp. 157-188.

23. Dunders, J. and Comninou, M., "On the Exterior Crack with Contact Zones", International Journal of Engineering Science, Vol. 21, No. 3, 1983, pp. 223-230.

24. Roark, F.J. and Young, W.C., Formulas for Stress and Strain, 5th ed., McGraw-Hill Book Company, 1975.

APPENDIX I

CLOSURE MODE - INTERNAL CRACK CLOSURE

The closure mode which is the subject of this analysis is that where the crack mouth closes first and closure progresses toward the crack tip. It has been noted that this mode of closure requires a closing (negative) bending moment and either a tensile (positive) or compressive membrane force. If an opening bending moment is applied a compressive membrane force is required to close the crack. The resulting closure begins at the crack tip and progresses toward the mouth. In this mode a cusp is formed at the crack tip. Applying superposition of the stress intensity factor gives:

$$K_I = Nk'_N + Mk'_N = 0. \qquad \text{(I-1)}$$

Defining $\bar{\lambda}_k$ to be the load ratio required to satisfy equation (I-1) the result becomes

$$\bar{\lambda}_k = -6 \frac{0.923 + 0.199(1-\sin \phi)^4}{0.752 + 2.02\, \xi_a + 0.37(1-\sin \phi)^3} \qquad \text{(I-2)}$$

where k'_N and k'_M are obtained from Tada et al [20] and $\phi = \pi \xi_a / 2$.

Figure I-1 presents the load ratio required for the onset of internal ($\bar{\lambda}_k$) and external ($\bar{\lambda}_{crit}$) closure versus crack depth. To determine which closure mode occurs first under various loading combinations the crack opening displacement profile and the stress intensity factor are required. The findings are as follows:

Case 1 - $N > 0$, $M > 0$ No closure of either type.

FIGURE I-1
CRACK CLOSURE MODE
CRITICAL LOAD RATIO vs CRACK DEPTH

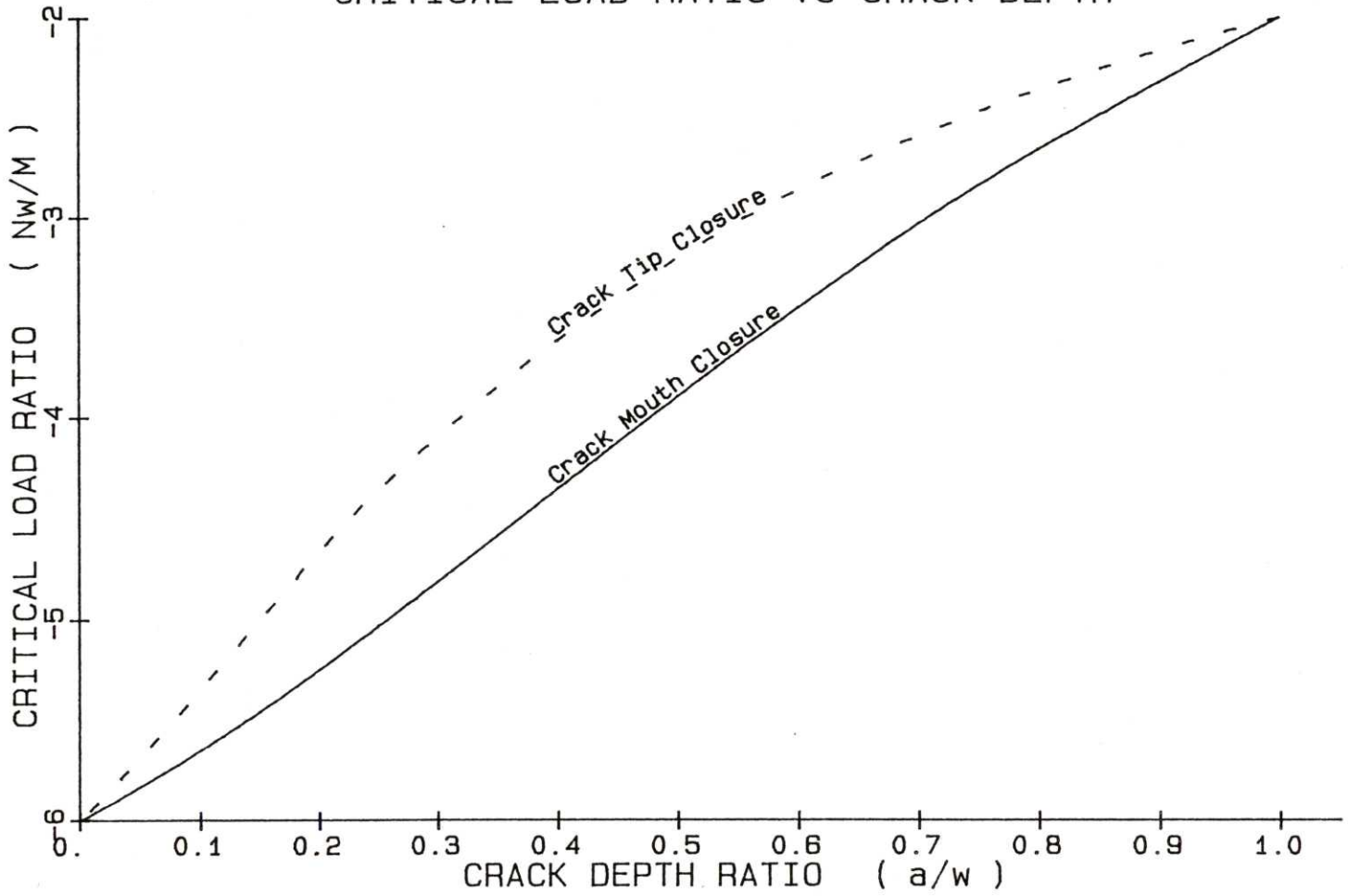

Case 2 - $N>0$, $M<0$	$\bar{\lambda}=\bar{\lambda}_k$ - overlapping C.O.D.
	$\bar{\lambda}=\bar{\lambda}_{crit}$ - positive SIF.
Case 3 - $N<0$, $M>0$	$\bar{\lambda}=\bar{\lambda}_k$ - separating C.O.D.
	$\bar{\lambda}=\bar{\lambda}_{crit}$ - negative SIF.
Case 4 - $N<0$, $M<0$	Full external closure ($\xi_a \leq 0.5$).
	Possible full external closure
	($\xi_a > 0.5$).

In summary, the closure mode is dependent only upon the applied bending moment. For a closing (negative) moment closure begins at the crack mouth. For an opening moment closure begins at the crack tip.

APPENDIX II

REDUCTION OF PARAMETRIC DATA

Reduction of the parametric finite element data was discussed in Sections 3.2 and 3.3. At this time the actual data reduction will be performed on the data for a crack depth of 0.100.

For this crack depth three closure lengths were modeled; 0.0^-(fully open), 0.0^+ and 0.05. The uncracked contributions to the far-field deflections are 0.091 due to a unit membrane force and 1.092 due to a unit bending moment (equation 2.1-3) with E'=30/0.91 and w = 1.0.

Before proceeding with the actual data reduction the differences between the "modeled", "effective" and "actual" closure lengths should be discussed. Consider a portion of the finite element model presented in Figure 3.2-3. The "modeled" closure length is just that, the amount of closure corresponding to node i of the model. For 0.0^- modeled closure, i = 0; for 0.0^+ modeled closure, i = 1; etc. The "effective" closure length correpsonds to the closure at node i+1 and applies to the displacement contributions ($\delta_N, \delta_M = \theta_N, \theta_M$). With a given modeled closure (to node i) the model characteristics remain constant until the gap COD_{i+1} is zero. At this point the characteristics will change, again to remain constant until gap COD_{i+2} closes. Therefore, the displacement contributions for the effective closure length correspond to those for the modeled length. The "actual" closure length also corresponds to the closure at node i+1. However, it applies to the total displacements and stress intensity factor (δ^M, θ^M and k^M).

These values, as described in Sections 2.4 and 3.3 combine the displacement and SIF contributions corresponding to the modeled closure length. In summary, the term "effective" simply implies that the displacement contributions are applicable over the entire closure range from node i to node i+1 and are dependent on the finite element mesh size.

For the 0.0^- and 0.0^+ modeled closure lengths (0.0^+ and 0.025 effective) the data reduction is presented in Tables II-1 and II-2. Note that $k_{rat,N}$ and $k_{rat,M}$ relate the K_{IN} and K_{IM} estimates from the finite element analysis to those from reference [20] (Table 3.3-2). For the case of 0.05 closure a different approach is required. Consider the 0.05 closure model of Figure II-1. Application of equation (3.2-1) results in a load ratio of $\bar{\lambda} = -5.1$ with a closure length of 0.075 (node 4). However if node 4 has closed, then, to the accuracy of the finite element model, the crack is fully closed. From equation (2.3-9), full closure occurs at a load ratio of -4.8. The discrepancy lies in that what appears to be full closure as far as the model is concerned in reality represents the presence of a crack between nodes 4 and 5 (i.e., no traction is present on the surface between nodes 4 and 5).

Since full closure has in reality occured, the 0.05 modeled closure length data is neglected in favor of the full closure characteristics. This effect occurs for all crack depths.

Table II-3 presents a complete list of the reduced parametric data requred for the partial closure routines.

TABLE II-1

DATA REDUCTION FOR 0.0^- CLOSURE

CRACK DEPTH - 0.10

MODELED CLOSURE LENGTH - 0.0^-

Displacement (Far-Field)	0.091569 (N)	0.003152 (M)
Rotation (Far-Field)	0.003152 (N)	1.109473 (M)
COD_{i+1}	0.00847 (N)	0.049961 (M)
J-Integral	0.012948 (N)	0.3707 (M)

EFFECTIVE CLOSURE LENGTH - 0.0^+

$\frac{1}{2}\delta_N = E'(.091569-.091) = 0.01876$

$\frac{1}{2}\delta_M = \frac{1}{2}\Theta_N = E'(0.003152) = 0.10392$

$\frac{1}{2}\Theta_M = E'(1.109473-1.092) = 0.57603$

ACTUAL CLOSURE LENGTH - 0.0^+

$\bar{\lambda} = -0.049961/0.008847 = -5.64708$

$\frac{1}{2}\delta^M = \frac{1}{2}\delta_N \bar{\lambda} + \frac{1}{2}\delta_M = -0.002037$

$\frac{1}{2}\Theta^M = \frac{1}{2}\Theta_N \bar{\lambda} + \frac{1}{2}\Theta_M = -0.010819$

$k_{rat,N} = 0.6702/0.6533 = 1.0259$

$k_{rat,M} = 3.5003/3.4958 = 1.0013$

$k^M = \bar{\lambda}\, k_{rat,N} \sqrt{E'(0.012948)} + k_{rat,M} \sqrt{E'(0.3707)} = -0.28437$

TABLE II-2

DATA REDUCTION FOR 0.0^+ CLOSURE

CRACK DEPTH - 0.10

MODELED CLOSURE LENGTH - 0.0^+

Displacement (Far-Field)	0.091277 (N)	0.001502 (M)
Rotation (Far-Field)	0.001502 (N)	1.100153 (M)
COD_{i+1}	0.003536 (N)	0.019528 (M)
J-Integral	0.006561 (N)	0.1774 (M)

EFFECTIVE CLOSURE LENGTH - 0.025

$\frac{1}{2}\delta_N$ = E'(.091277-.091) = 0.00913

$\frac{1}{2}\delta_M = \frac{1}{2}\Theta_N$ = E'(0.001502) = 0.04951

$\frac{1}{2}\Theta_M$ = E'(1.100153-1.092) = 0.26879

ACTUAL CLOSURE LENGTH - 0.025

$\bar{\lambda}$ = -0.019528/0.003536 = -5.52209

$\frac{1}{2}\delta^M = \frac{1}{2}\delta_N \bar{\lambda} + \frac{1}{2}\delta_M$ = -0.00090

$\frac{1}{2}\Theta^M = \frac{1}{2}\Theta_N \bar{\lambda} + \frac{1}{2}\Theta_M$ = -0.00463

$k_{rat,N}$ = 0.6702/0.6533 = 1.0259

$k_{rat,M}$ = 3.5003/3.4958 = 1.0013

$k^M = \bar{\lambda}\, k_{rat,N} \sqrt{E'(0.006561)} + k_{rat,M} \sqrt{E'(0.1774)}$ = -0.21326

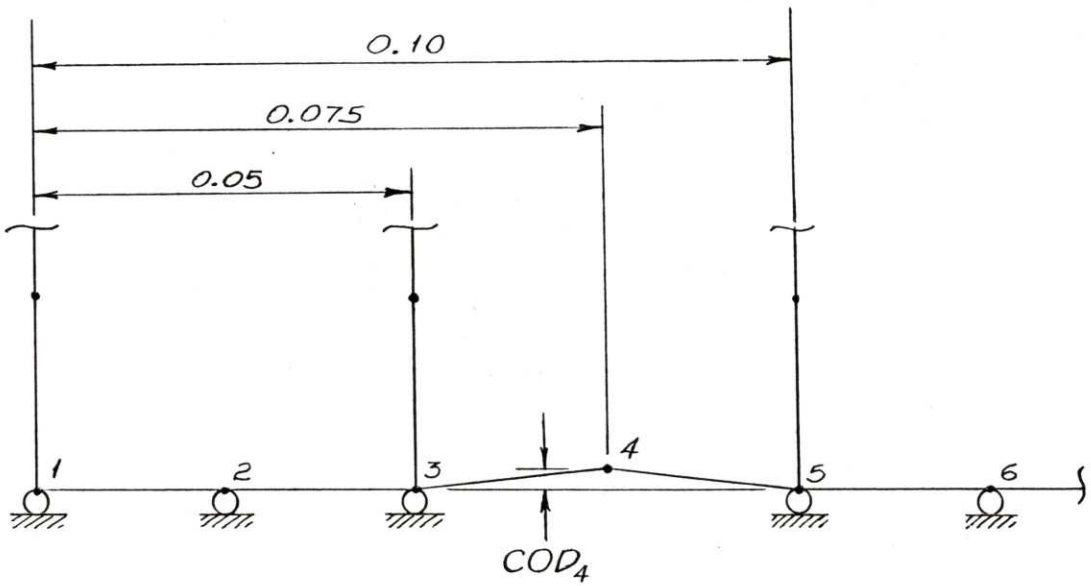

Figure II-1

Finite Element Model in the Vicinity of Modeled Closure Length 0.05
with Crack Depth Ratio of 0.100

TABLE II-3
PARTIAL CRACK CLOSURE - PARAMETRIC DATA

Number of Discreet Data Points Available for Crack Depth Ratio

0.1	0.2	0.3	0.4	0.5	0.6	0.7	0.8
3	5	7	9	11	13	15	17

Crack Depth = 0.10

$\bar{\lambda}_{crit}$	ξ_c	$\delta^M/2$	$\theta^M/2$	k^M	$\delta_N/2$	$\delta_M/2$	$\theta_M/2$
-5.64708	.000	-2.0371E-3	-1.0819E-2	-.28437	.0187634	.1039211	.5760317
-5.52209	.025	-8.9607E-4	-4.6304E-3	-.21326	.0091287	.0495130	.2687900
-4.80000	.100	0.0000000	0.0000000	.00000	.0000000	.0000000	.0000000

Crack Depth = 0.20

$\bar{\lambda}_{crit}$	ξ_c	$\delta^M/2$	$\theta^M/2$	k^M	$\delta_N/2$	$\delta_M/2$	$\theta_M/2$
-5.24679	.000	-1.7614E-2	-8.0639E-2	-.75905	.0922415	.4663580	2.366244
-5.13448	.025	-1.2219E-2	-5.4311E-2	-.63228	.0480350	.2344200	1.149300
-4.76670	.075	-4.4843E-3	-1.8879E-2	-.39294	.0172090	.0775440	.3507500
-4.33957	.125	-9.0437E-4	-3.5887E-3	-.19343	.0065008	.0273060	.1149100
-3.60000	.200	0.0000000	0.0000000	.00000	.0000000	.0000000	.0000000

Crack Depth = 0.30

$\bar{\lambda}_{crit}$	ξ_c	$\delta^M/2$	$\theta^M/2$	k^M	$\delta_N/2$	$\delta_M/2$	$\theta_M/2$
-4.81112	.000	-6.0228E-2	-2.3167E-1	-1.3360	.2651587	1.215482	5.616157
-4.71098	.025	-4.7201E-2	-1.7503E-1	-1.1582	.1300800	.5656100	2.489500
-4.38720	.075	-2.6125E-2	-9.0642E-2	-.86567	.0563050	.2209000	.8784800
-4.00480	.125	-1.2443E-2	-4.0326E-2	-.60850	.0311660	.1123700	.4096900
-3.58532	.175	-4.5211E-3	-1.3609E-2	-.37863	.0159090	.0525170	.1746800
-3.14211	.225	-9.0525E-4	-2.5065E-3	-.18291	.0063747	.0191250	.0575860
-2.40000	.300	0.0000000	0.0000000	.00000	.0000000	.0000000	.0000000

Crack Depth = 0.40

$\bar{\lambda}_{crit}$	ξ_c	$\delta^M/2$	$\theta^M/2$	k^M	$\delta_N/2$	$\delta_M/2$	$\theta_M/2$
-4.35286	.000	-1.4209E-1	-4.4258E-1	-1.9828	.6401989	2.644603	11.06900
-4.26558	.025	-1.1832E-1	-3.5147E-1	-1.7539	.2724800	1.044000	4.101700
-3.97712	.075	-7.7615E-2	-2.1143E-1	-1.4235	.1243000	.4167300	1.445900
-3.63400	.125	-4.7966E-2	-1.1972E-1	-1.1296	.0779270	.2352200	.7350600
-3.24489	.175	-2.6575E-2	-6.0300E-2	-.84978	.0493520	.1335700	.3731100
-2.82582	.225	-1.2526E-2	-2.5565E-2	-.59034	.0295510	.0709800	.1750100
-2.39119	.275	-4.5296E-3	-8.1993E-3	-.36201	.0155790	.0327220	.0700460

TABLE II-3
PARTIAL CRACK CLOSURE - PARAMETRIC DATA
(continued)

-1.94302	.325	-9.0543E-4	-1.4209E-3	-.17001	.0063326	.0113990	.0207270
-1.20000	.400	0.0000000	0.0000000	.00000	.0000000	.0000000	.0000000

Crack Depth = 0.50

$\bar{\lambda}_{crit}$	ξ_c	$\delta^M/2$	$\theta^M/2$	k^M	$\delta_N/2$	$\delta_M/2$	$\theta_M/2$
-3.89162	.000	-2.7534E-1	-6.5594E-1	-2.6925	1.460995	5.410300	20.39889
-3.81571	.025	-2.3798E-1	-5.3147E-1	-2.4105	.4920900	1.639700	5.725100
-3.55408	.075	-1.7148E-1	-3.3919E-1	-2.0591	.2257200	.6307500	1.902500
-3.24200	.125	-1.2036E-1	-2.1047E-1	-1.7413	.1500900	.3662200	.9768100
-2.88163	.175	-7.9582E-2	-1.2114E-1	-1.4251	.1041200	.2204700	.5141600
-2.48636	.225	-4.8657E-2	-6.3056E-2	-1.1196	.0716280	.1294400	.2587700
-2.06796	.275	-2.6759E-2	-2.8608E-2	-.83550	.0473250	.0711090	.1184400
-1.63435	.325	-1.2562E-2	-1.0563E-2	-.57530	.0289710	.0347860	.0462900
-1.19356	.375	-4.5336E-3	-2.7664E-3	-.34820	.0154520	.0139090	.0138350
-0.74337	.425	-9.0548E-4	-3.3448E-4	-.16057	.0063165	.0037900	.0024829
0.00000	.500	0.0000000	0.0000000	.00000	.0000000	.0000000	.0000000

Crack Depth = 0.60

$\bar{\lambda}_{crit}$	ξ_c	$\delta^M/2$	$\theta^M/2$	k^M	$\delta_N/2$	$\delta_M/2$	$\theta_M/2$
-3.44645	.000	-4.7628E-1	-7.8557E-1	-3.4946	3.374369	11.15332	37.65377
-3.37874	.025	-4.2227E-1	-6.3167E-1	-3.1624	.7976900	2.272900	7.048000
-3.13426	.075	-3.2279E-1	-3.9773E-1	-2.7976	.3630000	.8149600	2.156600
-2.84305	.125	-2.4403E-1	-2.4415E-1	-2.4578	.2501600	.4672000	1.084100
-2.50443	.175	-1.7767E-1	-1.3749E-1	-2.1113	.1827300	.2799700	.5636700
-2.12905	.225	-1.2337E-1	-6.7611E-2	-1.7667	.1349000	.1638300	.2812000
-1.72738	.275	-8.0800E-2	-2.6034E-2	-1.3605	.0983610	.0891070	.1278900
-1.30774	.325	-4.9078E-2	-4.7092E-3	-1.1148	.0695410	.0418640	.0500370
-0.87642	.375	-2.6878E-2	3.5180E-3	-.82275	.0466650	.0140210	.0150860
-0.43689	.425	-1.2587E-2	4.5196E-3	-.56311	.0288100	.0000000	.0045196
0.00602	.475	-4.5366E-3	2.6758E-3	-.33804	.0154290	-.0046295	.0027036
0.45665	.525	-9.0544E-4	7.5226E-4	-.14939	.0063165	-.0037899	.0024829
1.20000	.600	0.0000000	0.0000000	.00000	.0000000	.0000000	.0000000

Crack Depth = 0.70

$\bar{\lambda}_{crit}$	ξ_c	$\delta^M/2$	$\theta^M/2$	k^M	$\delta_N/2$	$\delta_M/2$	$\theta_M/2$
-3.03154	.000	-7.7607E-1	-7.1091E-1	-4.4927	8.445548	24.82695	74.55299
-2.96777	.025	-7.0055E-1	-5.3147E-1	-4.1000	1.184800	2.815600	7.824600
-2.72858	.075	-5.5677E-1	-2.7089E-1	-3.7147	.5386900	.9130900	2.220600
-2.44620	.125	-4.4094E-1	-1.1111E-1	-3.3391	.3820800	.4937100	1.096600
-2.11894	.175	-3.4027E-1	-8.3404E-3	-2.9518	.2894000	.2729500	.5700200
-1.75586	.225	-2.5423E-1	5.1161E-2	-2.5592	.2234400	.1381100	.2936600

TABLE II-3
PARTIAL CRACK CLOSURE - PARAMETRIC DATA
(continued)

-1.36644	.275	-1.8292E-1	7.8043E-2	-2.1723	.1724300	.0526920	.1500400
-0.95859	.325	-1.2582E-1	8.2055E-2	-1.7999	.1312600	.0000000	.0820550
-0.53820	.375	-8.1836E-2	7.1846E-2	-1.4485	.0974130	-.0294090	.0560180
-0.10926	.425	-4.9462E-2	5.4612E-2	-1.1228	.0695410	-.0418630	.0500370
0.32551	.475	-2.6996E-2	3.5929E-2	-.82670	.0468750	-.0422540	.0496830
0.76535	.525	-1.2614E-2	1.9666E-2	-.56283	.0289710	-.0347860	.0462900
1.20734	.575	-4.5402E-3	8.1266E-3	-.33586	.0154990	-.0232530	.0362010
1.65702	.625	-9.0554E-4	1.8394E-3	-.14735	.0063326	-.0113990	.0207270
2.40000	.700	0.0000000	0.0000000	.00000	.0000000	.0000000	.0000000

Crack Depth = 0.80

$\bar{\lambda}_{crit}$	ξ_c	$\delta^M/2$	$\theta^M/2$	k^M	$\delta_N/2$	$\delta_M/2$	$\theta_M/2$
-2.65483	.000	-1.2525000	-2.2619E-1	-6.0106	25.69929	66.97476	177.5804
-2.58921	.025	-1.1446000	-2.2047E-2	-5.4998	1.645400	3.115700	8.045000
-2.33836	.075	-9.3191E-1	2.4371E-1	-5.0432	.7649000	.8567100	2.247000
-2.04842	.125	-7.5900E-1	3.7913E-1	-4.5891	.5591900	.3864600	1.170800
-1.71790	.175	-6.0655E-1	4.4165E-1	-4.1162	.4370700	.1443000	.6895500
-1.35542	.225	-4.7337E-1	4.5156E-1	-3.6361	.3492500	.0000000	.4515600
-0.96994	.275	-3.5972E-1	4.2403E-1	-3.1617	.2802400	-.0878970	.3387700
-0.56890	.325	-2.6522E-1	3.7222E-1	-2.7035	.2234400	-.1381100	.2936600
-0.15769	.375	-1.8878E-1	3.0737E-1	-2.2682	.1755700	-.1610900	.2819600
0.26018	.425	-1.2874E-1	2.3857E-1	-1.8627	.1349000	-.1638300	.2812000
0.68268	.475	-8.3166E-2	1.7287E-1	-1.4874	.1004400	-.1517300	.2764500
1.10903	.525	-4.9998E-2	1.1522E-1	-1.1464	.0716280	-.1294300	.2587700
1.53896	.575	-2.7177E-2	7.8788E-2	-.83979	.0480930	-.1011900	.2245100
1.97352	.625	-1.2660E-2	3.4932E-2	-.56982	.0295510	-.0709800	.1750100
2.41111	.675	-4.5475E-3	1.3597E-2	-.33894	.0157040	-.0424120	.1158600
2.85799	.725	-9.0579E-4	2.9277E-3	-.14829	.0063747	-.0191250	.0575860
3.60000	.800	0.0000000	0.0000000	.00000	.0000000	.0000000	.0000000

Data for 99% Closure for Each Crack Depth

$\bar{\lambda}$	$\partial\xi_c/\partial\bar{\lambda}$
-4.81198	.083574
-3.62382	.084625
-2.43558	.085326
-1.24724	.086008
-.058824	.086683
1.12968	.087355
2.31828	.088020
3.46572	.088685

APPENDIX III

MODIFIED MATLS ROUTINE

A listing of the modified version of MATLS is contained on the following pages. The modifications are lumped into five major blocks, each identified on the listing. A brief description of the function of each block is given below.

Block A - Storage Initialization

Storage locations are dimensioned for up to 30 nodes connected to line-spring elements. The discrete parametric data will be stored in arrays CJ, ALAM9, and SXIC9. Arrays STF_, EEPR_, FOR_, STF_A, and EE1_A are used for storage of stiffnesses, displacements and forces at various intermediate solution states.

Block B - Data Initialization/Update

Discrete parametric data are read from an external file and stored in the arrays CJ, ALAM9 and SXIC9. Array NPT contains the number of parametric data points which are available for each crack depth analyzed. Subroutine INIT determines the number of line-spring element nodes and initializes and updates several of the arrays (see Appendix IV).

Block C - Data Initialization/Update

The variables FC1, FC2, and FC3 are factors which multiply the partially-closed crack stiffnesses to ensure continuity across the fully-open/partially-closed interface. This topic is described in more detail in Section 4.2 and in the Discussion.

Block D - Closure Check/Evaluation and Data Update

A linear solution is obtained (array SE1) to determine if closure will occur. Three possibilities exist at this point. If closure is predicted but incremental displacements are zero (ICOUNT = 1 from subroutine INIT) then this is a first pass through after a converged increment. In this case the stiffnesses are updated and the closure routines are bypassed. If closure is predicted and the incremental displacements are non-zero then the closure routines are called and the closure characteristics are evaluated. If closure is not predicted the linear solution scheme is continued. Also, if closure is predicted but, due to the convergence tolerance limits, an "open crack" solution is obtained, the stress intensity factor is evaluated linearly.

Block E - Data Update

If no closure is predicted in block D the arguments of subroutine INIT1 are updated. This update is performed within block D if closure occurs.

Subroutine MATLS

```
      SUBROUTINE MATLS(JMATYP,AMK,AMPK,TEMP,DTEMP,EVAL,AMTAB,EPAR,
     1A,C,EE1,DEE1,DSE1,AMKO,GELA,S1,SVAR)
      IMPLICIT REAL*8(A-H,O-Z)
      DIMENSION JMATYP(2,1)
      DIMENSION AMK(1),AMPK(1),TEMP(1),DTEMP(1),EVAL(1),AMTAB(1),
     1EPAR(1),A(1),C(1),EE1(1),DEE1(1),DSE1(1),AMKO(1),GELA(1),
     2S1(1),SVAR(1)
C*********************************************************************
      DIMENSION CJ(8,17,10),SE1(2),ALAM9(8),SXIC9(8),NPT(8)
      DIMENSION STF11(30),STF12(30),STF22(30),EEPR1(30),EEPR2(30)
     1,FORN(30),FORM(30),STF11A(30),STF12A(30),STF22A(30)
     2,EE11A(30),EE12A(30),KFCL(30)
C
      COMMON /JJL/CJ,THCK,XIA,EPRIME,NPT /LOC/ICL,ICLP
      COMMON /RNGE/ALAM1,ALAM2,ALAM9,SXIC9 /FCT/FC1,FC2,FC3
C*********************************************************************
      COMMON/CEL/LELOP,JETP,JETP1,KEL,KINTK,KINTL,KINTSL,KSPT,NEMCRD,
     1 JINTYP,JEXTYP,JEXTY2,JLIB,NAN24,MDOF,MCRD,
     1 NNODE,NNODU,NTENS,NDI,NSHR,NPR,NINTK,NINTM,NINTSL,NINTLL,NMP,
     4 NPARS,NSHL,NBM,NELZM,NINTTS,NEINT,NDOFEL,JUNSYM,NEGEOM,
     5 LNODEK,NNODEP,LBASIS,NNODET,NTENST,NTDOFN,LLUMPM,NOFFT,
     1 NSPT,NNOD2,NNOD3,NNOD4,NTDOFE,KSPTT
      COMMON/CMATS/JMATP,NMPROP,LCONFA,LGSECT,AMPTEM,
     1 LACTP1,JELA,JEXP,JHARD,JCREEP,JSWELL,JVISCP,JHYPO,JPERMB,
     2 JSOILE,SLAMDA,SKAPPA,SMRAT2,SVOID0,SVOID1,SCONST,
     3 JFRIC,LNOTC,JORNL,LUNSMD,LCONCR,LMROT,JCRK,NCRKS,LCRKD(3)
     4,LMORI,LUNSMT,NTENSA,NDIA,NSHRA,LNWCRK
      COMMON/CMATSZ/NMVARB,NMZ
      COMMON/CONSTS/PI,SIN60,COS60,KCROS2(3),KCROS3(3),ZERO,LZERO,LONE,
     1 ONE,TWO,HALF,ABIG,ASMALL,BCBIG,LOCSHR(2,3),THIRD,PRECIS,BLANK
      COMMON/CSMDB/IECR,IESW,IEPL,ISTRE,IPDISS,ICDISS,IEHAT,IORIG,
     1 IORNL,ISTVAR,IIRSET,ICONFA
C
C*********************************************************************
      DATA ITTHL,ITTH /0,0/
      IF (ITTHL.EQ.0) THEN
         READ(90,*) (NPT(I),I=1,8)
         DO 75 I=1,8
            DO 76 J=1,NPT(I)
               READ(90,*) (CJ(I,J,K),K=1,10)
 76            CONTINUE
 75         CONTINUE
         DO 77 I=1,8
            READ(90,*) ALAM9(I),SXIC9(I)
 77         CONTINUE
         XIC=ZERO
         SVAR(3)=ZERO
         SVAR(4)=ZERO
      END IF
```

```
      CALL INIT(ITTHL,ITTH,ICNT,ICLCNT,EE1,DEE1,EE11A,EE12A,STF11,
     1STF12,STF22,STF11A,STF12A,STF22A)
      THCK=EPAR(2)
      DEPTH=A(NMVARB)
      XIA=DABS(DEPTH/EPAR(2))
      ICL=10*XIA
      ICLP=ICL+1
      ALAM1=(CJ(ICLP,1,3)-CJ(ICL,1,3))*(10.D0*XIA-ICL)+CJ(ICL,1,3)
      ALAM2=6.D0*(2.D0*XIA-1.D0)
C*********************************************************************
      I1=6
      DO 10 K=1,NMPROP
      JPROP=JMATYP(1,I1)
      IF(JPROP.EQ.1) GO TO 11
         I1=I1+2
   10    CONTINUE
         GO TO 990
   11    CONTINUE
      DO 201 K1=1,NMZ
         AMK(K1)=ZERO
  201    CONTINUE
      IADDR=JMATYP(1,I1+1)
      NPDEP=JMATYP(1,IADDR)
      ICOLS=IADDR+1+NPDEP
      NCOLS=JMATYP(1,ICOLS)
   21 CONTINUE
      NROWS=JMATYP(1,ICOLS+1)
      NEVAL=2
      CALL TABVAL(JMATYP(1,ICOLS+2),EVAL,TEMP,NROWS,NCOLS,NEVAL,NPDEP,
     1AMTAB)
      CALL MATLS1(EVAL,AMK,DEPTH,EPAR(2),C(2),C(101),C(200),C(299),
     1C(398),C(497))
      EPRIME=EVAL(1)/(ONE-EVAL(2)**2)
C*********************************************************************
      CALL CLOSE(XIC,SXIC,KCL,ALAM1)
      CALL COMPL(XIC,SXIC,PDM,PRM,ALAM1,C11,C12,C21,C22,CM,KDEFI,
     1KDEFIP)
      FC1=AMK(1)/(CM*C22)
      FC2=-AMK(2)/(CM*C12)
      FC3=AMK(3)/(CM*C11)
      IF (DEPTH.LT.ZERO) FC2=-FC2
C*********************************************************************
      DO 23 K1=1,NMZ
         AMPK(K1)=AMK(K1)
   23    CONTINUE
      IF(DTEMP(1).EQ.ZERO) GO TO 50
   24    CONTINUE
      IF(NCOLS.LT.2) GO TO 50
      DO 25 K=1,NMVARB
```

B

C

```
         IF(EE1(K).NE.ZERO) GO TO 26
   25    CONTINUE
      GO TO 50
   26    CONTINUE
      TT=TEMP(1)-DTEMP(1)
      CALL TABVAL(JMATYP(1,ICOLS+2),EVAL,TT,NROWS,NCOLS,NEVAL,NPDEP,
     1AMTAB)
      CALL MATLS1(EVAL,AMKO,DEPTH,EPAR(2),C(2),C(101),C(200),C(299),
     1C(398),C(497))
      DO 46 K1=1,NMZ
         AMKO(K1)=AMPK(K1)-AMKO(K1)
   46    CONTINUE
      CALL ASET(GELA,ZERO,NMVARB)
      CALL APRDTA(AMKO,EE1,GELA,NMVARB)
      DO 47 K1=1,NMVARB
         DSE1(K1)=DSE1(K1)+GELA(K1)
   47    CONTINUE
   50    CONTINUE
      DO 51 K1=1,NMVARB
         EE1(K1)=EE1(K1)+DEE1(K1)
   51    CONTINUE
C*******************************************************************************
      SE1(1)=ZERO
      SE1(2)=ZERO
      CALL APRDTA(AMPK,EE1,SE1,NMVARB)
      IF (SE1(2)*DEPTH.GE.ZERO) GOTO 52
      ALMBDA=SE1(1)*EPAR(2)/SE1(2)
      IF (DEPTH.LT.ZERO) ALMBDA=-ALMBDA
      IF (ALMBDA.LT.ALAM1) GOTO 52
      IF (ICLCNT.EQ.1) THEN
         CALL ICOUNT(ICNT,ICLCNT,AMK,AMPK,STF11A,STF12A,STF22A)
         GOTO 52
      END IF
      IF (FM.EQ.ZERO.AND.FN.EQ.ZERO) THEN
         WRITE(6,100)
 100     FORMAT(' ','THE FIRST LOAD STEP INCREMENT OF THE ANALYSIS
     1 HAS RESULTED IN CLOSURE'//2X,'THE PARTIAL CLOSURE ROUTINES
     2 REQUIRE A PREVIOUSLY CONVERGED (LINEAR) SOLUTION'//2X,'PLEA
     3SE REDEFINE THE LOADS SO A LINEAR SOLUTION WILL BE OBTAINED')
         GOTO 999
      END IF
      CALL PRTCLL(ICNT,EE1,DEE1,S1,DSE1,AMK,AMPK,A(2),STF11,STF12,
     1STF22,FORN,FORM,EEPR1,EEPR2,KFCL,DEPTH,NMVARB,XIC,THCK,KCL)
      SVAR(3)=XIC
      IF (KCL.EQ.-1) GOTO 53
      GOTO 60
   52    CONTINUE
      SVAR(3)=ZERO
C*******************************************************************************
```

D

```
      CALL APRDTA(AMPK,DEE1,DSE1,NMVARB)
C*****************************************************************************
      IF (ICNT.GE.1) THEN                                                      ^
         CALL INIT1(ICNT,EE1,S1,DSE1,AMPK,STF11,STF12,STF22,FORN,              |
     1   FORM,EEPR1,EEPR2)                                                     | E
      END IF                                                                   |
   53 CONTINUE                                                                 v
C*****************************************************************************
      AABS=DABS(DEPTH)
      CALL MATLS2(AABS,EPAR(2),F1,F2,F3,F4,F5)
      IF(DEPTH.GE.ZERO) GO TO 55
      F2=-F2
      F5=-F5
   55 CONTINUE
C     GPLASO=A(1)-A(2)**2/EPRIME
      A(2)=F1*DSE1(1)+F2*DSE1(2)+A(2)
C     IF(ISTVAR.EQ.0) GO TO 59
C     CALL MATLS3(DEPTH,EPAR(2),COD1,COD2)
C     SVAR(2)=SVAR(2)+(DSE1(1)*COD1+DSE1(2)*COD2)/EPRIME
   59 CONTINUE
      IF(JINTYP.EQ.2403) GO TO 60
      A(3)=F3*DSE1(3)+A(3)
      A(4)=F4*DSE1(5)+F5*DSE1(6)+A(4)
      A(1)=A(2)**2+A(3)**2+A(4)**2/(ONE-EVAL(2))
      GO TO 70
   60 CONTINUE
C     A(1)=GPLASO+A(2)**2/EPRIME
C     GO TO 990
      A(1)=A(2)**2
   70 CONTINUE
      A(1)=A(1)/EPRIME
      SVAR(4)=THCK*SVAR(3)
  990 CONTINUE
      RETURN
  999 STOP
      END
```

APPENDIX IV

PARTIAL CLOSURE SUBROUTINES

A listing of each of the 18 partial closure subroutines and the parametric data file is presented in the following pages. The subroutines are grouped and contained in the following order.

ICOUNT INIT INIT1 PRTCLL	Data initialization, updating and partial closure check/evaluation routines
PART	Main partial closure routine
CLOSE CLOSEA COMPL DEFL DEFLA FULL PDEFL PDEFLA SIFAC SIFACA	Support routines to evaluate closure, deflections, compliances and stress intensity factor
CUBIC QUADL QUADR	Interpolation routines
CLOSEDAT.DAT	Parametric Data File

Subroutine ICOUNT

```
      SUBROUTINE ICOUNT(ICNT,ICLCNT,AMK,AMPK,STF11A,STF12A,STF22A)
CCCCCCCCCCCCCCCCCCCCCCCCCCCCCCCCCCCCCCCCCCCCCCCCCCCCCCCCCCCCCCCCCCCCCCCCC
C SUBROUTINE ICOUNT
C
C     SET STIFFNESSES TO PREVIOUS INCREMENT STIFFNESSES RATHER THAN
C        CALLING ROUTINE 'PART' IF DISPLACEMENT INCREMENTS ARE ZERO.
C
CCCCCCCCCCCCCCCCCCCCCCCCCCCCCCCCCCCCCCCCCCCCCCCCCCCCCCCCCCCCCCCCCCCCCCCCC
      IMPLICIT REAL*8(A-H,O-Z)
      DIMENSION AMK(1),AMPK(1)
      DIMENSION STF11A(1),STF12A(1),STF22A(1)
C
      AMK(1)=STF11A(ICNT)
      AMK(2)=STF12A(ICNT)
      AMK(3)=STF22A(ICNT)
      ICLCNT=0
      DO 79 KK1=1,3
         AMPK(KK1)=AMK(KK1)
  79     CONTINUE
      RETURN
      END
```

Subroutine INIT

```
      SUBROUTINE INIT(ITTHL,ITTH,ICNT,ICLCNT,EE1,DEE1,EE11A,EE12A,
     1STF11,STF12,STF22,STF11A,STF12A,STF22A)
CCCCCCCCCCCCCCCCCCCCCCCCCCCCCCCCCCCCCCCCCCCCCCCCCCCCCCCCCCCCCCCCCCCCCCCCCC
C SUBROUTINE JINIT
C
C     INITIALIZE STORAGE LOCATIONS AND DETERMINE THE NUMBER
C        OF LINE-SPRING ELEMENTS
C
CCCCCCCCCCCCCCCCCCCCCCCCCCCCCCCCCCCCCCCCCCCCCCCCCCCCCCCCCCCCCCCCCCCCCCCCCC
      IMPLICIT REAL*8(A-H,O-Z)
      DIMENSION EE1(1),DEE1(1)
      DIMENSION STF11(1),STF12(1),STF22(1),STF11A(1),STF12A(1),
     1STF22A(1),EE11A(1),EE12A(1)
C
      COMMON/CONSTS/PI,SIN60,COS60,KCROS2(3),KCROS3(3),ZERO,LZERO,LONE,
     1 ONE,TWO,HALF,ABIG,ASMALL,BCBIG,LOCSHR(2,3),THIRD,PRECIS,BLANK
C
C  ITTHL IS EQUAL TO THE NUMBER OF LINE-SPRINGS TIMES 3 (NUMBER OF
C     L-S NODES).  EE11A AND EE12A ARE THE 'PREVIOUSLY CONVERGED
C     INCREMENT' DISPLACEMENTS (EE1).
C
C  IF ALL DISPLACEMENTS ARE ZERO THEN THIS IS STILL THE FIRST PASS
C     THROUGH THE MODEL SO ITTHL IS INCREMENTED.
C
      IF (DEE1(1).EQ.ZERO .AND. DEE1(2).EQ.ZERO .AND. EE1(1).EQ.ZERO
     1.AND. EE1(2).EQ.ZERO) THEN
         ITTHL=ITTHL+1
         EE11A(ITTHL)=ZERO
         EE12A(ITTHL)=ZERO
      END IF
C
C  DO NOT ACCESS ROUTINE 'PART' IF DISPLACEMENT INCREMENTS ARE
C     ZERO (ICLCNT=1).  INSTEAD, THE CURRENTLY STORED STIFFNESSES
C     WILL BE SENT BACK TO MATLSA.
C
      IF (DEE1(1).EQ.ZERO .AND. DEE1(2).EQ.ZERO) THEN
         ICLCNT=1
         IF (ITTH.GE.2*ITTHL) ITTH=ITTH-ITTHL
      ELSE
         ICLCNT=0
      END IF
      IF (ITTH.EQ.3*ITTHL) ITTH=ITTH-ITTHL
      ITTH=ITTH+1
      ICNT=ITTH-ITTHL
      IF(ICNT.GT.ITTHL) ICNT=ICNT-ITTHL
C
C  IF DISPLACEMENT (EE1) HAS CHANGED THEN THE INCREMENT HAS CONVERGED
C     AND THE 'PREVIOUSLY CONVERGED INCREMENT' DATA IS UPDATED.
C
```

Subroutine INIT (page 2)

```
      IF (ICNT.GE.1 .AND. ICLCNT.EQ.1) THEN
         IF (EE11A(ICNT).EQ.ZERO) EE11A(ICNT)=EE1(1)
         IF (EE12A(ICNT).EQ.ZERO) EE12A(ICNT)=EE1(2)
         DBS1=DABS((EE1(1)-EE11A(ICNT))/EE11A(ICNT))
         DBS2=DABS((EE1(2)-EE12A(ICNT))/EE12A(ICNT))
         IF (DBS1.GT.1.0E-4 .OR. DBS2.GT.1.0E-4) THEN
            EE11A(ICNT)=EE1(1)
            EE12A(ICNT)=EE1(2)
            STF11A(ICNT)=STF11(ICNT)
            STF12A(ICNT)=STF12(ICNT)
            STF22A(ICNT)=STF22(ICNT)
         END IF
      END IF
      RETURN
      END
```

Subroutine INIT1

```
      SUBROUTINE INIT1(ICNT,EE1,S1,DSE1,AMPK,STF11,STF12,STF22,
     1FORN,FORM,EEPR1,EEPR2)
CCCCCCCCCCCCCCCCCCCCCCCCCCCCCCCCCCCCCCCCCCCCCCCCCCCCCCCCCCCCCCCCCCCCCCCCCC
C SUBROUTINE INIT1
C
C     UPDATE DISPLACEMENT,STIFFNESS, AND FORCE QUANTITIES FOR USE
C        IN ROUTINE 'PRTCLL'.
C
CCCCCCCCCCCCCCCCCCCCCCCCCCCCCCCCCCCCCCCCCCCCCCCCCCCCCCCCCCCCCCCCCCCCCCCCCC
      IMPLICIT REAL*8(A-H,O-Z)
      DIMENSION AMPK(1),EE1(1),DSE1(1),S1(1)
      DIMENSION STF11(1),STF12(1),STF22(1),EEPR1(1),EEPR2(1),
     1FORN(1),FORM(1)
C
      EEPR1(ICNT)=EE1(1)
      EEPR2(ICNT)=EE1(2)
      STF11(ICNT)=AMPK(1)
      STF12(ICNT)=AMPK(2)
      STF22(ICNT)=AMPK(3)
      FORN(ICNT)=S1(1)+DSE1(1)
      FORM(ICNT)=S1(2)+DSE1(2)
C
      RETURN
      END
```

Subroutine PRTCLL

```
      SUBROUTINE PRTCLL(ICNT,EE1,DEE1,S1,DSE1,AMK,AMPK,ASIF,STF11,
     1STF12,STF22,FORN,FORM,EEPR1,EEPR2,KFCL,DEPTH,NMVARB,XIC,THCK,KCL)
CCCCCCCCCCCCCCCCCCCCCCCCCCCCCCCCCCCCCCCCCCCCCCCCCCCCCCCCCCCCCCCCCCCCCCCC
C SUBROUTINE PRTCLL
C
C     CALCULATE THE PREVIOUS SOLUTION RESULTS TO TRANSMIT TO ROUTINE
C        'PART'.  THE RESULTS WILL EITHER BE FROM THE PREVIOUSLY
C        CONVERGED INCREMENT OR FROM THE PREVIOUS ITERATION.
C
CCCCCCCCCCCCCCCCCCCCCCCCCCCCCCCCCCCCCCCCCCCCCCCCCCCCCCCCCCCCCCCCCCCCCCCC
      IMPLICIT REAL*8(A-H,O-Z)
      DIMENSION AMK(1),AMPK(1),EE1(1),DEE1(1),DSE1(1),S1(1),DFNM(2)
      DIMENSION STF11(1),STF12(1),STF22(1),EEPR1(1),EEPR2(1)
     1,FORN(1),FORM(1),KFCL(1)
C
      COMMON /RNGE/ALAM1,ALAM2,ALAM9,SXIC9
      COMMON/CONSTS/PI,SIN60,COS60,KCROS2(3),KCROS3(3),ZERO,LZERO,LONE,
     1 ONE,TWO,HALF,ABIG,ASMALL,BCBIG,LOCSHR(2,3),THIRD,PRECIS,BLANK
C
      DELTA=EE1(1)
      THETA=EE1(2)
C
C  IF FULL CLOSURE HAS OCCURED USE PCI, IF NOT USE LAST ITERATION.
C
      IF (KFCL(ICNT).EQ.1) THEN
         FN=S1(1)
         FM=S1(2)
         DDELTA=DEE1(1)
         DTHETA=DEE1(2)
      ELSE
         FN=FORN(ICNT)
         FM=FORM(ICNT)
         DDELTA=DELTA-EEPR1(ICNT)
         DTHETA=THETA-EEPR2(ICNT)
      END IF
C
C  UPDATE THE LAST ITERATION DISPLACEMENTS
C
      EEPR1(ICNT)=EE1(1)
      EEPR2(ICNT)=EE1(2)
      DFNM(1)=ZERO
      DFNM(2)=ZERO
C
C  SEND IN THE LINEAR STIFFNESSES IN CASE EXTRAPOLATION TO
C     THE ONSET OF CLOSURE IS NECESSARY
C
      STF11(ICNT)=AMPK(1)
      STF12(ICNT)=AMPK(2)
      STF22(ICNT)=AMPK(3)
```

```
      IF (DEPTH.LT.ZERO) THEN
         FM=-FM
         THETA=-THETA
         DTHETA=-DTHETA
         STF12(ICNT)=-STF12(ICNT)
      END IF
C
C  IF CLOSURE DID NOT OCCUR IN THE PREVIOUS ITERATION (OR INCREMENT)
C     CALCULATE THE INCREMENTAL FORCES BASED ON LINEARITY
C
      IF (FM*DEPTH.LE.ZERO.OR.(FN*THCK/FM).LT.(1.000001*ALAM1)) THEN
         KCL=-1
         CALL APRDTA(AMPK,DEE1,DFNM,NMVARB)
         IF (DEPTH.LT.ZERO) DFNM(2)=-DFNM(2)
      ELSE IF (FN*THCK/FM.GT.ALAM2) THEN
         KCL=1
      ELSE
         KCL=0
      END IF
   53 CONTINUE
C
C  EVALUATE THE PARTIALLY-CLOSED CRACK CHARACTERISTICS
C
      CALL PART(FN,FM,DELTA,THETA,DDELTA,DTHETA,XIC,KCL,STF11(ICNT)
     1,STF12(ICNT),STF22(ICNT),ASIF,DFNM(1),DFNM(2),KDCR,KFCL(ICNT))
      IF (DEPTH.LT.ZERO) THEN
         FM=-FM
         STF12(ICNT)=-STF12(ICNT)
      END IF
C
C  UPDATE STIFFNESS, FORCE, AND INCREMENTAL FORCE VALUES
C
      AMK(1)=STF11(ICNT)
      AMK(2)=STF12(ICNT)
      AMK(3)=STF22(ICNT)
      FORN(ICNT)=FN
      FORM(ICNT)=FM
      DO 80 K1=1,3
         AMPK(K1)=AMK(K1)
   80    CONTINUE
      DSE1(1)=FN-S1(1)
      DSE1(2)=FM-S1(2)
      IF (DSE1(1)/S1(1).GE.10.D0.AND.DSE1(2)/S1(2).GE.10.D0)
     1 KFCL(ICNT)=1
      RETURN
      END
```

Subroutine PART

```
       SUBROUTINE PART(FN,FM,TDCR,TRCR,DTDCR,DTRCR,XIC,KCL,
     1 S11,S12,S22,SIF,DFN,DFM,KFCL)
CCCCCCCCCCCCCCCCCCCCCCCCCCCCCCCCCCCCCCCCCCCCCCCCCCCCCCCCCCCCCCCCCCCCCCCCCCCCCC
C SUBROUTINE PART
C
C     EVALUATION OF CLOSURE PARAMETERS
C
C  DISCRETE PARAMETRIC DATA:
C      CJ(I,J,K) - FINITE ELEMENT DATA
C        I=1 TO 8 - CRACK DEPTH RATIO (TIMES 10)
C        J=1 TO 2*I+1 - DATA POINT NUMBER
C        K=1 - I
C        K=2 - J
C        K=3 - LOAD RATIO (ALMBDA_BAR)
C        K=4 - CORRESPONDING CLOSURE DEPTH RATIO
C        K=5 - ONE-HALF TOTAL 'CRACKED' DISPLACEMENT PER UNIT FM
C        K=6 - ONE-HALF TOTAL 'CRACKED' ROTATION PER UNIT FN
C        K=7 - STRESS INTENSITY FACTOR PER UNIT FM
C        K=8 - ONE-HALF 'CRACKED' DISPLACEMENT DUE TO FN
C        K=9 - ONE-HALF 'CRACKED' DISPLACEMENT DUE TO FM
C        K=10 - ONE-HALF 'CRACKED' ROTATION DUE TO FM
C      ALAM9(I) - LOAD RATIO FOR 99% CLOSURE
C        I=1 TO 8 - CRACK DEPTH RATIO (TIMES 10)
C      SXIC9(I) - SLOPE OF CLOSURE VERSUS LOAD RATIO AT 99% CLOSURE
C        I=1 TO 8 - CRACK DEPTH RATIO (TIMES 10)
C      NPT(I) - NUMBER OF DATA POINTS (CLOSURE LENGTHS)
C        I=1 TO 8 - CRACK DEPTH RATIO (TIMES 10)
C
C  INCOMING INFORMATION
C    AT TIME T:
C      FN - APPLIED FAR-FIELD TENSILE FORCE
C      FM - APPLIED FAR-FIELD BENDING MOMENT
C      XIC - CLOSURE LENGTH RATIO
C      SIF - STRESS INTENSITY FACTOR
C    AT TIME T+DT:
C      TDCR - 'CRACKED' FAR-FIELD TOTAL DISPLACEMENT
C      TRCR - 'CRACKED' FAR-FIELD TOTAL ROTATION
C      DTDCR - INCREMENTAL 'CRACKED' FAR-FIELD TOTAL DISPLACEMENT
C      DTRCR - INCREMENTAL 'CRACKED' FAR-FIELD TOTAL ROTATION
C  RETURNED DATA AT TIME T+DT:
C      FN - REQUIRED FAR-FIELD TENSILE FORCE
C      FM - REQUIRED FAR-FIELD BENDING MOMENT
C      XIC - CLOSURE LENGTH RATIO
C      S** - STIFFNESS MATRIX ELEMENTS
C      SIF - STRESS INTENSITY FACTOR
C
CCCCCCCCCCCCCCCCCCCCCCCCCCCCCCCCCCCCCCCCCCCCCCCCCCCCCCCCCCCCCCCCCCCCCCCCCCCCCC
       IMPLICIT REAL*8 (A-H,O-Z)
       DIMENSION CJ(8,17,10),ALAM9(8),SXIC9(8),NPT(8)
```

Subroutine PART (page 2)

```
C
      COMMON /JJL/CJ,THCK,XIA,EPRIME,NPT /LOC/ICL,ICLP
      COMMON /RNGE/ALAM1,ALAM2,ALAM9,SXIC9 /FCT/FC1,FC2,FC3
C
      IF (ICL.EQ.0) THEN
         ALAM9A=11.8802D0*XIA-6.D0
         SXIC9A=1.D0/12.D0
      ELSE
         ALAM9A=(ALAM9(ICLP)-ALAM9(ICL))*(10.D0*XIA-ICL)+ALAM9(ICL)
         SXIC9A=(SXIC9(ICLP)-SXIC9(ICL))*(10.D0*XIA-ICL)+SXIC9(ICL)
      END IF
C
C   CHECK FOR FULL CLOSURE BASED ON INCOMING TDCR AND TRCR
C
      CALL FULL(XIC,SXIC9A,PDM,PRM,ALAM9A,C11,C12,C21,C22,
     1      CM,KDEFI,KDEFIP,1)
      TFN=C22*CM*TDCR
      TFM=C11*CM*TRCR
      KFCL=0
      IF ((TFN*THCK/TFM).GE.ALAM2.AND.TFM.LT.0.D0) THEN
         KFCL=1
         KCL=1
         XIC=XIA
         S11=CM*C22
         S12=0.0D0
         S22=CM*C11
         GOTO 1030
      END IF
      IF (KCL.EQ.-1) THEN
         ALPH=(FM*ALAM1-FN*THCK)/(DFN*THCK-DFM*ALAM1)
         FN=FN+ALPH*DFN
         FM=FM+ALPH*DFM
         ALMBDA=ALAM1
         SM=1.D0/(S11*S22-S12*S12)
         DTDCR=TDCR-SM*(S22*FN-S12*FM)
         DTRCR=TRCR-SM*(S11*FM-S12*FN)
      ELSE
         ALMBDA=FN*THCK/FM
      END IF
      IF (KCL.EQ.0 .AND. ALMBDA.LT.ALAM1) ALMBDA=ALAM1
      CALL CLOSE(XIC,SXIC,KCL,ALMBDA)
      IF (KCL) 1010,1020,1020
C
C  LINE 1010 - CHECK BASED ON ALMBDA AT TIME T+DT
C  LINE 1020 - PARTIAL OR FULL CLOSURE WILL OCCUR
C
C  FIRST PASS (FIRST ESTIMATE AT NEW LOADS)
C
 1020     CONTINUE
```

```
      IF (XIC.GT.(0.99D0*XIA).OR.KCL.EQ.1) THEN
         CALL FULL(XIC,SXIC9A,PDM,PRM,ALAM9A,C11,C12,C21,C22,
     1         CM,KDEFI,KDEFIP,KCL)
      ELSE
         CALL COMPL(XIC,SXIC,PDM,PRM,ALMBDA,C11,C12,C21,
     1         C22,CM,KDEFI,KDEFIP)
      END IF
      BXIC=XIA
      AFC=XIC/BXIC
      IF (AFC.GE.1.D0) AFC=1.D0
      C22=C22*(AFC*(1.D0-FC1)+1.D0)
      C11=C11*(AFC*(1.D0-FC1)+1.D0)
      C12=C12*(AFC*(1.D0-FC1)+1.D0)
      C21=C21*(AFC*(1.D0-FC1)+1.D0)
      TDFN=CM*(C22*DTDCR-C12*DTRCR)
      TDFM=CM*(C11*DTRCR-C21*DTDCR)
      N=0
C
C  BEGINNING OF NEWTON-RAPHSON ITERATION
C
 1050    CONTINUE
      TFN=FN+TDFN
      TFM=FM+TDFM
      N=N+1
C
C  SUBSEQUENT LOAD ESTIMATIONS
C
      IF (TFM.GE.0.D0) THEN
         KCL=-1
         GOTO 1010
      END IF
      TTLAM=TFN*THCK/TFM
      CALL CLOSE(XIC,SXIC,KCL,TTLAM)
      IF (KCL.EQ.-1) THEN
         FN=TFN
         FM=TFM
         GOTO 1010
      END IF
 1040    CONTINUE
      IF (XIC.GT.(0.99D0*XIA).OR.KCL.EQ.1) THEN
         CALL FULL(XIC,SXIC9A,PDM,PRM,ALAM9A,C11,C12,C21,C22,
     1         CM,KDEFI,KDEFIP,KCL)
      ELSE
         CALL COMPL(XIC,SXIC,PDM,PRM,TTLAM,C11,C12,C21,
     1         C22,CM,KDEFI,KDEFIP)
      END IF
      AFC=XIC/BXIC
      IF (AFC.GE.1.D0) AFC=1.D0
      C22=C22*(AFC*(1.D0-FC1)+1.D0)
```

```
      C11=C11*(AFC*(1.D0-FC1)+1.D0)
      C12=C12*(AFC*(1.D0-FC1)+1.D0)
      C21=C21*(AFC*(1.D0-FC1)+1.D0)
C
C  ESTIMATION OF ERROR
C
      ERRD=TDCR-TFM*PDM/THCK/EPRIME
      ERRR=TRCR-TFM*PRM/THCK/THCK/EPRIME
      DTDFN=CM*(C22*ERRD-C12*ERRR)
      DTDFM=CM*(C11*ERRR-C21*ERRD)
      TDFN=TDFN+DTDFN
      TDFM=TDFM+DTDFM
      IF (N.EQ.1) THEN
         ERRD1=ERRD
         ERRR1=ERRR
      END IF
      DERRD = DABS(ERRD/TDCR)
      DERRR = DABS(ERRR/TRCR)
      DERRD1 = DABS(ERRD/ERRD1)
      DERRR1 = DABS(ERRR/ERRR1)
      DABN = DABS(DTDFN/TDFN)
      DABM = DABS(DTDFM/TDFM)
      DABTN = DABS(DTDFN/TFN)
      DABTM = DABS(DTDFM/TFM)
      IF ((DERRD .LT. 1.0E-3 .OR. DERRD1 .LT. 1.0E-3) .AND.
     1 (DERRR .LT. 1.0E-3 .OR. DERRR1 .LT. 1.0E-3) .AND.
     1 (DABN .LT. 1.0E-3 .OR. DABTN .LT. 1.0E-4) .AND.
     1 (DABM .LT. 1.0E-3 .OR. DABTM .LT. 1.0E-4)) GOTO 1030
      IF (N.GE.200) GOTO 1010
      GOTO 1050
 1030    CONTINUE
      FN=TFN
      FM=TFM
      IF (KCL.EQ.1) THEN
         SIF=0.0D0
      ELSE
         CALL SIFAC(KDEFI,KDEFIP,TFM,SIF,XIC)
      END IF
 1010    CONTINUE
      S11=C22*CM
      S22=C11*CM
      S12=-C12*CM
      IF (KCL.EQ.-1) XIC=0.0D0
      RETURN
      END
```

Subroutine CLOSE

```
      SUBROUTINE CLOSE(ZC,SZC,KCL,TLAM)
CCCCCCCCCCCCCCCCCCCCCCCCCCCCCCCCCCCCCCCCCCCCCCCCCCCCCCCCCCCCCCCCCCCCCCCCCCCCCCC
C SUBROUTINE CLOSE
C
C      CALCULATE THE NEW CRACK CLOSURE LENGTH BASED ON INCOMING LOAD
C         RATIO 'TLAM'
C
CCCCCCCCCCCCCCCCCCCCCCCCCCCCCCCCCCCCCCCCCCCCCCCCCCCCCCCCCCCCCCCCCCCCCCCCCCCCCCC
      IMPLICIT REAL*8 (A-H,O-Z)
      DIMENSION CJ(8,17,10),ALAM9(8),SXIC9(8),NPT(8)
C
      COMMON /JJL/CJ,THCK,XIA,EPRIME,NPT /LOC/ICL,ICLP
      COMMON /RNGE/ALAM1,ALAM2,ALAM9,SXIC9
C
C   DETERMINE TYPE OF CLOSURE (NONE, PARTIAL OR FULL)
C
      IF (TLAM.LT.ALAM1) THEN
         KCL=-1
         RETURN
      ELSE IF (TLAM.GE.ALAM2) THEN
         KCL=1
         ZC=1.D0
         SZC=0.D0
         RETURN
      END IF
      KCL=0
C
C   DETERMINE THE REGIME OF TLAM RELATIVE TO THE
C      DISCRETE DATA POINTS
C
C   REGIME 1 - TLAM>ALAM1(I)  ; TLAM<ALAM1(IP)
C   REGIME 2 - TLAM>ALAM1(IP) ; TLAM<ALAM2(I)
C   REGIME 3 - TLAM>ALAM2(I)  ; TLAM<ALAM2(IP)
C
      DO 1125 J=1,NPT(ICLP)
         IF (TLAM.GT.CJ(ICLP,J,3)) GOTO 1125
            NIP=J-1
            GOTO 1130
 1125    CONTINUE
 1130 CONTINUE
      IF (ICL.EQ.0) GOTO 1160
      DO 1135 J=1,NPT(ICL)
         NI=NPT(ICL)+1-J
         IF (TLAM.LT.CJ(ICL,NI,3)) GOTO 1135
            GOTO 1140
 1135    CONTINUE
 1140 CONTINUE
      IF (NI.LT.NPT(ICL).AND.NIP.GT.0) GOTO 1145
         IF (NIP.EQ.0) GOTO 1150
```

```
C
C   REGIME 3
C
       CALL CLOSEA(ICLP,NIP,ZCIP,SZCIP,TLAM)
       SZCI=1.D0/12.D0
       ZCI=TLAM*SZCI+0.5D0
       ZC=(ZCIP-ZCI)*(XIA-ZCI)*10.D0/(ICLP-10.D0*ZCI)+ZCI
       SZC=(SZCIP-SZCI)*(XIA-ZCI)*10.D0/(ICLP-10.D0*ZCI)+SZCI
       RETURN
C
C   REGIME 1
C
 1150  CONTINUE
       CALL CLOSEA(ICL,NI,ZCI,SZCI,TLAM)
       ZCIP=0.D0
       DLTLAM=(TLAM-CJ(ICL,1,3))/(CJ(ICLP,1,3)-CJ(ICL,1,3))
       IF (DLTLAM/ICL.LT.1.E-2) THEN
          ZC=ZCI
          SZC=SZCI
          RETURN
       END IF
       ZP=DLTLAM+1.D0*ICL
       CALL CLOSEA(ICL,1,ZTMP,SZTMP,CJ(ICL,1,3))
       CALL CLOSEA(ICLP,1,ZTMPP,SZTMPP,CJ(ICLP,1,3))
       SZCIP=DLTLAM*(SZTMPP-SZTMP)+SZTMP
       ZC=(ZCIP-ZCI)*(10.D0*XIA-ICL)/(ZP-ICL)+ZCI
       SZC=(SZCIP-SZCI)*(10.D0*XIA-ICL)/(ZP-ICL)+SZCI
       RETURN
C
C   REGIME 2
C
 1145  CONTINUE
       CALL CLOSEA(ICL,NI,ZCI,SZCI,TLAM)
       CALL CLOSEA(ICLP,NIP,ZCIP,SZCIP,TLAM)
       ZC=(ZCIP-ZCI)*(10.D0*XIA-ICL)+ZCI
       SZC=(SZCIP-SZCI)*(10.D0*XIA-ICL)+SZCI
       RETURN
C
C   DO THE FOLLOWING IF XIA < 0.100
C
 1160     CONTINUE
       SZCI=1.D0/12.D0
       ZCI=TLAM*SZCI+0.5D0
       IF (NIP.EQ.0) THEN
          DLTLAM=(TLAM+6.D0)/0.35292D0
          ZP=DLTLAM
          CALL CLOSEA(ICLP,1,ZTMPP,SZTMPP,CJ(ICLP,1,3))
          SZCIP=DLTLAM*(SZTMPP-SZCI)+SZCI
          ZC=(ZCIP-ZCI)*10.D0*XIA/ZP+ZCI
```

```
         SZC=(SZCIP-SZCI)*10.D0*XIA/ZP+SZCI
      ELSE
         CALL CLOSEA(ICLP,NIP,ZCIP,SZCIP,TLAM)
         ZC=(ZCIP-ZCI)*(XIA-ZCI)*10.D0/(1.D0-10.D0*ZCI)+ZCI
         SZC=(SZCIP-SZCI)*(XIA-ZCI)*10.D0/(1.D0-10.D0*ZCI)+SZCI
      END IF
      RETURN
      END
```

Subroutine CLOSEA

```
      SUBROUTINE CLOSEA(IC,NIC,ZCIC,SZCIC,TLAMT)
CCCCCCCCCCCCCCCCCCCCCCCCCCCCCCCCCCCCCCCCCCCCCCCCCCCCCCCCCCCCCCCCCCCCCCCC
C SUBROUTINE CLOSEA
C
C      CALCULATE CRACK CLOSURE DATA FOR USE IN SUBROUTINE CLOSE
C
CCCCCCCCCCCCCCCCCCCCCCCCCCCCCCCCCCCCCCCCCCCCCCCCCCCCCCCCCCCCCCCCCCCCCCCC
      IMPLICIT REAL*8 (A-H,O-Z)
      DIMENSION CJ(8,17,10),NPT(8)
C
      COMMON /JJL/CJ,THCK,XIA,EPRIME,NPT
C
C   X - LOAD RATIO; Z - CLOSURE
C
      XL=CJ(IC,NIC,3)
      XR=CJ(IC,NIC+1,3)
      ZL=CJ(IC,NIC,4)
      ZR=CJ(IC,NIC+1,4)
      XRMXL=XR-XL
      IF (NIC.GT.1) THEN
         XLM=CJ(IC,NIC-1,3)
         ZLM=CJ(IC,NIC-1,4)
      END IF
      IF (NIC.LT.NPT(IC)-1) THEN
         XRP=CJ(IC,NIC+2,3)
         ZRP=CJ(IC,NIC+2,4)
      END IF
C
C   EVALUATE THE REQUIRED SLOPES USING A WEIGHTED CENTRAL DIFFERENCE
C      METHOD AND USE APPLICABLE SPLINE FIT (CUBIC OR QUADRATIC)
C
      IF (NIC.LT.NPT(IC)-1) THEN
         AMR=((ZR-ZL)*(XRP-XR)/XRMXL+(ZRP-ZR)*XRMXL/(XRP-XR))/(XRP-XL)
      ELSE
         AMR=1.D0/12.D0
      END IF
      IF (NIC.GT.1) THEN
         AML=((ZL-ZLM)*XRMXL/(XL-XLM)+(ZR-ZL)*(XL-XLM)/XRMXL)/(XR-XLM)
         CALL CUBIC(AML,AMR,XL,XR,ZL,ZR,TLAMT,ZCIC,SZCIC)
      ELSE
         CALL QUADR(AMR,XL,XR,ZL,ZR,TLAMT,ZCIC,SZCIC)
      END IF
      RETURN
      END
```

Subroutine COMPL

```
      SUBROUTINE COMPL(ZC,SZC,PDM,PRM,TLAMT,C11,C12,C21,C22,CM,KDEFI,
     1 KDEFIP)
CCCCCCCCCCCCCCCCCCCCCCCCCCCCCCCCCCCCCCCCCCCCCCCCCCCCCCCCCCCCCCCCCCCCCCCCCC
C SUBROUTINE COMPL
C
C      CALCULATE COMPLIANCE MATRIX COEFFICIENTS FOR PARTIALLY
C         CLOSED CASE (CLOSURE LESS THAN 99%)
C
CCCCCCCCCCCCCCCCCCCCCCCCCCCCCCCCCCCCCCCCCCCCCCCCCCCCCCCCCCCCCCCCCCCCCCCCCC
      IMPLICIT REAL*8 (A-H,O-Z)
      DIMENSION CJ(8,17,10),NPT(8)
C
      COMMON /JJL/CJ,THCK,XIA,EPRIME,NPT
C
C   DETERMINE DISPLACEMENTS AND SLOPES
C
      CALL PDEFL(ZC,PDM,PRM,SPDM,SPRM,KDEFI,KDEFIP)
      CALL DEFL(ZC,DN,DM,RM,KDEFI,KDEFIP)
C
C   CALCULATE COEFFICIENTS
C
      C11=SZC*SPDM+DN
      C12=(DM-SZC*TLAMT*SPDM)/THCK
      C21=(SZC*SPRM+DM)/THCK
      C22=(RM-SZC*TLAMT*SPRM)/THCK/THCK
      C12=(DABS(C12*C21))**(1.D0/2.D0)
      IF (ZC .GT. 1.D0-XIA) C12=-C12
      C21=C12
      CM=EPRIME/(C11*C22-C12*C21)
      RETURN
      END
```

Subroutine DEFL

```
      SUBROUTINE DEFL(ZC,DN,DM,RM,KDEFI,KDEFIP)
CCCCCCCCCCCCCCCCCCCCCCCCCCCCCCCCCCCCCCCCCCCCCCCCCCCCCCCCCCCCCCCCCCCCCCCCCCCCCCC
C SUBROUTINE DEFL
C
C       CALCULATE THE FAR-FIELD DISPLACEMENTS DUE TO THE
C          INDIVIDUAL FORCE AND MOMENT
C
CCCCCCCCCCCCCCCCCCCCCCCCCCCCCCCCCCCCCCCCCCCCCCCCCCCCCCCCCCCCCCCCCCCCCCCCCCCCCCC
      IMPLICIT REAL*8 (A-H,O-Z)
      DIMENSION CJ(8,17,10),NPT(8)
C
      COMMON /JJL/CJ,THCK,XIA,EPRIME,NPT /LOC/ICL,ICLP
C
C   CALCULATE END POINT DISPLACEMENTS AND SLOPES FOR
C       LINEAR INTERPOLATION IN XIA
C
      IF (KDEFI.LT.NPT(ICL)) THEN
         ZI=1.D0*ICL
         CALL DEFLA(ICL,KDEFI,DNI,DMI,RMI,ZC)
      ELSE
         DNI=0.D0
         DMI=0.D0
         RMI=0.D0
         ZI=10.D0*ZC
      END IF
      CALL DEFLA(ICLP,KDEFIP,DNIP,DMIP,RMIP,ZC)
      DN=(DNIP-DNI)*(10.D0*XIA-ZI)/(ICLP-ZI)+DNI
      DM=(DMIP-DMI)*(10.D0*XIA-ZI)/(ICLP-ZI)+DMI
      RM=(RMIP-RMI)*(10.D0*XIA-ZI)/(ICLP-ZI)+RMI
      RETURN
      END
```

Subroutine DEFLA

```
      SUBROUTINE DEFLA(IC,KDEF,DNIC,DMIC,RMIC,ZC)
CCCCCCCCCCCCCCCCCCCCCCCCCCCCCCCCCCCCCCCCCCCCCCCCCCCCCCCCCCCCCCCCCCCCCCCC
C SUBROUTINE DEFLA
C
C      CALCULATE FAR-FIELD DISPLACEMENT DATA FOR USE IN
C         SUBROUTINE DEFL
C
CCCCCCCCCCCCCCCCCCCCCCCCCCCCCCCCCCCCCCCCCCCCCCCCCCCCCCCCCCCCCCCCCCCCCCCC
      IMPLICIT REAL*8 (A-H,O-Z)
      DIMENSION CJ(8,17,10),NPT(8)
C
      COMMON /JJL/CJ,THCK,XIA,EPRIME,NPT
C
C   X - CLOSURE; Z-8 - DISP DUE TO FORCE; Z-9 - DISP DUE TO MOMENT
C      AND ROTA DUE TO FORCE; Z-10 - ROTA DUE TO MOMENT
C
      XL=CJ(IC,KDEF,4)
      XR=CJ(IC,KDEF+1,4)
      XRMXL=XR-XL
      ZL8=2.D0*CJ(IC,KDEF,8)
      ZR8=2.D0*CJ(IC,KDEF+1,8)
      ZL9=2.D0*CJ(IC,KDEF,9)
      ZR9=2.D0*CJ(IC,KDEF+1,9)
      ZL10=2.D0*CJ(IC,KDEF,10)
      ZR10=2.D0*CJ(IC,KDEF+1,10)
      IF (KDEF.GT.1) THEN
         XLM=CJ(IC,KDEF-1,4)
         ZLM8=2.D0*CJ(IC,KDEF-1,8)
         ZLM9=2.D0*CJ(IC,KDEF-1,9)
         ZLM10=2.D0*CJ(IC,KDEF-1,10)
      END IF
      IF (KDEF.LT.NPT(IC)-1) THEN
         XRP=CJ(IC,KDEF+2,4)
         ZRP8=2.D0*CJ(IC,KDEF+2,8)
         ZRP9=2.D0*CJ(IC,KDEF+2,9)
         ZRP10=2.D0*CJ(IC,KDEF+2,10)
      END IF
C
C   EVALUATE THE REQUIRED SLOPES USING A WEIGHTED DIFFERENCE METHOD
C      AND USE APPLICABLE SPLINE FIT (CUBIC OR QUADRATIC)
C
      IF (KDEF.EQ.NPT(IC)-1) THEN
         AMR8=0.D0
         AMR9=0.D0
         AMR10=0.D0
      ELSE
         XRPMXL=XRP-XL
         XRPMXR=XRP-XR
         AMR8=((ZR8-ZL8)*XRPMXR/XRMXL+(ZRP8-ZR8)*XRMXL/XRPMXR)/XRPMXL
```

```
          AMR9=((ZR9-ZL9)*XRPMXR/XRMXL+(ZRP9-ZR9)*XRMXL/XRPMXR)/XRPMXL
          AMR10=((ZR10-ZL10)*XRPMXR/XRMXL+(ZRP10-ZR10)*XRMXL/XRPMXR)
     1    /XRPMXL
        END IF
        IF (KDEF.EQ.1) THEN
          CALL QUADR(AMR8,XL,XR,ZL8,ZR8,ZC,DNIC,SDNIC)
          CALL QUADR(AMR9,XL,XR,ZL9,ZR9,ZC,DMIC,SDMIC)
          CALL QUADR(AMR10,XL,XR,ZL10,ZR10,ZC,RMIC,SRMIC)
        ELSE
          XRMXLM=XR-XLM
          XLMXLM=XL-XLM
          AML8=((ZL8-ZLM8)*XRMXL/XLMXLM+(ZR8-ZL8)*XLMXLM/XRMXL)/XRMXLM
          AML9=((ZL9-ZLM9)*XRMXL/XLMXLM+(ZR9-ZL9)*XLMXLM/XRMXL)/XRMXLM
          AML10=((ZL10-ZLM10)*XRMXL/XLMXLM+(ZR10-ZL10)*XLMXLM/XRMXL)
     1    /XRMXLM
          CALL CUBIC(AML8,AMR8,XL,XR,ZL8,ZR8,ZC,DNIC,SDNIC)
          CALL CUBIC(AML9,AMR9,XL,XR,ZL9,ZR9,ZC,DMIC,SDMIC)
          CALL CUBIC(AML10,AMR10,XL,XR,ZL10,ZR10,ZC,RMIC,SRMIC)
        END IF
        RETURN
        END
```

Subroutine FULL

```
      SUBROUTINE FULL(XIC,SXIC9A,PDM,PRM,ALAM9A,C11,C12,C21,C22,
     1 CM,KDEFI,KDEFIP,KCL)
CCCCCCCCCCCCCCCCCCCCCCCCCCCCCCCCCCCCCCCCCCCCCCCCCCCCCCCCCCCCCCCCCCCCCCCCCC
C SUBROUTINE FULL
C
C      CALCULATE THE COMPLIANCE COEFFICIENTS FOR CLOSURE LENGTHS
C         GREATER THAN 0.99*(CRACK DEPTH)
C
CCCCCCCCCCCCCCCCCCCCCCCCCCCCCCCCCCCCCCCCCCCCCCCCCCCCCCCCCCCCCCCCCCCCCCCCCC
      IMPLICIT REAL*8 (A-H,O-Z)
      DIMENSION CJ(8,17,10),NPT(8)
C
      COMMON /JJL/CJ,THCK,XIA,EPRIME,NPT
C
      NETA=0
      IF (KCL.NE.1) THEN
         ETA=100.D0*(XIC/XIA-0.99D0)
         OMETA=1.D0-ETA
      ELSE
         NETA=1
      END IF
      XCL=0.99D0*XIA
      CALL COMPL(XCL,SXIC9A,PDM,PRM,ALAM9A,C11,C12,C21,
     1      C22,CM,KDEFI,KDEFIP)
C
C   FOR FULL CLOSURE LET C12=C21=0 AND DECREASE THE DIAGONAL
C      TERM BY A FACTOR OF 1000
C
      C11P=C11/1000.D0
      C22P=C22/1000.D0
C
C   USE LINEAR INTERPOLATION BETWEEN 99% CLOSURE AND FULL
C      CLOSURE
C
      IF (NETA.EQ.1) THEN
         C11=C11P
         C12=0.D0
         C21=0.D0
         C22=C22P
      ELSE
         C11=C11*OMETA+ETA*C11P
         C12=C12*OMETA
         C21=C21*OMETA
         C22=C22*OMETA+ETA*C22P
      END IF
      CM=EPRIME/(C11*C22-C12*C21)
      RETURN
      END
```

Subroutine PDEFL

```
      SUBROUTINE PDEFL(ZC,PDM,PRM,SPDM,SPRM,KDEFI,KDEFIP)
CCCCCCCCCCCCCCCCCCCCCCCCCCCCCCCCCCCCCCCCCCCCCCCCCCCCCCCCCCCCCCCCCCCCCCCCCCC
C SUBROUTINE PDEFL
C
C      CALCULATE FAR-FIELD DISPLACEMENTS AND ROTATIONS PER UNIT
C         MOMENT 'TFM'
C
CCCCCCCCCCCCCCCCCCCCCCCCCCCCCCCCCCCCCCCCCCCCCCCCCCCCCCCCCCCCCCCCCCCCCCCCCCC
      IMPLICIT REAL*8 (A-H,O-Z)
      DIMENSION CJ(8,17,10),NPT(8)
C
      COMMON /JJL/CJ,THCK,XIA,EPRIME,NPT /LOC/ICL,ICLP
C
C   CALCULATE END POINT DISPLACEMENTS AND SLOPES FOR
C      LINEAR INTERPOLATION IN XIA
C
      DO 100 NICLP=1,NPT(ICLP)-1
         IF (ZC.GE.CJ(ICLP,NICLP,4)) KDEFIP=NICLP
 100     CONTINUE
      DO 110 NICL=1,NPT(ICL)
         IF (ZC.GE.CJ(ICL,NICL,4)) KDEFI=NICL
 110     CONTINUE
      IF (KDEFI.LT.NPT(ICL)) THEN
         ZI=1.D0*ICL
         CALL PDEFLA(ICL,KDEFI,PDMI,PRMI,SPDMI,SPRMI,ZC)
      ELSE
         PDMI=0.D0
         PRMI=0.D0
         SPDMI=0.D0
         SPRMI=0.D0
         ZI=10.D0*ZC
      END IF
      CALL PDEFLA(ICLP,KDEFIP,PDMIP,PRMIP,SPDMIP,SPRMIP,ZC)
      PDM=(PDMIP-PDMI)*(10.D0*XIA-ZI)/(ICLP-ZI)+PDMI
      PRM=(PRMIP-PRMI)*(10.D0*XIA-ZI)/(ICLP-ZI)+PRMI
      SPDM=(SPDMIP-SPDMI)*(10.D0*XIA-ZI)/(ICLP-ZI)+SPDMI
      SPRM=(SPRMIP-SPRMI)*(10.D0*XIA-ZI)/(ICLP-ZI)+SPRMI
      RETURN
      END
```

Subroutine PDEFLA

```
      SUBROUTINE PDEFLA(IC,KPDEF,PDMIC,PRMIC,SPDMIC,SPRMIC,ZC)
CCCCCCCCCCCCCCCCCCCCCCCCCCCCCCCCCCCCCCCCCCCCCCCCCCCCCCCCCCCCCCCCCCCCCCCCCCCCCCC
C SUBROUTINE PDEFLA
C
C      CALCULATE FAR-FIELD DISPLACEMENT AND SLOPE DATA FOR USE
C         IN SUBROUTINE PDEFL
C
CCCCCCCCCCCCCCCCCCCCCCCCCCCCCCCCCCCCCCCCCCCCCCCCCCCCCCCCCCCCCCCCCCCCCCCCCCCCCCC
      IMPLICIT REAL*8 (A-H,O-Z)
      DIMENSION CJ(8,17,10),NPT(8)
C
      COMMON /JJL/CJ,THCK,XIA,EPRIME,NPT
C
C   X - CLOSURE; Z-D - FAR-FIELD DISP; Z-R - FAR-FIELD ROTA
C
      XL=CJ(IC,KPDEF,4)
      XR=CJ(IC,KPDEF+1,4)
      XRMXL=XR-XL
      ZLD=2.D0*CJ(IC,KPDEF,5)
      ZRD=2.D0*CJ(IC,KPDEF+1,5)
      ZLR=2.D0*CJ(IC,KPDEF,6)
      ZRR=2.D0*CJ(IC,KPDEF+1,6)
      ZRMZLD=ZRD-ZLD
      ZRMZLR=ZRR-ZLR
      IF (KPDEF.GT.1) THEN
         XLM=CJ(IC,KPDEF-1,4)
         ZLDM=2.D0*CJ(IC,KPDEF-1,5)
         ZLRM=2.D0*CJ(IC,KPDEF-1,6)
      END IF
      IF (KPDEF.LT.NPT(IC)-1) THEN
         XRP=CJ(IC,KPDEF+2,4)
         ZRDP=2.D0*CJ(IC,KPDEF+2,5)
         ZRRP=2.D0*CJ(IC,KPDEF+2,6)
      END IF
C
C   EVALUATE THE REQUIRED SLOPES USING A WEIGHTED DIFFERENCE METHOD
C      AND USE APPLICABLE SPLINE FIT (CUBIC OR QUADRATIC)
C
      IF (KPDEF.EQ.NPT(IC)-1) THEN
         AMRD=0.D0
         AMRR=0.D0
      ELSE
         XRPMXL=XRP-XL
         XRPMXR=XRP-XR
         AMRD=(ZRMZLD*XRPMXR/XRMXL+(ZRDP-ZRD)*XRMXL/XRPMXR)/XRPMXL
         AMRR=(ZRMZLR*XRPMXR/XRMXL+(ZRRP-ZRR)*XRMXL/XRPMXR)/XRPMXL
      END IF
      IF (KPDEF.EQ.1) THEN
         CALL QUADR(AMRD,XL,XR,ZLD,ZRD,ZC,PDMIC,SPDMIC)
```

```
         CALL QUADR(AMRR,XL,XR,ZLR,ZRR,ZC,PRMIC,SPRMIC)
      ELSE
         XRMXLM=XR-XLM
         XLMXLM=XL-XLM
         AMLD=((ZLD-ZLDM)*XRMXL/XLMXLM+ZRMZLD*XLMXLM/XRMXL)/XRMXLM
         AMLR=((ZLR-ZLRM)*XRMXL/XLMXLM+ZRMZLR*XLMXLM/XRMXL)/XRMXLM
         CALL CUBIC(AMLD,AMRD,XL,XR,ZLD,ZRD,ZC,PDMIC,SPDMIC)
         CALL CUBIC(AMLR,AMRR,XL,XR,ZLR,ZRR,ZC,PRMIC,SPRMIC)
      END IF
      RETURN
      END
```

Subroutine SIFAC

```
      SUBROUTINE SIFAC(KDEFI,KDEFIP,TFM,SIF,ZC)
CCCCCCCCCCCCCCCCCCCCCCCCCCCCCCCCCCCCCCCCCCCCCCCCCCCCCCCCCCCCCCCCCCCCCCCCCCCCCCC
C SUBROUTINE SIFAC
C
C       CALCULATE STRESS INTENSITY FACTOR CALIBRATION BASED ON
C          A UNIT APPLIED MOMENT 'TFM'
C
CCCCCCCCCCCCCCCCCCCCCCCCCCCCCCCCCCCCCCCCCCCCCCCCCCCCCCCCCCCCCCCCCCCCCCCCCCCCCCC
      IMPLICIT REAL*8 (A-H,O-Z)
      DIMENSION CJ(8,17,10),NPT(8)
C
      COMMON /JJL/CJ,THCK,XIA,EPRIME,NPT /LOC/ICL,ICLP
C
C   CALCULATE END POINT DISPLACEMENTS AND SLOPES FOR
C      LINEAR INTERPOLATION IN XIA
C
      IF (KDEFI.LT.NPT(ICL)) THEN
         ZI=1.D0*ICL
         CALL SIFACA(ICL,KDEFI,SIFI,ZC)
      ELSE
         SIFI=0.D0
         ZI=10.D0*ZC
      END IF
      CALL SIFACA(ICLP,KDEFIP,SIFIP,ZC)
      SIF=((SIFIP-SIFI)*(10.D0*XIA-ZI)/(ICLP-ZI)+SIFI)*TFM/THCK**1.5D0
      RETURN
      END
```

Subroutine SIFACA

```
      SUBROUTINE SIFACA(IC,KPDEF,SIFIC,ZC)
CCCCCCCCCCCCCCCCCCCCCCCCCCCCCCCCCCCCCCCCCCCCCCCCCCCCCCCCCCCCCCCCCCCCCCCCCCCCCCC
C SUBROUTINE SIFACA
C
C      CALCULATE SIF CALIBRATION DATA FOR USE IN SUBROUTINE SIFAC
C
CCCCCCCCCCCCCCCCCCCCCCCCCCCCCCCCCCCCCCCCCCCCCCCCCCCCCCCCCCCCCCCCCCCCCCCCCCCCCCC
      IMPLICIT REAL*8 (A-H,O-Z)
      DIMENSION CJ(8,17,10),NPT(8)
C
      COMMON /JJL/CJ,THCK,XIA,EPRIME,NPT
C
C   X - CLOSURE; Z - SIF CALIBRATION
C
      XL=CJ(IC,KPDEF,4)
      XR=CJ(IC,KPDEF+1,4)
      ZL=CJ(IC,KPDEF,7)
      ZR=CJ(IC,KPDEF+1,7)
      XRMXL=XR-XL
      IF (KPDEF.GT.1) THEN
         XLM=CJ(IC,KPDEF-1,4)
         ZLM=CJ(IC,KPDEF-1,7)
      END IF
      IF (KPDEF.LT.NPT(IC)-1) THEN
         XRP=CJ(IC,KPDEF+2,4)
         ZRP=CJ(IC,KPDEF+2,7)
      END IF
C
C   EVALUATE THE REQUIRED SLOPES USING A WEIGHTED DIFFERENCE METHOD
C      AND USE APPLICABLE SPLINE FIT (CUBIC OR QUADRATIC)
C
      IF (KPDEF.EQ.1) THEN
         AMR=((ZR-ZL)*(XRP-XR)/XRMXL+(ZRP-ZR)*XRMXL/(XRP-XR))/(XRP-XL)
         CALL QUADR(AMR,XL,XR,ZL,ZR,ZC,SIFIC,DSIFIC)
      ELSE IF (KPDEF.EQ.NPT(IC)-1) THEN
         AML=((ZL-ZLM)*XRMXL/(XL-XLM)+(ZR-ZL)*(XL-XLM)/XRMXL)/(XR-XLM)
         CALL QUADL(AML,XL,XR,ZL,ZR,ZC,SIFIC,DSIFIC)
      ELSE
         AMR=((ZR-ZL)*(XRP-XR)/XRMXL+(ZRP-ZR)*XRMXL/(XRP-XR))/(XRP-XL)
         AML=((ZL-ZLM)*XRMXL/(XL-XLM)+(ZR-ZL)*(XL-XLM)/XRMXL)/(XR-XLM)
         CALL CUBIC(AML,AMR,XL,XR,ZL,ZR,ZC,SIFIC,DSIFIC)
      END IF
      RETURN
      END
```

Subroutine CUBIC

```
      SUBROUTINE CUBIC(AML,AMR,XL,XR,ZL,ZR,XC,DIC,SDIC)
CCCCCCCCCCCCCCCCCCCCCCCCCCCCCCCCCCCCCCCCCCCCCCCCCCCCCCCCCCCCCCCCCCCCCCCC
C SUBROUTINE CUBIC
C
C       CALCULATE REQUIRED DATA USING CUBIC INTERPOLATION BETWEEN
C          TWO POINTS WITH KNOWN SLOPE AT EACH END
C
CCCCCCCCCCCCCCCCCCCCCCCCCCCCCCCCCCCCCCCCCCCCCCCCCCCCCCCCCCCCCCCCCCCCCCCC
      IMPLICIT REAL*8 (A-H,O-Z)
C
      XRMXL=XR-XL
      ZRMZL=ZR-ZL
C
C    CALCULATE COEFFICIENTS OF CUBIC EQUATION
C
      A3=((AMR+AML)*XRMXL-2.D0*ZRMZL)/XRMXL**3
      A2=(AMR-AML-3.D0*A3*(XR*XR-XL*XL))/(2.D0*XRMXL)
      A1=(ZRMZL-A3*(XR**3-XL**3)-A2*(XR*XR-XL*XL))/XRMXL
      A0=ZL-((A3*XL+A2)*XL+A1)*XL
C
C    CALCULATE DISPLACEMENT AND SLOPE
C
      DIC=((A3*XC+A2)*XC+A1)*XC+A0
      SDIC=(3.D0*A3*XC+2.D0*A2)*XC+A1
      RETURN
      END
```

Subroutine QUADL

```
      SUBROUTINE QUADL(AML,XL,XR,ZL,ZR,XC,DIC,SDIC)
CCCCCCCCCCCCCCCCCCCCCCCCCCCCCCCCCCCCCCCCCCCCCCCCCCCCCCCCCCCCCCCCCCCCCCC
C SUBROUTINE QUADL
C
C      CALCULATE REQUIRED DATA USING QUADRATIC INTERPOLATION
C         BETWEEN TWO POINTS WITH KNOWN SLOPE AT THE LEFT POINT
C
CCCCCCCCCCCCCCCCCCCCCCCCCCCCCCCCCCCCCCCCCCCCCCCCCCCCCCCCCCCCCCCCCCCCCCC
      IMPLICIT REAL*8 (A-H,O-Z)
C
      XRMXL=XR-XL
      ZRMZL=ZR-ZL
C
C   CALCULATE COEFFICIENTS OF QUADRATIC EQUATION
C
      A2=(ZRMZL-AML*XRMXL)/(XRMXL*XRMXL)
      A1=AML-2.D0*A2*XL
      A0=ZL-(A2*XL+A1)*XL
C
C   CALCULATE DISPLACEMENT AND SLOPE
C
      DIC=(A2*XC+A1)*XC+A0
      SDIC=2.D0*A2*XC+A1
      RETURN
      END
```

Subroutine QUADR

```
      SUBROUTINE QUADR(AMR,XL,XR,ZL,ZR,XC,DIC,SDIC)
CCCCCCCCCCCCCCCCCCCCCCCCCCCCCCCCCCCCCCCCCCCCCCCCCCCCCCCCCCCCCCCCCCCCCCCC
C SUBROUTINE QUADR
C
C      CALCULATE REQUIRED DATA USING QUADRATIC INTERPOLATION
C         BETWEEN TWO POINTS WITH KNOWN SLOPE AT THE RIGHT POINT
C
CCCCCCCCCCCCCCCCCCCCCCCCCCCCCCCCCCCCCCCCCCCCCCCCCCCCCCCCCCCCCCCCCCCCCCCC
      IMPLICIT REAL*8 (A-H,O-Z)
C
      XRMXL=XR-XL
      ZRMZL=ZR-ZL
C
C   CALCULATE COEFFICIENTS OF QUADRATIC EQUATION
C
      A2=(AMR*XRMXL-ZRMZL)/(XRMXL*XRMXL)
      A1=AMR-2.D0*A2*XR
      A0=ZL-(A2*XL+A1)*XL
C
C   CALCULATE DISPLACEMENT AND SLOPE
C
      DIC=(A2*XC+A1)*XC+A0
      SDIC=2.D0*A2*XC+A1
      RETURN
      END
```

Parametric Data File - CLOSEDAT.DAT

```
 3  5  7  9 11 13 15 17
1  1 -5.64708 .000 -2.0371E-3 -1.0819E-2 -.28437 .0187634  .1039211 .5760317
1  2 -5.52209 .025 -8.9607E-4 -4.6304E-3 -.21326 .0091287  .0495130 .2687900
1  3 -4.80000 .100  0.0000000  0.0000000  .00000 .0000000  .0000000 .0000000
2  1 -5.24679 .000 -1.7614E-2 -8.0639E-2 -.75905 .0922415  .4663580 2.366244
2  2 -5.13448 .025 -1.2219E-2 -5.4311E-2 -.63228 .0480350  .2344200 1.149300
2  3 -4.76670 .075 -4.4843E-3 -1.8879E-2 -.39294 .0172090  .0775440 .3507500
2  4 -4.33957 .125 -9.0437E-4 -3.5887E-3 -.19343 .0065008  .0273060 .1149100
2  5 -3.60000 .200  0.0000000  0.0000000  .00000 .0000000  .0000000 .0000000
3  1 -4.81112 .000 -6.0228E-2 -2.3167E-1 -1.3360 .2651587  1.215482 5.616157
3  2 -4.71098 .025 -4.7201E-2 -1.7503E-1 -1.1582 .1300800  .5656100 2.489500
3  3 -4.38720 .075 -2.6125E-2 -9.0642E-2 -.86567 .0563050  .2209000 .8784800
3  4 -4.00480 .125 -1.2443E-2 -4.0326E-2 -.60850 .0311660  .1123700 .4096900
3  5 -3.58532 .175 -4.5211E-3 -1.3609E-2 -.37863 .0159090  .0525170 .1746800
3  6 -3.14211 .225 -9.0525E-4 -2.5065E-3 -.18291 .0063747  .0191250 .0575860
3  7 -2.40000 .300  0.0000000  0.0000000  .00000 .0000000  .0000000 .0000000
4  1 -4.35286 .000 -1.4209E-1 -4.4258E-1 -1.9828 .6401989  2.644603 11.06900
4  2 -4.26558 .025 -1.1832E-1 -3.5147E-1 -1.7539 .2724800  1.044000 4.101700
4  3 -3.97712 .075 -7.7615E-2 -2.1143E-1 -1.4235 .1243000  .4167300 1.445900
4  4 -3.63400 .125 -4.7966E-2 -1.1972E-1 -1.1296 .0779270  .2352200 .7350600
4  5 -3.24489 .175 -2.6575E-2 -6.0300E-2 -.84978 .0493520  .1335700 .3731100
4  6 -2.82582 .225 -1.2526E-2 -2.5565E-2 -.59034 .0295510  .0709800 .1750100
4  7 -2.39119 .275 -4.5296E-3 -8.1993E-3 -.36201 .0155790  .0327220 .0700460
4  8 -1.94302 .325 -9.0543E-4 -1.4209E-3 -.17001 .0063326  .0113990 .0207270
4  9 -1.20000 .400  0.0000000  0.0000000  .00000 .0000000  .0000000 .0000000
5  1 -3.89162 .000 -2.7534E-1 -6.5594E-1 -2.6925 1.460995  5.410300 20.39889
5  2 -3.81571 .025 -2.3798E-1 -5.3147E-1 -2.4105 .4920900  1.639700 5.725100
5  3 -3.55408 .075 -1.7148E-1 -3.3919E-1 -2.0591 .2257200  .6307500 1.902500
5  4 -3.24200 .125 -1.2036E-1 -2.1047E-1 -1.7413 .1500900  .3662200 .9768100
5  5 -2.88163 .175 -7.9582E-2 -1.2114E-1 -1.4251 .1041200  .2204700 .5141600
5  6 -2.48636 .225 -4.8657E-2 -6.3056E-2 -1.1196 .0716280  .1294400 .2587700
5  7 -2.06796 .275 -2.6759E-2 -2.8608E-2 -.83550 .0473250  .0711090 .1184400
5  8 -1.63435 .325 -1.2562E-2 -1.0563E-2 -.57530 .0289710  .0347860 .0462900
5  9 -1.19356 .375 -4.5336E-3 -2.7664E-3 -.34820 .0154520  .0139090 .0138350
5 10 -0.74337 .425 -9.0548E-4 -3.3448E-4 -.16057 .0063165  .0037900 .0024829
5 11  0.00000 .500  0.0000000  0.0000000  .00000 .0000000  .0000000 .0000000
6  1 -3.44645 .000 -4.7628E-1 -7.8557E-1 -3.4946 3.374369  11.15332 37.65377
6  2 -3.37874 .025 -4.2227E-1 -6.3167E-1 -3.1624 .7976900  2.272900 7.048000
6  3 -3.13426 .075 -3.2279E-1 -3.9773E-1 -2.7976 .3630000  .8149600 2.156600
6  4 -2.84305 .125 -2.4403E-1 -2.4415E-1 -2.4578 .2501600  .4672000 1.084100
6  5 -2.50443 .175 -1.7767E-1 -1.3749E-1 -2.1113 .1827300  .2799700 .5636700
6  6 -2.12905 .225 -1.2337E-1 -6.7611E-2 -1.7667 .1349000  .1638300 .2812000
6  7 -1.72738 .275 -8.0800E-2 -2.6034E-2 -1.3605 .0983610  .0891070 .1278900
6  8 -1.30774 .325 -4.9078E-2 -4.7092E-3 -1.1148 .0695410  .0418640 .0500370
6  9 -0.87642 .375 -2.6878E-2  3.5180E-3 -.82275 .0466650  .0140210 .0150860
6 10 -0.43689 .425 -1.2587E-2  4.5196E-3 -.56311 .0288100  .0000000 .0045196
6 11  0.00602 .475 -4.5366E-3  2.6758E-3 -.33804 .0154290 -.0046295 .0027036
6 12  0.45665 .525 -9.0544E-4  7.5226E-4 -.14939 .0063165 -.0037899 .0024829
```

```
 6 13  1.20000 .600  0.0000000  0.0000000  .00000 .0000000  .0000000 .0000000
 7  1 -3.03154 .000 -7.7607E-1 -7.1091E-1 -4.4927 8.445548  24.82695 74.55299
 7  2 -2.96777 .025 -7.0055E-1 -5.3147E-1 -4.1000 1.184800  2.815600 7.824600
 7  3 -2.72858 .075 -5.5677E-1 -2.7089E-1 -3.7147 .5386900  .9130900 2.220600
 7  4 -2.44620 .125 -4.4094E-1 -1.1111E-1 -3.3391 .3820800  .4937100 1.096600
 7  5 -2.11894 .175 -3.4027E-1 -8.3404E-3 -2.9518 .2894000  .2729500 .5700200
 7  6 -1.75586 .225 -2.5423E-1  5.1161E-2 -2.5592 .2234400  .1381100 .2936600
 7  7 -1.36644 .275 -1.8292E-1  7.8043E-2 -2.1723 .1724300  .0526920 .1500400
 7  8 -0.95859 .325 -1.2582E-1  8.2055E-2 -1.7999 .1312600  .0000000 .0820550
 7  9 -0.53820 .375 -8.1836E-2  7.1846E-2 -1.4485 .0974130 -.0294090 .0560180
 7 10 -0.10926 .425 -4.9462E-2  5.4612E-2 -1.1228 .0695410 -.0418630 .0500370
 7 11  0.32551 .475 -2.6996E-2  3.5929E-2 -.82670 .0468750 -.0422540 .0496830
 7 12  0.76535 .525 -1.2614E-2  1.9666E-2 -.56283 .0289710 -.0347860 .0462900
 7 13  1.20734 .575 -4.5402E-3  8.1266E-3 -.33586 .0154990 -.0232530 .0362010
 7 14  1.65702 .625 -9.0554E-4  1.8394E-3 -.14735 .0063326 -.0113990 .0207270
 7 15  2.40000 .700  0.0000000  0.0000000  .00000 .0000000  .0000000 .0000000
 8  1 -2.65483 .000 -1.2525000 -2.2619E-1 -6.0106 25.69929  66.97476 177.5804
 8  2 -2.58921 .025 -1.1446000 -2.2047E-2 -5.4998 1.645400  3.115700 8.045000
 8  3 -2.33836 .075 -9.3191E-1  2.4371E-1 -5.0432 .7649000  .8567100 2.247000
 8  4 -2.04842 .125 -7.5900E-1  3.7913E-1 -4.5891 .5591900  .3864600 1.170800
 8  5 -1.71790 .175 -6.0655E-1  4.4165E-1 -4.1162 .4370700  .1443000 .6895500
 8  6 -1.35542 .225 -4.7337E-1  4.5156E-1 -3.6361 .3492500  .0000000 .4515600
 8  7 -0.96994 .275 -3.5972E-1  4.2403E-1 -3.1617 .2802400 -.0878970 .3387700
 8  8 -0.56890 .325 -2.6522E-1  3.7222E-1 -2.7035 .2234400 -.1381100 .2936600
 8  9 -0.15769 .375 -1.8878E-1  3.0737E-1 -2.2682 .1755700 -.1610900 .2819600
 8 10  0.26018 .425 -1.2874E-1  2.3857E-1 -1.8627 .1349000 -.1638300 .2812000
 8 11  0.68268 .475 -8.3166E-2  1.7287E-1 -1.4874 .1004400 -.1517300 .2764500
 8 12  1.10903 .525 -4.9998E-2  1.1522E-1 -1.1464 .0716280 -.1294300 .2587700
 8 13  1.53896 .575 -2.7177E-2  7.8788E-2 -.83979 .0480930 -.1011900 .2245100
 8 14  1.97352 .625 -1.2660E-2  3.4932E-2 -.56982 .0295510 -.0709800 .1750100
 8 15  2.41111 .675 -4.5475E-3  1.3597E-2 -.33894 .0157040 -.0424120 .1158600
 8 16  2.85799 .725 -9.0579E-4  2.9277E-3 -.14829 .0063747 -.0191250 .0575860
 8 17  3.60000 .800  0.0000000  0.0000000  .00000 .0000000  .0000000 .0000000
-4.81198 .083574
-3.62382 .084625
-2.43558 .085326
-1.24724 .086008
-.058824 .086683
 1.12968 .087355
 2.31828 .088020
 3.46572 .088685
```

APPENDIX V

NEWTON-RAPHSON ITERATION

In Section 4.2 a very brief description of the Newton-Raphson iteration scheme used in the secondary iteration loop was given. At this time a more in-depth description will be presented in outline form.

Given: ${}^{t}F$, ${}^{t}U$ = force and displacement distributions of previous solution state (time t)

${}^{t+}\Delta U$ = current state incremental displacement distribution (time $t+ = t + \Delta t$)

Assume: ${}^{t}\bar{\lambda}$, ${}^{t+}\bar{\lambda}$ are within range of closure

Newton-Raphson Initialization

1. Evaluate ${}^{t}C$; tangent compliance matrix for ${}^{t}F$. (equations 2.4-7)
2. Calculate ${}^{t+}\Delta F^{o}$; first approximation of incremental loads. $({}^{t}C)^{-1}({}^{t+}\Delta U)$
3. Estimate ${}^{t+}F^{o}$; first estimate of new loads. $= {}^{t}F + {}^{t+}\Delta F^{o}$
4. Calculate ${}^{t+}U^{o}$; first estimation of total displacements for ${}^{t+}F^{o}$. (equations 2.4-1)
5. Determine ${}^{t+}e^{o}$; displacement estimate error. $= {}^{t}U + {}^{t+}\Delta U - {}^{t+}U^{o}$

Newton-Raphson Iteration

6. Evaluate ${}^{t+}C^{i-1}$; tangent compliance matrix for ${}^{t+}F$. (equations 2.4-7)
7. Calculate ${}^{t+}d\Delta F^{i-1}$; incremental load correction. $({}^{t+}C^{i-1})^{-1}({}^{t+}e^{i-1})$
8. Estimate ${}^{t+}\Delta F^{i}$; incremental load estimate. $= {}^{t+}\Delta F^{i-1} + {}^{t+}d\Delta F^{i-1}$
9. Compare both ${}^{t+}e^{i-1}$ and ${}^{t+}d\Delta F^{i-1}$ to convergence limits. If within limits, solution is complete.
10. Estimate ${}^{t+}F^{i}$; total load estimate. $= {}^{t}F + {}^{t+}\Delta F^{i}$
11. Calculate ${}^{t+}U^{i}$; total displacement estimate for ${}^{t+}C^{i-1}$ and ${}^{t+}F^{i}$. (equations 2.4-1)
12. Determine ${}^{t+}e^{i}$; displacement estimate error. $= {}^{t}U + {}^{t+}\Delta U - {}^{t+}U^{i}$
13. Return to step 6.

With regard to this algorithm several points should be made. As was discussed in Section 4.1 a linear solution is performed initially to determine if closure will occur. Therefore this iteration loop will only be performed for conditions where closure will occur. In this light, it was assumed that both ${}^{t}\bar{\lambda}$ and ${}^{t+}\bar{\lambda}$ are within the closure range. Consider the remaining three possibilities. If ${}^{t}\bar{\lambda}$ is outside the range and ${}^{t+}\bar{\lambda}$ remains inside the range the previous solution state is linearly modified (internally) to coincide with the onset of closure. In this way the original assumption remains valid. If ${}^{t}\bar{\lambda}$ is inside the range and ${}^{t+}\bar{\lambda}$ falls outside the iteration is stopped with current tangent compliance and load distribution estimates sent out. Finally, ${}^{t}\bar{\lambda}$ outside the range and ${}^{t+}\bar{\lambda}$ falling outside corresponds to a combination of the previous two cases.

Note that ${}^{t+}\bar{\lambda}$ can (and typically will) fall outside the range of closure when a very small amount of closure is obtained from a previously fully open solution state. This is simply due to the increase in stiffness with closure which causes displacement increments to decrease. In this situation, the iteration scheme is stopped. However, since the latest (closed) tangent compliance estimates are returned a linear solution will not be obtained unless the tolerance limits are satisfied.

As a final note, step 10 indicates that the incoming load distribution, ${}^{t}F$ is retained throughout the iteration loop. This is consistent with the approach used in the primary loop as described in Section 4.1.

APPENDIX VI

MODIFICATIONS TO PARTIAL CLOSURE ROUTINES

Several features of the partial closure routines can be modified quite easily to introduce additional parametric data or to modify the stiffness factor reduction procedure. The tasks required to institute these modification are outlined below.

Additional Parametric Data

Any additional data (acquired at crack depth ratio 0.1, 0.2,...0.8) must be reduced as shown in Appendix II and it must be added to the parametric data file CLOSEDAT.DAT. The first line of the data file gives the number of data points available for each crack depth. The data must then be formatted as shown in Table II-3 with two additional entries: the integral crack depth (i.e., 1 for 0.1, 2 for 0.2, etc.) and the data point number. The parametric data file is presented in Appendix IV. Each column of the file is defined within the listing of subroutine PART.

Stiffness Factor Reduction

The stiffness factors are calculated in block C of routine MATLS. The actual factor reduction is performed in subroutine PART. To use the partially-closed stiffnesses only the factors must be set to 1.0 and the stiffnesses defined as

AMK(1) = CM*C22

AMK(2) = -CM*C12 (for positive crack depths)

AMK(2) = CM*C12 (for negative crack depth)

AMK(3) = CM*C11

within block C. In this way, no factor reduction will be performed in subroutine PART.

The factor reduction is defined by the function by which the reduction is performed (linear, quadratic, etc.) and the closure length at which reduction is complete (BXIC). The reducing functions are applied at two locations within subroutine PART and are defined such that the factor is FC=FC1 (or FC2 or FC3) at AFC=0.0 and FC=1.0 for AFC=1.0.

Interpolation of Parametric Data

The linear interpolation with respect to crack length is performed in subroutines CLOSE, DEFL, PDEFL, and SIFAC. The cubic and/or quadratic interpolation with respect to load ratio is performed in subroutine CLOSEA and with respect to closure length in subroutines DEFLA, PDEFLA, and SIFACA. The weighted central difference approximation is applied in the _A subroutines. Any change in the interpolation scheme will impact each of these routines.

Stationary vs. Progressive Iteration

The "previous solution state" data which is input to subroutine PART is controlled by subroutine PRTCLL. To force stationary iteration at all time, the first IF-ELSE-END_IF loop (beginning with IF (KFCL(ICNT).EQ.1) THEN) must be replaced by

```
FN     =  S1(1)
FM     =  S1(2)
DDELTA =  DEE1(1)
DTHETA =  DEE1(2)
```

The data S1 and DEE1 represent the results based on the previous converged increment versus the previous converged iteration.

INFERNOS ADEAT LABOR